Adaptive Inverse Control for Rotorcraft Vibration Reduction

Stephen A. Jacklin

October 1985

NASA
National Aeronautics and
Space Administration

Adaptive Inverse Control for Rotorcraft Vibration Reduction

Stephen A. Jacklin, Ames Research Center, Moffett Field, California

October 1985

NASA

National Aeronautics and
Space Administration

Ames Research Center
Moffett Field, California 94035

ABSTRACT

This thesis extends the Least Mean Square (LMS) algorithm to solve the multiple-input, multiple-output problem of alleviating N/Rev helicopter fuselage vibration by means of adaptive inverse control. A frequency domain locally linear model is used to represent the transfer matrix relating the higher harmonic pitch control inputs to the harmonic vibration outputs to be controlled. By using the inverse matrix as the controller gain matrix, an adaptive inverse regulator is formed to alleviate the N/Rev vibration. The stability and rate of convergence properties of the extended LMS algorithm are discussed. It is shown that the stability ranges for the elements of the stability gain matrix are directly related to the eigenvalues of the vibration signal information matrix for the learning phase, but not for the control phase. The overall conclusion is that the LMS adaptive inverse control method can form a robust vibration control system, but will require some tuning of the input sensor gains, the stability gain matrix, and the amount of control relaxation to be used. The learning curve of the controller during the learning phase is shown to be quantitatively close to that predicted by averaging the learning curves of the normal modes. For higher order transfer matrices, a rough estimate of the inverse is needed to start the algorithm efficiently. The simulation results indicate that the factor which most influences LMS adaptive inverse control is the product of the control relaxation and the the stability gain matrix. A small stability gain matrix makes the controller less sensitive to relaxation selection, and permits faster and more stable vibration reduction, than by choosing the stability gain matrix large and the control relaxation term small. It is shown that the best selections of the stability gain matrix elements and the amount of control relaxation is basically a compromise between slow, stable convergence and fast convergence with increased possibility of unstable identification. In the simulation studies, the LMS adaptive inverse control algorithm is shown to be capable of adapting the inverse (controller) matrix to track changes in the flight conditions. The algorithm converges quickly for moderate disturbances, while taking longer for larger disturbances. Perfect knowledge of the inverse matrix is not required for good control of the N/Rev vibration. However it is shown that measurement noise will prevent the LMS adaptive inverse control technique from controlling the vibration, unless the signal averaging method presented is incorporated into the algorithm.

TABLE OF CONTENTS

iii , iv

LIST OF FIGURES

xiii

LIST OF TABLES

LIST OF SYMBOLS

C .... Controller Matrix (Inverse of T)

C_i^T .... i^{th} Row of C Matrix

$C(0)$ .... Controller Matrix Initial Conditions

e .... LMS Error Vector

e_i .... i^{th} Element of LMS Error Vector

I .... Identity Matrix

k_i .... i^{th} Element of Stability Gain (Row) Vector

K_S .... LMS Stability Gain Matrix

N .... Number of Blades in Rotor

$S_{z,z}$ ....Vibration Signal Information Matrix

$S_{z,\theta}$ .... Vibration Pitch Row Vector

R .... Matrix of Signal Information Matrix Eigenvectors

T .... Transfer Matrix Relating Harmonics of Pitch

   Harmonics of Vibration

Z .... Measured vibration Vector

Z_0 .... Uncontrolled Vibration Vector

ΔZ .... Vector of Changes in Vibration Vector Elements

$\Delta \Theta$ .... Vector of Changes in Cyclic Pitch

$\Delta \Theta_i$ .... i^{th} Element of $\Delta \Theta$ Vector

Θ .... Cyclic Pitch Vector

Λ .... Diagonal Matrix of Signal Information Matrix

   Eigenvalues

λ_i .... i^{th} Eigenvalue of Signal Information Matrix

λ_{max} .... Maximum Eigenvalue of Signal Information Matrix

Ψ .... Rotor Azimuth Angle

τ_i .... i^{th} Normal Mode Time Constant

Subscript: i   ...... Denotes i^{th} Row

Superscript: T   ...... Denotes Transpose

Superscript: *   ...... Denotes Optimal Inverse Control

Superscript: -1   ...... Denotes Inverse

Special Symbol: .E[ ]   Denotes Expectation

I. INTRODUCTION

This thesis presents an extension of the Least Mean Square (LMS) algorithm to solve the multiple-input, multiple-output problem of alleviating N/Rev helicopter fuselage vibration by means of adaptive inverse control. The reduction or alleviation of helicopter N/Rev vibration will reduce maintenance requirements, while at the same time increase ride quality and helicopter reliability. The solution presented in this paper uses the extended LMS algorithm to estimate the local inverse of the transfer matrix relating the higher harmonic pitch control inputs to the harmonic vibration outputs to be controlled. By using the inverse matrix as the controller gain matrix, an adaptive inverse regulator is formed to alleviate the N/Rev vibration. The contributions made in this thesis are first to extend the LMS algorithm of Widrow and Hoff to solve the multiple-input, multiple-output helicopter vibration control problem, and second to formulate the helicopter vibration problem in a manner suitable for solution by the LMS adaptive inverse control technique.

Prior to presenting the multiple-input, multiple-output LMS adaptive inverse control algorithm extension, the nature of the helicopter vibration control problem will be explained. A literature review of previous work follows this introduction. Though not intended to review previous work in an exhaustive fashion, work relevant to the control of helicopter vibration by active blade pitch controls, and work related to the development of the LMS algorithm are cited. A complete description of the vibration control problem is then given in terms of inverse modeling concepts and terminology related to modeling the helicopter as a linear system in the frequency domain. Once the control problem nomenclature and

formulation are clearly delineated, the extended LMS algorithm is presented and used to solve the vibration control problem. In the analysis section which follows, the stability and rate of convergence properties are discussed. Here, the effect of controller initial conditions and the choice of the stability gain matrix elements play an important role in overall algorithm performance. It will be shown that the stability ranges for the elements of the stability gain matrix are directly related to the eigenvalues of the vibration signal information matrix. Lastly, the results obtained from simulation will be presented for a variety of cases, including the effects of measurement noise and changes in operating conditions.

II. PREVIOUS WORK

This section presents a review of previous work. The review has been divided into two sections. The first section reviews work related to the active control of helicopter vibration using frequency domain models and inverse control techniques. The second part presents the development of the LMS algorithm. Though this review of previous work is not comprehensive, it will serve to acquaint the reader with most of the important contributions upon which this thesis builds.

2.1

ACTIVE CONTROL OF HELICOPTER VIBRATION
USING FREQUENCY DOMAIN MODELS

In forward flight, asymmetrical airflow through the rotor disk of the helicopter produces a fuselage vibration spectrum which tends to be dominated by multiples of the N/Rev component (Johnson, 1980). Here, N denotes the number of blades in the rotor. As viewed from the nonrotating or fuselage reference frame, the N rotor blades produce N cycles of vibration per rotor revolution. The vertical hub shears and blade stresses also have a similar periodic nature.

Researchers in rotorcraft development recognized early on that the elimination of these periodic vibrations and loads would be valuable in extending the useful life of the helicopter and improve its ride quality. Hence, passive vibration control mechanisms have been engineered into the helicopter almost from

its inception (Gessow and Meyers, 1952). Though these passive devices enhance vehicle operation, they typically have the disadvantages of adding to the gross weight of the helicopter and increasing the profile drag power loss. In recent years, advances in digital computation circuitry have offered the the option of implementing computer-controlled, active vibration reduction methods. These methods hold the potential for not only reducing the weight of the helicopter, but also the capability to adaptively reduce the periodic rotor loads and vibrations at their source.

Though it is difficult to say who was first in beginning the active vibration control studies, McCloud and Kretz (1974, 1975) seem to have developed the first linear, frequency domain model concept. In 1974 they examined the effects of introducing higher harmonic control into the rotating system of the jet-flap rotor. The jet-flap was excited at harmonics of 2, 3, 4, 5, 6, and 7 per Rev, and the 2, 3, 4, 5, and 6 harmonics of blade stress and rotor loads were obtained. The objective of the test was to see what effect higher harmonic blade pitch had on the periodic nature of the rotor loads and blade stresses. With the assistance of Jean N. Aubrun, a frequency domain model was developed to relate the various harmonics of rotor loads and vibration to the higher harmonics of jet-flap excitation. This model postulated that for a quasi-static wind tunnel operating condition, the higher harmonic amplitudes of fuselage vibration and rotor loads could be linearly related to the harmonics of jet-flap excitation. The matrix relating these harmonics was calculated by an off-line weighted least square error technique. This transfer matrix was termed the T matrix. In later theoretical studies the optimal control was formed as a deterministic function of the T matrix and sensed vibration. Further open-loop studies were subsequently tested by McCloud and Weisbrich on the Multicyclic Controllable

4

Twist Rotor (MCTR). This rotor was similar to the jet-flap rotor in that higher harmonic control was introduced directly into the rotating system. Again a frequency domain transfer function or T matrix was identified by an off-line least square error technique. The optimal open-loop deterministic control was calculated off-line using the test data, but not directly applied to the rotor.

The next key development in higher harmonic vibration control was to introduce the higher harmonic controls directly into the rotating system by means of swashplate oscillation. In 1974, Sissingh and Donham conducted a test in which the swashplate was oscillated at higher harmonic frequencies. They then identified transfer matrices relating higher harmonics of cyclic pitch to the higher harmonics of vibratory hub moment and vertical shears with an off-line least square error technique. Using sensed vibration data and the inverse of the T matrix, a control law was computed and applied to the rotor.

In the years that followed, several other experimenters closed the loop with respect to sensed vibration, and various versions of inverse control were presented. In 1978, Powers studied the harmonic response of hub forces to harmonic swashplate oscillation. The loop was closed only with respect to the operator, who calculated the control off-line, using direct inversion of the T matrix. In 1980, Shaw and Albion tested a fully closed-loop version of the inverse control scheme. The control used was swashplate oscillation at N/Rev and the sensed feedback parameters were the third, fourth, and fifth harmonics of root flapwise bending. The transfer matrix was computed by an off-line least squares method and inverted. This inverse matrix was then used as a fixed-gain controller matrix, since it effectively described the

relationship between the swashplate oscillation inputs, and the flapwise bending outputs. This method of inverse control worked well at one speed, but not at others, because at other flight conditions the control authority was exceeded, or perhaps because the transfer function was no longer valid at the new control point. In any event, it seemed that on-line identification and variable control authority would be required to make the inverse control method viable.

However, rather than pursuing these issues, the majority of researchers have since studied stochastic methods to identify and track the transfer matrix, and LQG theory to compute the control as either deterministic or stochastic functions of the transfer matrix and the measured or identified vibration. The interested reader is referred to optimal control texts such as Bryson and Ho, Goodwin and Payne, or Sage and Melsa to gain an appreciation of these modern estimation and control techniques. Johnson (1982), however, provides an excellent analysis of these state of the art identification and control techniques in the context of the helicopter vibration control problem. Davis (1983) presents a computer simulation of these methodologies including the Kalman Filter approach of Taylor, Farrar, and Mio (1980) and the cautious and dual control approaches as given by Molusis, Hammond, and Cline (1981).

Though some of these concepts appear very promising, the complexity of their implementation encourages efforts to find a simpler approach, if possible. The LMS algorithm of Widrow and Hoff was studied and extended in an effort to find such a simpler approach. Inverse control is simple to implement, but only effective if good knowledge of the local transfer matrix inverse is available. The LMS algorithm may serve as a means

6

of providing this knowledge, in a computationally fast and efficient manner.

2.2

DEVELOPMENT OF THE LMS ALGORITHM

The Least Mean Square (LMS) algorithm of Widrow and Hoff was initially designed to tune or adjust filters. In these studies, Widrow considered filters to be broadly defined as any device or system that processed incoming signals or other data in such a way as to eliminate noise, smooth the signals, or identify each signal as belonging to a class, or predict the next input signal from moment to moment (Widrow 1970). The early development of the LMS algorithm was focused on electrical engineering problems.

Widrow and his colleagues derived the LMS algorithm for single-input, single-output systems (Widrow 1960). The typical plant model considered a single input signal, which was delayed several times. After each delay, the signal was sent to the next delay, and also to a summer node after having been multiplied by a gain. All the signals were summed together to form a single output. The optimization problem was to find the value of the gains and/or delays which would tune the filter in some optimal sense. This type of model had many useful applications.

In 1967, Widrow, Mantey, Griffiths, and Goode proposed to optimally tune

antenna sensitivity using the LMS algorithm. In this case the tapped delay line model was used to represent a single signal source received by an array of antennas. Due to the configuration of the antennas in space, each antenna would receive the signal with a slightly different transmission delay time. It was postulated that the signals from different antennas could be optimally delayed such that when added together they would produce a maximum signal output. In this problem, the LMS algorithm was used to identify a vector of signal delay times.

A similar method was proposed to identify signals in the presence of interfering noise sources. As in the previous example, the concept involved optimally delaying the signals from several sensors, and adding them together to achieve the desired result. One application was a fetal heart monitor (Widrow 1975), in which the purpose was to track the fetal heart EKG in the presense of the mother's EKG, an interfering noise source. Microphones were placed in an array on the mother's abdomen. Since the microphones were located at varying distances from the mother and fetal hearts, it was postulated that by delaying the signal from each microphone by just the right amount, it would be possible to amplify the fetal heart EKG, while attenuating the mother's EKG at the same time. The model used to represent the filter was a tapped delay line, as in the previous example. The LMS algorithm was again used to tune the filter, by finding the optimal vector of time delays.

In 1979, Widrow, McCool, and Medoff proposed using the LMS algorithm for the purposes of adaptive inverse identification. They proposed that if a plant inverse were known, a servo device could be made to follow an input command signal. No modeling or simulation of a multiple-

input, multiple-output plant was presented in the paper. The model used in the paper was again the tapped delay line model, indicating that the present work concerned the single-input, single-output case. An allusion to adaptive inverse control of multiple-input, multiple-output systems was made, but with no examples, target applications, or models referenced.

The next section presents the helicopter vibration control problem as a multiple-input, multiple-output adaptive inverse control application problem.

III. INVERSE CONTROL OF HELICOPTER VIBRATION

The multiple-input, multiple-output control problem presented here involves determining the higher harmonic blade pitch motions to reduce the N/Rev fuselage vibration. In order to use active controls to reduce vibration, a model is needed to mathematically state how the input higher harmonic blade pitch is related to the measured harmonics of fuselage vibration. The formulation of such a model based on the helicopter structural motion constraints and aerodynamic loadings is, at present, an intractable problem. It is therefore necessary to identify the elements of an assumed model from the higher harmonic pitch inputs and vibration outputs. In this section, the concept of inverse active control will be presented, which will serve to define the vibration control problem at hand, as well as explain the nomenclature used herein.

3.1

HIGHER HARMONIC BLADE PITCH CONTROL

The control proposed to reduce fuselage vibration is termed *higher harmonic* or *multicyclic* blade pitch oscillation. As the names imply, the blade pitch is forced or oscillated at multiples of the rotor rotational frequency. It is convenient to express the blade pitch motion as a Fourier series expansion as follows:

$$\Theta = \theta_0 + \theta_{1C} Cos(\Psi) + \theta_{1S} Sin(\Psi) + \theta_{2C} Cos(2\Psi) + \theta_{2S} Sin(2\Psi)$$

$$+\theta_{3C} Cos(3\Psi) + \theta_{3S} Sin(3\Psi) + \theta_{4C} Cos(4\Psi) + \theta_{4S} Sin(4\Psi) + ...$$

where,

$$\theta_0 = \qquad Collective \;\; Cyclic \;\; Pitch$$
$$\theta_{1C} = \qquad Lateral \;\; Cyclic \;\; Pitch$$
$$\theta_{1S} = \qquad Longitudinal \;\; Cyclic \;\; Pitch$$

and,

$$\theta_{2C} =$$
$$\theta_{2S} =$$
$$\theta_{3C} =$$
$$\theta_{3S} = \qquad The \;\; Higher \;\; Harmonics \;\; of$$
$$\theta_{4C} = \qquad Cyclic \;\; Blade \;\; Pitch$$
$$\theta_{4S} =$$
$$\theta_{5C} =$$
$$\theta_{5S} =$$

The first three coefficients specify the primary controls which are used to trim the helicopter to a desired flight attitude. The remaining coefficients are the higher harmonic terms, and are potentially available to control vibration.

The blade pitch control is considered to be implemented from actuators located in the nonrotating system. (It is possible to introduce blade pitch control from the rotating system, as well.) The control is transferred from the nonrotating system to the rotating system by means of the swashplate.

The swashplate is basically a pair of annular plates, positioned around the rotor shaft. While the lower swashplate is stationary, and attached to the fixed system actuators, the upper swashplate rotates with the rotor, and is attached to the blade pitch control rods. Differential control of rotor blade pitch is obtained by tilting the swashplate. For helicopter trim control, the swashplate tilt is held quasi-steady. Higher harmonic control is implemented by oscillating the swashplate tilt in a sinusoidal fashion, relative to the reference blade angle.

Because the higher harmonic control is of different frequency and amplitude than the trim controls, separate actuation systems are typically required. Figures 1 and 2 are presented to give the reader some insight as to how the higher harmonic motion used to alleviate vibration may be mechanically superimposed on the primary controls used to trim the helicopter. In figure 1, the higher harmonic actuators move the pivot point of the bell crank of the trim control actuator linkage. An in-line actuator arrangement is also possible, as shown in figure 2. Note that in both cases, the actuators are in the fixed system and move the stationary swashplate. The rotating swashplate follows the stationary swashplate and introduces cyclic blade pitch proportional to the swashplate position.
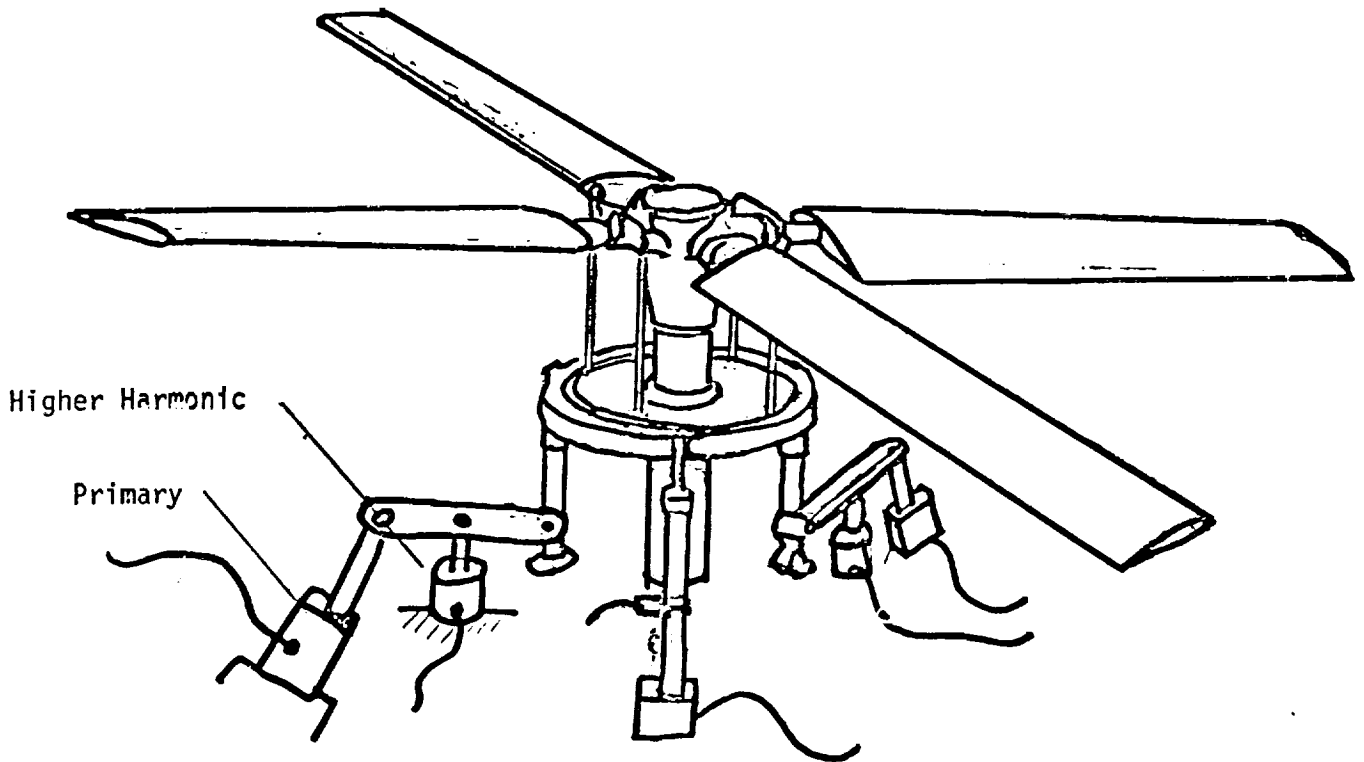
Figure 1. Mechanical Superposition of Trim and Higher Harmonic (Multicyclic) Pitch Controls; Bell Crank Arrangement
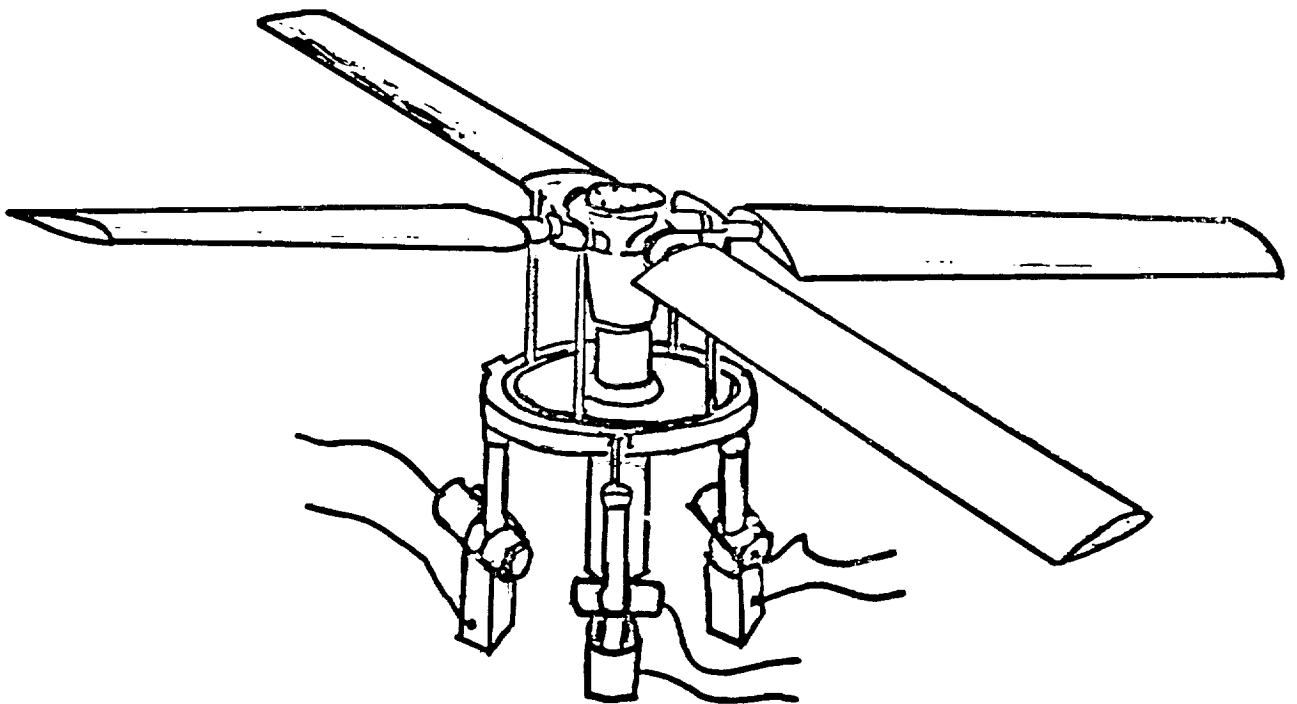
Figure 2. Mechanical Superposition of Trim and Higher Harmonic (Multicyclic) Pitch Controls; In-Line Actuator Arrangement

The control problem is to determine the phase and amplitude of cyclic pitch (swashplate) oscillation at N/Rev necessary to reduce fuselage vibration at N/Rev. Although other alternatives are possible, oscillation at N/Rev has the advantage of keeping all the blades "in track". That is, if the pitch of an N-bladed rotor is oscillated at N/Rev, then every blade will experience the same aerodynamic loading going around the azimuth. This is desirable, as it tends to aerodynamically balance the rotor (McCloud and Biggers 1978).

Higher harmonic pitch oscillation at N/Rev in the fixed system allows for six control degrees of freedom. Figure 3 defines the angle Ψ made by the reference blade and the tail of the helicopter. With respect to this reference, the magnitude and phase of collective, lateral, and longitudinal cyclic pitch motion at N/Rev frequency may be specified. These degrees of freedom are also shown in figure 3. However, instead of presenting the components as magnitude and phase, the relation,

$$A Cos(N\Psi + \phi) = C_1 Cos(N\Psi) + C_2 Sin(N\Psi)$$

will be used to form an expression using sine and cosine coefficients. Hence the control vector, Θ, consists of the sine and cosine Fourier coefficients of collective, lateral, and longitudinal higher harmonic motion at N/Rev,

$$\Theta \;=\; \begin{bmatrix} \theta_{C,Lon} \\[4pt] \theta_{S,Lon} \\[4pt] \theta_{C,Col} \\[4pt] \theta_{S,Col} \\[4pt] \theta_{C,Lat} \\[4pt] \theta_{S,Lat} \end{bmatrix} \quad \begin{array}{l} \textit{Longitudinal, Cosine} \\[4pt] \textit{Longitudinal, Sine} \\[4pt] \textit{Collective, Cosine} \\[4pt] \textit{Collective, Sine} \\[4pt] \textit{Lateral, Cosine} \\[4pt] \textit{Lateral, Sine} \end{array}$$

and will always be a (6x1) vector.
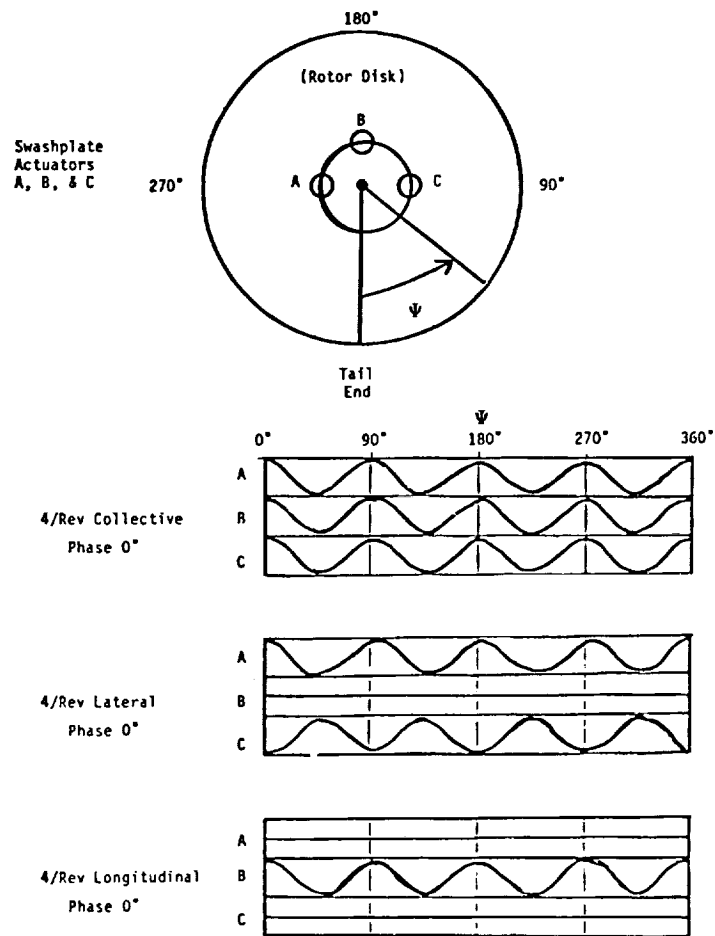
Figure 3: Example of N/Rev Collective, Lateral, and Longitudinal Pitch Controls for N=4.

MEASURED N/REV VIBRATION

The measured vibration vector, Z, represents the quantity to be minimized. It is formed by processing signals from accelerometers placed at various locations on the fuselage. By orienting the accelerometers in different spatial directions, vibration forces on all three axes may be sensed. The signal from each accelerometer may be represented as a Fourier series, using one rotor revolution as the fundamental period, as,

$$Z = z_0 + z_{1c}Cos(\Psi) + z_{1s}Sin(\Psi) + z_{2c}Cos(2\Psi) + z_{2s}Sin(2\Psi) + z_{3c}Cos(3\Psi)$$

$$z_{3s}Sin(3\Psi) + z_{4c}Cos(4\Psi) + z_{4s}Sin(4\Psi) + z_{5c}Cos(5\Psi) + z_{5s}Sin(5\Psi)...$$

If the vibration signal from the accelerometers is processed by a Fast Fourier Transform (FFT) algorithm, the N/Rev coefficients may be used to form the vibration vector. The vibration measurement vector will therefore be defined as a (2n x 1) vector whose elements are the N/Rev Fourier sine and cosine coefficients of the "n" accelerometers (figure 4).

The dimension of the vibration vector is thus proportional to the number of accelerometers used. Since only six controls have been proposed, it is obvious that good control of the (2n x 1) Z vector can only be attained by restricting n. The choice of n is a compromise between good vibration control at a few areas, or less vibration control at more areas. The number of locations in which vibration may be controlled well is dependent upon the structural constraints imposed by the fuselage between the accelerometers. If no constraints existed

among the selected accelerometer locations, it would be possible to control the magnitude and phase of at most three accelerometers, with the (6 x 1) control vector. Control at a greater number of locations is possible depending upon the fuselage constraints. With three appropriately placed accelerometers, it may be possible to alleviate the N/Rev vibration throughout the entire fuselage.
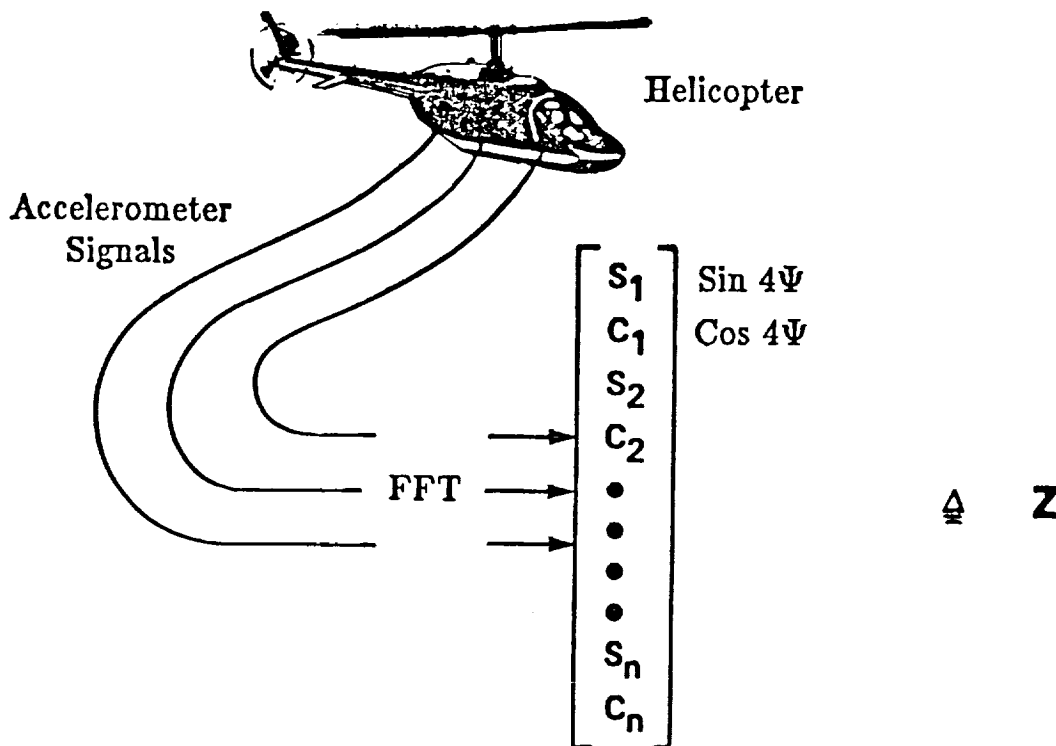
Figure 4: Formation of the (2n x 1) Vibration Measurement Vector from "n" Accelerometers on the Helicopter Fuselage

INVERSE VIBRATION CONTROL USING
LINEAR FREQUENCY DOMAIN MODELS

The higher harmonic fuselage vibration can be thought of as arising from two sources: 1) the aerodynamic interaction of the rotating N blades with the airflow, and, 2) the N/Rev cyclic pitch control input. The objective is to use the latter to cancel the former. To do so requires a mathematical model of the relationship between the higher harmonics of sensed vibration and the higher harmonics of pitch control.

Vibration control by inverse modeling requires that this relationship be linear. Linear models which describe the system may be of the global type,

$$Z(k) = [T]\Theta(k) + Z_0$$

where the vibration harmonics, Z, are linearly related to the pitch harmonics, Θ, about the vibration level Z_0 where Θ equals zero. However, for adaptive inverse control, it is more useful to use a local model of the form,

$$\Delta Z(k) = [T]\Delta\Theta(k)$$

where,

$$\Delta Z(k) = Z(k) - Z(k-1)$$

$$\Delta\Theta(k) = \Theta(k) - \Theta(k-1)$$

in which small changes in the N/Rev coefficients of vibration, ΔZ, are linearly related to small changes in the N/Rev coefficients of cyclic pitch, $\Delta\Theta$, about a local control point. Here $\Delta Z(k)$ is a column vector whose elements represent the difference in the sine and cosine Fourier coefficients between two successive steps. Similarly, $\Delta\Theta(k)$ is a column vector whose elements represent the difference in the N/Rev sine and cosine Fourier coefficients from one step to the next. T is the postulated transfer matrix which relates the changes in the higher harmonics of vibration to the changes in the higher harmonics of cyclic pitch control.

The idea behind adaptive inverse control is to make the controller matrix be the local inverse of the helicopter (plant) transfer function. The inverse control feedback loop may be modeled as in figure 5, where C denotes the inverse of the helicopter transfer matrix, T. From this figure, it is seen that the total sensed vibration level, Z, is fed into the inverse controller matrix. This is done to generate a corresponding change in the higher harmonic pitch to alleviate the total sensed vibration. Or,

$$\Delta\Theta^* = -[C]Z_{measured} \qquad (1)$$

The change in higher harmonic pitch necessary to alleviate the sensed vibration is produced by simply changing the sign on the sensed vibration. Note that the $\Delta\Theta^*$ vector has an asterisk superscript to distinguish it as a commanded change in higher harmonic pitch based on an imperfect estimate of the inverse matrix, C.

This approach has been used by previous researchers to implement inverse control by inverting a transfer matrix identified at a particular flight condition. However, the T matrix identified at one flight condition is generally not representative of the T matrix identified at another flight condition. As a result, good control may be achieved at one flight condition, but not at others. Because the T matrix is apparently not constant throughout the flight envelope, it is necessary to identify the local inverse transfer matrix adaptively. Adaptive inverse control, as presented here, thus refers to identifying the locally linear inverse at the current operating conditions. In the next section, the extension of the LMS algorithm to handle the problem of adaptively identifying the local inverse transfer matrix will be discussed.
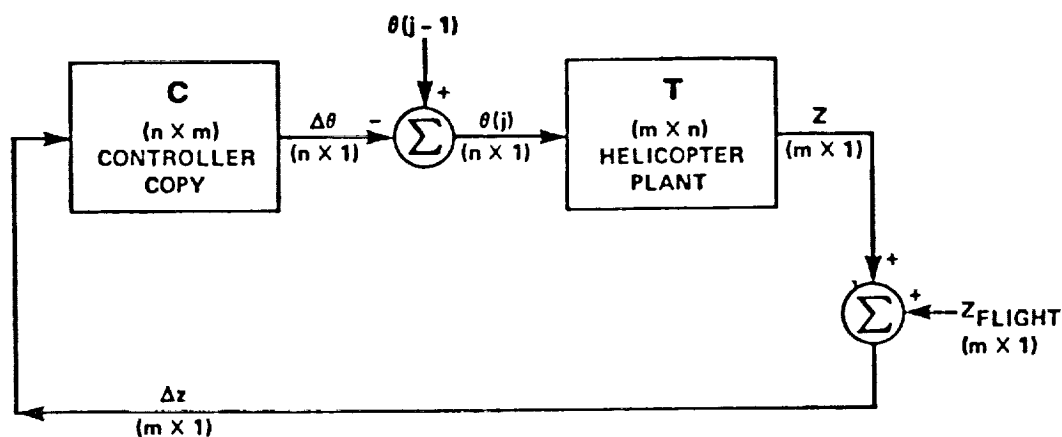
Figure 5: An Inverse Controller, Where C is the Inverse of T.

IV. LMS ADAPTIVE INVERSE CONTROL OF HELICOPTER N/REV VIBRATION

As mentioned previously, it is necessary to adaptively identify the local helicopter transfer function inverse in order for inverse control to work in all flight regimes. In this section, the LMS algorithm is extended to the multiple-input, multiple-output form and applied to the helicopter vibration control problem. The convergence and stability analysis of this formulation will be discussed in the next section.

4.1

FORMATION OF LMS ADAPTIVE INVERSE
IDENTIFICATION ERROR VECTOR

The LMS algorithm has been extended to exploit the differences between the actual and estimated changes in the higher harmonic blade pitch FFT N/Rev coefficients. The estimated change in higher harmonic pitch is computed using the inverse estimate as in equation 1. Hence, these differences may be used to form an error vector which can be used to adaptively identify the inverse transfer matrix. The error vector formation is shown in figure 6. Note that the controller has been placed downstream of the plant for the express purpose of forming this error vector. Referring to figure 6,

$$Adaptation\ Error\ Vector\ = \Delta\Theta - \Delta\Theta^*$$

$$e = \Delta\Theta - [C]\Delta Z$$

$$e = \Delta\Theta - [C][T]\Delta\Theta$$

Here $\Delta\Theta$ is the change in N/Rev blade pitch, which produces a corresponding change in vibration, ΔZ. When this ΔZ is multiplied by the controller matrix, C, the change in blade pitch would be reproduced exactly, if C were the exact inverse of T. However, this calculated change in pitch is usually not quite the same as the original change in blade pitch due to identification errors in the inverse matrix, C.
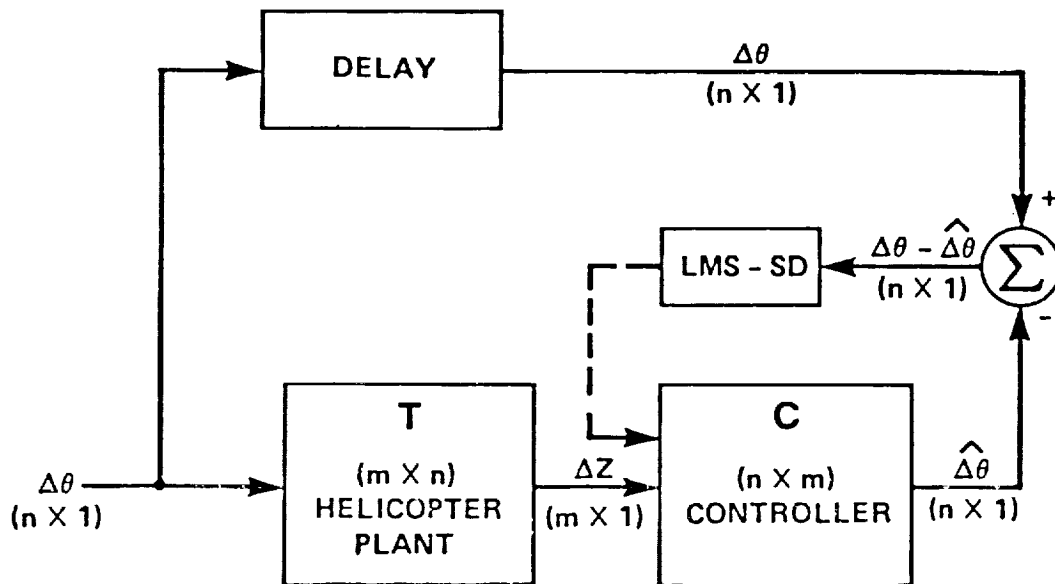
Figure 6: Formation of the Adaptation Error Vector Used by the Extended LMS Algorithm to Identify and Track the Inverse Matrix, C.

22

TRACKING THE INVERSE ESTIMATE
WITH THE EXTENDED LMS ALGORITHM

The extended LMS algorithm is an iterative technique which uses the method of steepest descent to update the estimate of the inverse plant transfer function. The form of the equations presented here basically follows and extends the single-input, single-output LMS algorithm work of Widrow and Hoff. The stability gain term has been made into a diagonal matrix, as has the gradient, in order to extend the LMS algorithm to solve the multiple-input, multiple-output vibration control problem.

The extended LMS algorithm identifies and tracks the local inverse transfer function by making corrections to the inverse estimate which are proportional to the gradient of the error vector squared, with respect to the inverse matrix elements. In steepest descent form, the equation for updating the estimate of the inverse may be written as:

$$C(k+1) = C(k) - K_s \left(\frac{\partial e^2}{\partial C(k)} \right) \tag{2}$$

To understand the form of the equation, it is helpful to think about correcting only one value of the inverse matrix. If the square of the error of element $C_{i,j}$ is plotted as a function of the $C_{i,j}$ estimate, a plot such as that shown in figure 7 may be made. For this case, the gradient has degenerated to the slope of the error squared line. It is seen that for two successive estimates of $C_{i,j}$, that if the square error increases with increases in $C_{i,j}$, then the update to correct the

estimate must be negative. This is why the correction term is preceded by a minus sign in equation 2. K_s is a gain term which governs the amount of correction to be made. If K_s is made too large, convergence to the minimum may not occur.

Identification
Error
in
C_{ij}

.. Error(k+1)

.... Error(k)

(correction k+2)

C_{ij}
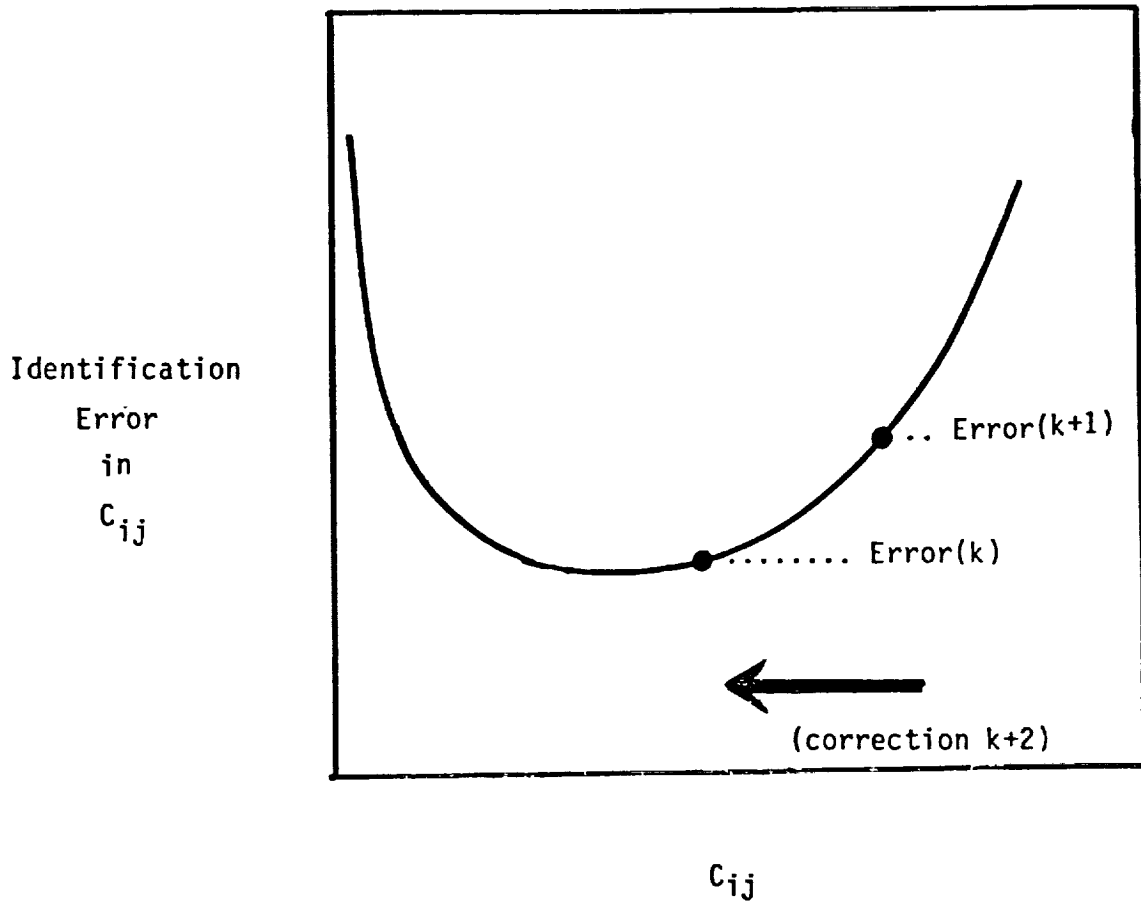
Figure 7:   Steepest Descent Approach for Estimation of only one
parameter, C_{ij} .

The extension of the LMS algorithm to the n dimensional case is made by finding an estimate of the error vector squared with respect to the current value of the inverse estimate. An estimate is needed for the gradient of the square error, or,

$$\frac{\partial e^2}{\partial C(k)}$$

where the error vector squared has been defined as

$$e^2 = [e_1^2, e_2^2, e_3^2, .., e_n^2]$$

By defining the error vector in this fashion, an error is associated with each row of the inverse estimate. Hence for each row i of the inverse C matrix, the square error may be expressed as,

$$e_i^2 = (e_i)(e_i^T)$$

$$e_i^2 = (\Delta\Theta_i - C_i^T \Delta Z^T)(\Delta\Theta_i - \Delta Z C_i)$$

$$e_i^2 = (\Delta\Theta_i \Delta\Theta_i - \Delta\Theta_i \Delta Z C_i - C_i^T \Delta Z^T \Delta\Theta_i + C_i^T \Delta Z^T \Delta Z C_i) \qquad (3)$$

where e_i is the scalar error term associated with the ith row of the inverse matrix, C_i^T. Note that ΔZ^T is a column vector, and that $\Delta\Theta_i$ is a scalar.

An approximation of the gradient of the error squared for the ith row may then be found by differentiating the ith error squared (equation 3) with respect to the ith row of the C matrix, C^T, as follows:

$$\frac{\partial e_i^2}{\partial C_i^T} = -\Delta Z^T \Delta\Theta_i - \Delta Z^T \Delta\Theta_i + \Delta Z^T \Delta Z C_i + \Delta Z^T \Delta Z C_i$$

$$= -2\Delta Z^T \Delta\Theta_i + 2\Delta Z^T \Delta Z C_i$$

$$= -2\Delta Z^T(\Delta\Theta_i - \Delta Z C_i)$$

and thus,

$$\frac{\partial e_i^2}{\partial C_i^T} = -2\Delta Z(\Delta\Theta_i - C_i^T \Delta Z^T) \qquad (4)$$

This expression is used by the extended LMS algorithm as an estimate of the gradient of the square error for the ith row of the inverse matrix. It is an approximation because it does not account for measurement errors in Z, or identification errors in C.

Using the row error squared gradient estimate provided by Equation 4, in the steepest descent equation 2, the extended LMS inverse update equation is formed:

$$C_i^T(k+1) = C_i^T(k) + 2k_i\Delta Z(k)(\Delta\Theta_i(k) - C_i^T(k)\Delta Z^T(k)) \qquad (5)$$

It is this equation that adaptively identifies and tracks the estimate of the inverse matrix. It has been presented in a row by row fashion to assist the reader in seeing that it applies to square and nonsquare plant transfer matrices alike.

ADAPTIVE INVERSE CONTROL OF HELICOPTER VIBRATION

When the controller update equation (5) is combined with the inverse control law (1), the adaptive inverse control scheme is realized. These two relations form the estimator and controller of the adaptive inverse regulator:

$$C_i^T(k+1) = C_i^T(k) + 2k_i \Delta Z(k)(\Delta \Theta_i(k) - C_i^T(k)\Delta Z^T(k))$$

as the inverse estimate update equation, and

$$\Theta(k+1) = \Theta(k) + \Delta \Theta^*$$

or,

$$\Theta(k+1) = \Theta(k) - K_{CR}C(k)Z_{measured}$$

for the inverse control law. Here, K_{CR} is a gain chosen between zero and one. It is termed the *controlrelaxation* constant, and is useful in modifying the convergence characteristics of the extended LMS algorithm.

These feedback loops are shown in figure 8. Note that the inverse matrix, C, has been shown in two places for conceptual purposes. In the top loop, the C (inverse) matrix has been placed downstream of the T transfer matrix (helicopter) for the purpose of generating the extended LMS error vector. The $LMS - SD$ box represents the extended LMS estimator, which uses the error vector information to track and identify the inverse matrix, C. The bottom loop shows another C matrix placed upstream of the helicopter

to serve as the controller matrix for the inverse control law. In actual implementation, though, only one inverse (C) matrix would be held in computer memory.
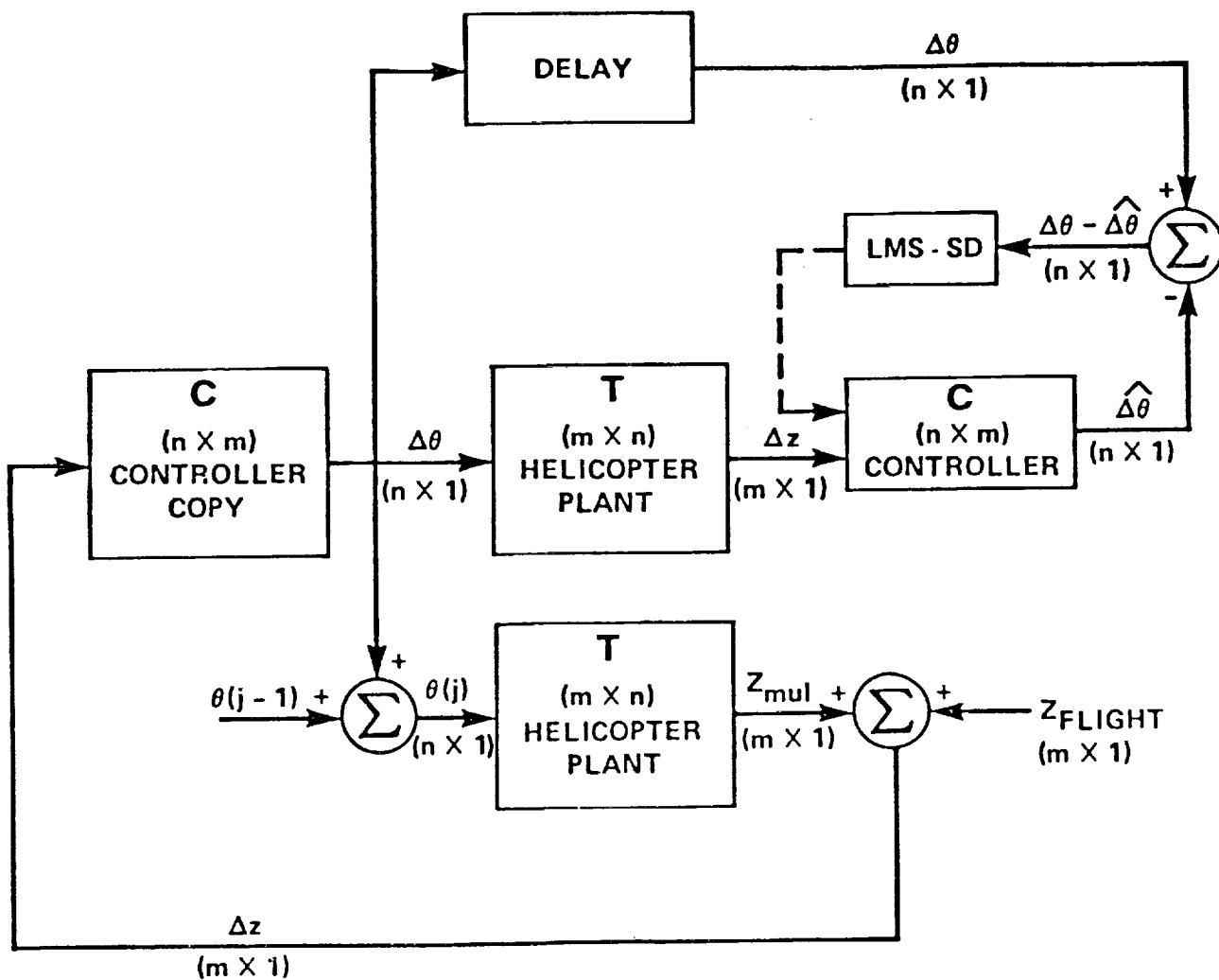
Figure 8 :   Adaptive Inverse Regulator, Combining Extended LMS Estimator with the Inverse Control Law.

From figure 8, the adaptive inverse control technique sequence of events can be seen. First, a change in the higher harmonic pitch vector, $\Delta\Theta$ is fed into the helicopter. This should produce a change in the measured vibration vector, ΔZ. If this change in N/Rev vibration is postmultiplied into the inverse estimate matrix, the original change in higher harmonic pitch should be produced, provided C is the inverse of T, in the least squares sense. The original ($\Delta\Theta$) and calculated ($\Delta\Theta^*$) higher harmonic pitch commands are compared, and the error vector for the extended LMS algorithm is generated. The extended LMS algorithm is then applied to update the estimate of the inverse matrix. After the updated inverse estimate is obtained, the *total* sensed vibration vector, $Z_{measured}$, is postmultiplied into the inverse estimate. This should then form the negative of the change in higher harmonic pitch necessary to alleviate the measured vibration. The new control is applied to the rotor, and the cycle repeated.

The question of how the adaptive inverse control technique should be started will be addressed in the next section, after some analysis of the method has been presented.

V. ANALYSIS OF ADAPTIVE INVERSE CONTROL

Analysis of the adaptive inverse control technique is centered on the identification characteristics of the extended LMS algorithm. The reason for this is that if convergence to the inverse can be achieved, then the inverse control law (by definition) will reduce the vibration, providing the control authority is not exceeded. Hence, aside from selecting the amount of control relaxation, the extended LMS algorithm convergence characteristics are governed by the selection of K_s. It is shown that the stability ranges for the elements of K_s are, in part, determined by the eigenvalues of the signal information matrix. The eigenvalues of the signal information matrix will, in turn, be related to the dynamics of the helicopter. Lastly, the learning characteristics of the algorithm are discussed as functions of the starting estimate of the inverse, and the elements of K_s.

CONDITIONS FOR CONVERGENCE TO THE INVERSE

The analysis of the multiple-input, multiple-output adaptive inverse control technique presented here involves determining the stability properties of the extended LMS estimator. In this section, considerations governing the selection of the K_s elements will be discussed. The learning properties associated with the extended LMS algorithm convergence characteristics will be discussed in the next section.

Analysis of the stability properties of the extended LMS estimator proceeds with the controller update equation for the ith row of the controller matrix:

$$C_i^T(k+1) = C_i^T(k) + 2(k_i)\Delta Z(\Delta\Theta_i - C_i^T(k)\Delta Z^T)$$

Recalling that

$$C_i^T(k)\Delta Z^T = (row)(col) = scalar,$$

the above equation may be written as,

$$C_i^T(k+1) = C_i^T(k) + 2(k_i)\Delta Z\Delta\Theta_i - 2(k_i)C_i^T(k)\Delta Z^T\Delta Z$$

Then taking the expected value of both sides,

$$E[C_i^T(k+1)] = E[C_i^T(k)] + 2(k_i)E[\Delta Z\Delta\Theta_i] - 2(k_i)E[C_i^T(k)]E[\Delta Z^T\Delta Z]$$

Defining

$$E[\Delta Z\Delta\Theta_i] = S_{z,\theta}$$

and,

$$E[\Delta Z^T \Delta Z] = S_{z,z}$$

the equation may be rewritten as

$$E[C_i^T(k+1)] = E[C_i^T(k)] + 2(k_i)S_{z,\theta} - 2(k_i)E[C_i^T(k)]S_{z,z}$$

Or,

$$E[C_i^T(k+1)] = E[C_i^T(k)][I - S_{z,z}2k_i] + 2k_i S_{z,\theta}$$

From this equation it can be seen that as long as the eigenvalues of

$$[I - S_{z,z}2k_i]$$

are less than 1, the algorithm is stable. Alternatively, it is possible to decompose the signal information matrix into modal form by letting

$$S_{z,z} = R^{-1}\Lambda R$$

where R is a matrix whose columns are the eigenvectors of $S_{z,z}$, and Λ is a diagonal matrix, whose elements are the eigenvalues of the $S_{z,z}$ matrix.

Hence for stable convergence, it is necessary to select the elements of the stability gain matrix, k_i, so that the eigenvalues of,

$$[I - S_{z,z}2k_i] \quad \text{are} \quad < 1$$

Thus, the stability range for the K_s gain elements are

$$0 < k_i < \frac{1}{\lambda_{max}}$$

where λ_{max} is the largest eigenvalue of the signal information matrix.

The signal information matrix is almost a diagonal matrix, so the upper limit specified by $\frac{1}{\lambda_{max}}$ may be replaced by roughly $\frac{1}{signal..power}$ of the largest mean signal of the measurement vector.

In the simulations, the effect of varying K_s is studied. Values of K_s near $\frac{1}{\lambda_{max}}$ will adapt rapidly, but will be more prone to tracking random noise after "convergence" has been achieved, and will tend to oscillate about the correct solution. A good value of K_s is one which results in convergence at a sufficiently rapid rate, yet does not track noise signals too closely.

The stability bound on K_s predicted by $\frac{1}{\lambda_{max}}$ is really not a known quantity, since the signal information matrix is, in general, not known. From

$$E[\Delta Z^T \Delta Z] = E[(T\Delta\Theta)^T(T\Delta\Theta)]$$

it is seen that the signal information matrix depends upon the local transfer matrix, T, as well as the applied multicyclic pitch control, $\Delta\Theta$, and any control relaxation used. Hence, the actual values for the K_s elements which allow for sufficiently fast and stable inverse identification must be found with some trial and error. The (6 x 6) simulation results will make this point clear, when the effects of control relaxation are examined.

CONVERGENCE PROPERTIES OF THE EXTENDED LMS ESTIMATOR

In the preceding section, the values of K_s which lead to stable convergence to an inverse estimate were found. In this section more is said about the solution to which the algorithm converges, and how fast it does so. By analyzing the controller update equation in modal form, it is possible to describe the convergence process in terms of *learning curve modes*, as that done for single-input, single-output systems by Widrow (1970).

Recall from the last section that for row i of the inverse update equation that

$$E[C_i^T(k+1)] = E[C_i^T(k)][I - S_{z,z}2k_i] + 2k_iS_{z,\theta}$$

To study the convergence and learning properties, it is necessary to express the effect of initial conditions on the inverse, as well as the value of the stability gain matrix, K_s. Letting $C(0)$ denote the initial estimate of the inverse, and

$$A = [I - S_{z,z}2k_i]$$
$$B = 2k_iS_{z,\theta}$$

Then,

$$E[C_i^T(1)] = E[C_i^T(0)][A] + B$$

$$E[C_i^T(2)] = E[C_i^T(1)][A] + B$$

$$E[C_i^T(3)] = E[C_i^T(2)][A] + B$$

$$E[C_i^T(n+1)] = E[C_i^T(n)][A] + B$$

And by substitution, a relationship between the initial inverse estimate, the stability gain matrix, and convergence may be derived.

$$E[C_i^T(3)] = (E[C_i^T(1)][A] + B)[A] + B$$
$$E[C_i^T(3)] = ((C_i^T(0)[A] + B) + B)[A] + B$$
$$E[C_i^T(3)] = (C_i^T(0)[A]^2 + BA + B)[A] + B$$
$$E[C_i^T(3)] = C_i^T(0)[A]^3 + B[A]^2 + B[A] + B$$
$$E[C_i^T(3)] = C_i^T(0)[A]^3 + \sum_{n=0}^{2} B[A]^n$$

Or, generalizing this expression,

$$E[C_i^T(k+1)] = C_i^T(0)[A]^{k+1} + \sum_{n=0}^{k} B[A]^n$$

And resubstituting for A and B,

$$E[C_i^T(k+1)] = C_i^T(0)[I - S_{z,z} 2k_i]^{k+1} + \sum_{n=0}^{k} 2k_i S_{z,\theta}[I - S_{z,z}k_i]^n \quad (6)$$

The assumption is now made that the K_s elements have been selected small enough so that the diagonal elements of the $[I - S_{z,z}2k_i]$ matrix are all less than one. Then as j approaches infinity, the first term of equation 6 will go to zero.

To see that the second term will converge, in the limit, to the same estimate as that found by the least square error method, it is necessary to place the second term in modal form. This is done by letting

$$S_{z,z} = R^{-1}\Lambda R$$

35

where R is a matrix whose columns are the eigenvectors of $S_{z,z}$, and Λ is a diagonal matrix, whose elements are the eigenvalues of the $S_{z,z}$ matrix. Rewriting the second term of equation 6 with this nomenclature, and recalling that the first term went to zero,

$$E[C_i^T(k+1)] = \sum_{n=0}^{k} 2k_i S_{z,\theta}[I - R^{-1}\Lambda R]^n$$

$$= 2k_i \sum_{n=0}^{k} S_{z,\theta}[I - R^{-1}\Lambda R]^n$$

and thus for each row,

$$E[C_i^T(k+1)] = 2k_i R^{-1} \sum_{n=0}^{k} (1 - 2k_i\lambda_i)^n RS_{z,\theta}$$

$$= 2k_i R^{-1}(\frac{1}{1-(1-2k_i\lambda_i)})RS_{z,\theta}$$

$$= 2k_i R^{-1}(\frac{1}{2k_i\lambda_i})RS_{z,\theta}$$

$$= R^{-1}\Lambda^{-1}RS_{z,\theta}$$

$$= S_{z,z}^{-1}S_{z,\theta}$$

$$= E[\Delta Z^T \Delta Z]^{-1}E[\Delta Z \Delta \Theta_i]$$

which is the same as that found by ordinary least squares, because if

$$\Delta \Theta_i = C_i^T \Delta Z^T$$

36

where C_i^T is the ith row of the inverse matrix, then

$$e_i^2 = (e_i)(e_i^T)$$

$$e_i^2 = (\Delta\Theta_i - C_i^T\Delta Z^T)(\Delta\Theta_i - \Delta Z C_i)$$

and,

$$\frac{\partial e^2}{\partial C_i^T} = (\Delta\Theta_i\Delta\Theta_i - \Delta\Theta_i\Delta Z^T - \Delta\Theta_i\Delta Z^T + 2\Delta Z\Delta Z^T C_i)$$

$$= -2\Delta\Theta_i\Delta Z^T + 2\Delta Z\Delta Z^T C_i$$

Setting the partial derivative equal to zero, the normal equations,

$$\Delta\Theta_i\Delta Z^T = \Delta Z\Delta Z^T C_i$$

are found, and hence,

$$C_i = [\Delta Z\Delta Z^T]^{-1}\Delta\Theta_i\Delta Z^T$$

Taking expectations,

$$E[C_i] = E[\Delta Z^T\Delta Z]^{-1}E[\Delta Z\Delta\Theta_i]$$

which is in exact agreement with the expected estimate of the extended LMS steepest descent approach. Hence, the extended LMS algorithm converges to the correct estimate of the inverse in the least squares sense.

The modal analysis also permits the rate of convergence to be expressed in terms of normal modes. That is, for an n dimensional matrix,

n geometric modes may be associated with the eigenvalues of the signal information matrix $S_{z,z}$. Letting p_i denote the geometric ratio of the ith mode,

$$p_i = (1 + 2k_i\lambda_i)$$

and assuming an exponential decay, it is possible to associate an adaptation or learning curve time constant, τ_i, with this mode. Hence,

$$p_i = \exp\frac{-1}{\tau_i}$$

or

$$p_i = 1 - \frac{1}{\tau_i} + \frac{1}{(2\tau_i\tau_i)} - \cdot\cdot$$

And equating these two expressions, an approximate learning curve time constant for the ith mode may be expressed as

$$\tau_i = \frac{1}{2k_i\lambda_i}$$

The exponential decay associated with this adaptation time constant is designated as the "learning curve" for the ith normal mode. If all eigenvalues of $S_{z,z}$ were the same, a single learning curve could be defined for the entire inverse matrix. In the more general case, however, the eigenvalues will not be equal. Then the overall learning curve will be a function of all of the eigenvalues corresponding to the various normal modes. It is expected that the faster modes will therefore produce rapid initial learning, whereas the slower modes will govern final convergence, since they will take longer to die out.

38

STARTING ADAPTIVE INVERSE CONTROL

A method for iteratively correcting the estimate of the helicopter inverse transfer matrix has been presented without regard as to how the algorithm should be started. That is, the initial conditions on the inverse matrix need to be specified.

The effect of the initial estimate of the $C_i^T(0)$ matrix was seen to be negligible as the number of iterations approached infinity, since the first term in equation 6,

$$C_i^T(0)[I - S_{z,z}o2K_s]^{j+1}$$

approached zero in the limit. However, the choice of the intial $C(0)$ matrix is important if the transient behavior is to be considered.

One method of selecting a starting estimate for the inverse would be to apply an off-line least square estimation algorithm to some input and output data taken near the expected mean operating condition. The identified matrix could then be used as the initial estimate for the $C(0)$ matrix. This approach, however, has the significant drawback that each helicopter has a slightly different flight regime, which requires a different starting estimate. Futhermore, it would make a difference whether the vibration control algorithm was started on the ground, in hover, or in a variety of forward flight conditions.

A more comprehensive method, although more complex to implement, involves determining the starting estimate during initial flight. In this ap-

proach, an initial identification phase, termed the *learning phase*, would be used to identify the starting inverse estimate in an open-loop fashion. During the learning phase, the blade pitch could be given small perturbations in higher harmonic pitch, and the corresponding small changes in vibration could be sensed. These measurements could then be used by the extended LMS adaptive inverse control algorithm to correct an initial coarse estimate of the inverse matrix, obtained from some off-line technique. No vibration control commands would be generated during the learning phase, to avoid large transients in control resulting from a poorly identified inverse.

The learning phase would be terminated and the closed-loop operation begun when the inverse estimate was then "close enough" for adaptive inverse control. This end point would be established when the sum of the squares of the adaptation errors, $\Delta\Theta_i - \Delta\Theta_i^*$, were deemed small enough. At this point, the learning signal would be discontinued, and the adaptive inverse control loop would be closed. The LMS algorithm would then update the estimate of the helicopter inverse transfer matrix to keep up with changes in the helicopter operating environment.

VI. DISCUSSION OF SIMULATION RESULTS

In order to explore and test the extended LMS adaptive inverse control method, two basic types of simulation studies were performed. The first study used a (3 x 3) matrix to represent the helicopter transfer function, whereas the second simulation runs used a (6 x 6) matrix. The (3 x 3) matrix was useful, in that, the low order matrix made it easy to examine the convergence properties of the extended LMS algorithm. The (6 x 6) matrix, on the other hand, was useful in simulating more realistic control effects such as scaling and noise rejection capability. Although both simulations involved square plant transfer matrices, this is not a requirement of the algorithm, since identification of the inverse transfer matrix is done in a row by row fashion. Square matrices were selected only because they facilitated calculation of the true inverse.

The simulation studies model the harmonic vibration-pitch dynamics as a linear relationship:

$$Z = [T]\Theta + Z_0$$

where Z is the vector of N/Rev vibration Fourier coefficients, Θ is the vector of the Fourier coefficients of cyclic pitch control, and Z_0 represents the vector of the uncontrolled vibration coefficients. The values for the (3 x 3) T matrix were selected so that the matrix would be symmetric and well conditioned. This was done to avoid mixing the extended LMS algorithm convergence characteristics with those characteristics associated with a transfer

matrix having bad numerical properties. The transfer matrix was represented
as,

$$
T = \begin{bmatrix} 2.0 & 1.0 & 0.0 \\ 1.0 & 3.0 & 1.0 \\ 0.0 & 1.0 & 2.0 \end{bmatrix}
$$

and the uncontrolled vibration harmonics were constant,

$$
Z_0 = \begin{bmatrix} 1.0 \\ 1.0 \\ 1.0 \end{bmatrix}
$$

The matrix used to represent the (6 x 6) transfer matrix will be presented later.
The (3 x 3) simulation runs were divided into two phases. In the first phase, the
LMS inverse identification, starting from an initial estimate, was accomplished by
introducing perturbations in the cyclic pitch vector, and measuring the associated
changes in the uncontrolled vibration harmonics. This phase of the adaptive in-
verse control scheme was referred to as the *Learning Phase*, to distinguish it
from the *Control Phase* which began when the inverse control loop was closed.
The (6 x 6) simulation runs, however, studied only the control phase, beginning
with some initial estimate of the inverse. This was done to avoid duplicating
learning phase results seen in the (3 x 3) simulation, and also to permit a more
thorough investigation of control phase problems, such as the effects of measure-
ment noise.

42

In most cases, the figures consist of three parts. Part A presents the inverse identification error and vibration level as a function of the iteration number. The top plot displays the three (or six) uncontrolled vibration levels responding from three (or six) sinusoidal pitch inputs, and the bottom graph displays the amount of identification error in the identified inverse over 100 iterations. After iteration 100, the control loop is closed and the inverse control of the vibration is begun. For all steps (1 - 200), the identification error was found by subtracting the known true inverse from the identified inverse, squaring the resulting elements, and adding them all together to form a scalar index for plotting purposes. It should be noted that for the (3 x 3) T matrix, the vibration signals produced were imaginary, since the transfer matrix was not derived from actual flight data. Part B of the figures lists a digital representation of the identification and vibration data. This is useful in cases where it is necessary to distinguish if the graphical results indicate convergence or very slow divergence from a given flat region on the graph. Part C gives the identified, true, and initial inverse estimate. This detailed breakdown makes the simulation results discussion lengthy, but comprehensive. In most cases, though, the reader may skip over the digital form of the results (i.e., parts B and C) without significant loss of content.

IDENTIFICATION OF THE INVERSE MATRIX
WITH ARBITRARY INITIAL CONDITIONS

One of the nice properties of the extended LMS algorithm is that it is theoretically capable of identifying its own initial conditions prior to closed-loop control. That is, it is possible to start from some arbitrary initial estimate of the inverse, and correct that estimate through open-loop perturbations in pitch control until it becomes close enough to the true inverse for use with the inverse control law.

The following set of figures present the simulation results from the (3 x 3) simulation. To simulate convergence (learning) properties during the learning phase, the initial estimate of the inverse matrix was all zero. The diagonal elements of K_s were then varied from 0.01 (Figure 9) to 0.47 (Figure 17). For simplicity of simulation, all elements of the diagonal K_s matrix were chosen to be the same, and the off-diagonal terms were zero. The results are presented in order of increasing K_s values, as summarized by Table 1. When viewing the figures, note the relationship between the magnitude of the stability gain matrix diagonal elements and the inverse identification convergence pattern. (Figure 18, page 69, presents a quick examination of this relationship.)

TABLE 1

Training Phase Runs for the (3x3) Simulation

K_S Stability Vector	Figure
0.01	10 A, B, C
0.10	11 A, B, C
0.15	12 A, B, C
0.20	13 A, B, C
0.30	14 A, B, C
0.35	15 A
0.40	16 A
0.45	17 A, C
0.47	18 A, B, C
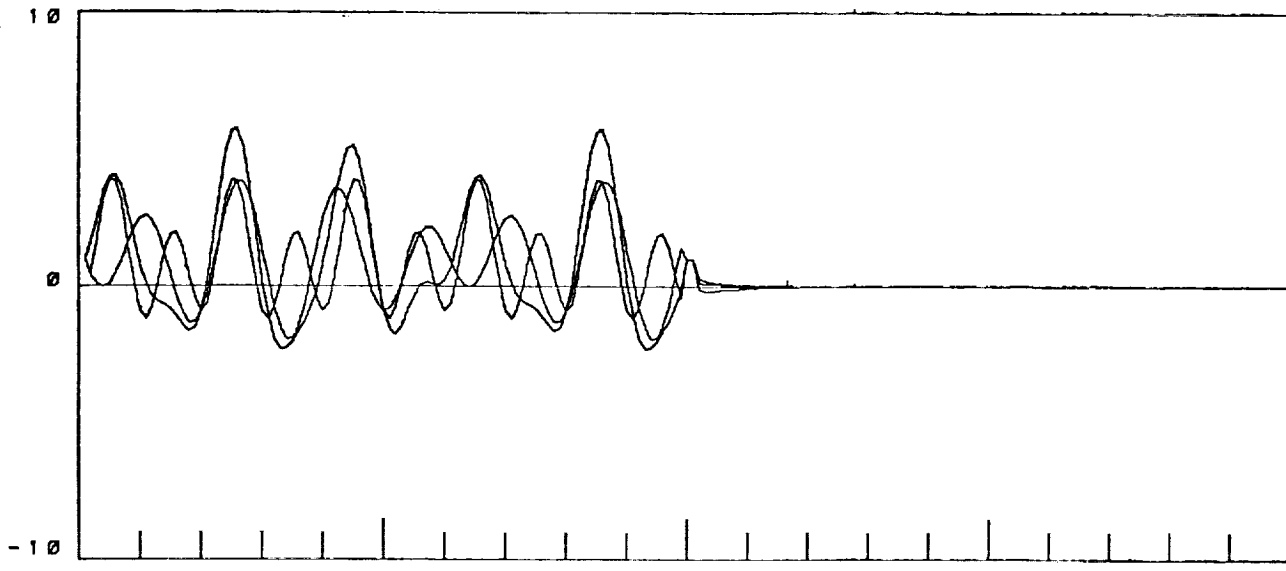
S E N S E D   V I B R A T I O N
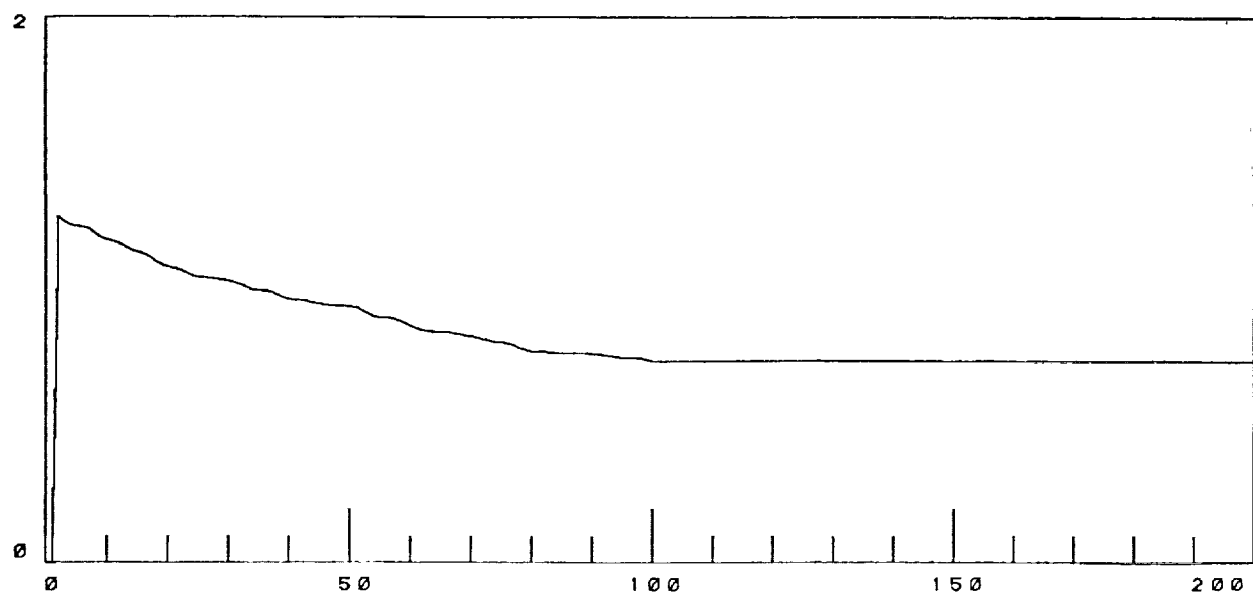
I N V E R S E   I D E N T I F I C A T I O N   E R R O R S

├────── LEARNING   PHASE ──────┼────── CONTROL   PHASE ──────┤

GAIN VECTOR: 0.0100   0.0100   0.0100
CONTROL RELAX:
        1.0000

Figure 9A   Learning Curve with Ks Diagonals = 0.01 for the (3 x 3)
Simulation (Note Learning and Control Phases).

ITERATION	I.D. ERROR	VIBRATION
1	0.00000	0.00000
2	1.27157	2.41634
3	1.25327	4.44880
4	1.24013	6.60944
5	1.23575	7.99706
6	1.23399	8.37584
7	1.22527	7.58645
8	1.20869	5.93930
9	1.19360	4.00408
10	1.18571	4.17732
15	1.14068	3.16234
20	1.08713	2.72247
25	1.04795	13.06231
30	1.03363	2.60947
35	0.99894	5.80914
40	0.96564	4.13753
45	0.95062	11.49648
50	0.94018	2.66334
55	0.89991	3.68004
60	0.86896	2.58204
65	0.84757	7.96703
70	0.83019	4.17401
75	0.80878	3.16856
80	0.77829	2.76308
85	0.76989	13.01733
90	0.76765	2.66917
95	0.75463	5.81383
100	0.74012	3.00000
105	0.73976	0.35476
110	0.73968	0.15914
115	0.73967	0.07123
120	0.73966	0.03188
125	0.73966	0.01427
130	0.73966	0.00639
135	0.73966	0.00286
140	0.73966	0.00128
145	0.73966	0.00057
150	0.73966	0.00026
155	0.73966	0.00011
160	0.73966	0.00005
165	0.73966	0.00002
170	0.73966	0.00001
175	0.73966	0.00000
180	0.73966	0.00000
185	0.73966	0.00000
190	0.73966	0.00000
195	073966	0.00000
200	0.73966	0.00000

Figure 9B   Identification Errors and Vibration Level,
Ks Diagonals = 0.01.

47

THE IDENTIFIED INVERSE

```
 0.2285      0.0532     -0.0325
 0.0267      0.1529     -0.0091
-0.0640      0.0629      0.3476
```

THE TRUE INVERSE

```
 0.6250     -0.2500      0.1250
-0.2500      0.5000     -0.2500
 0.1250     -0.2500      0.6250
```

INVERSE INITIAL ESTIMATE

```
 0.0000      0.0000      0.0000
 0.0000      0.0000      0.0000
 0.0000      0.0000      0.0000
```

Figure 9C   Identified, True, and Initial (3 x 3) Inverse Estimate,
Ks Diagonals = 0.01.
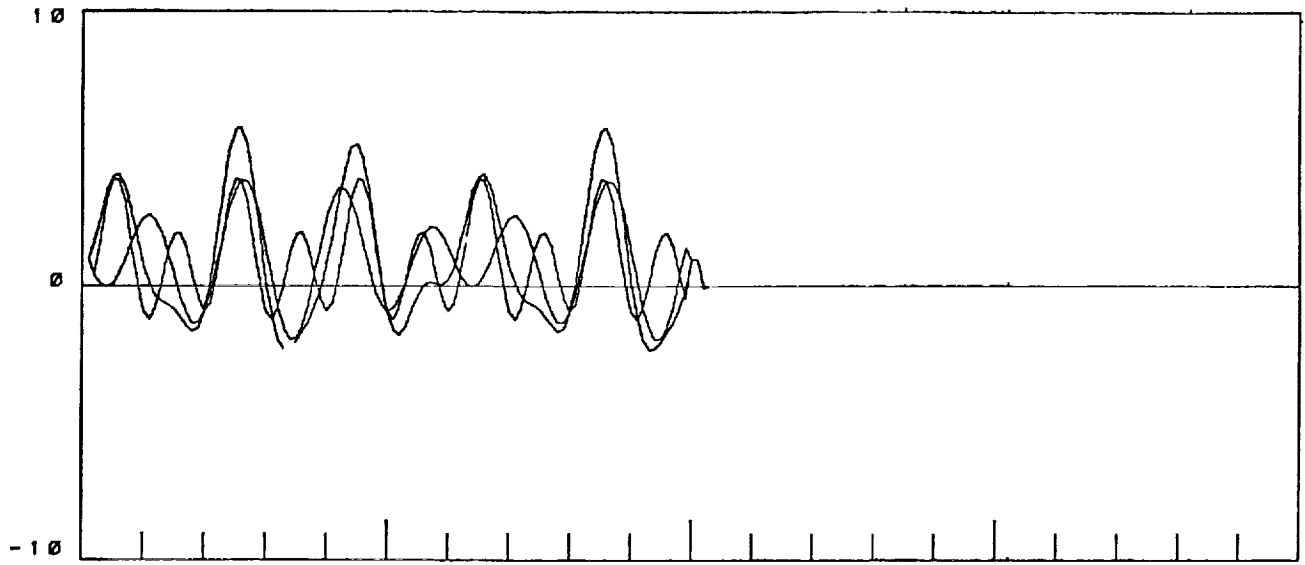
SENSED VIBRATION
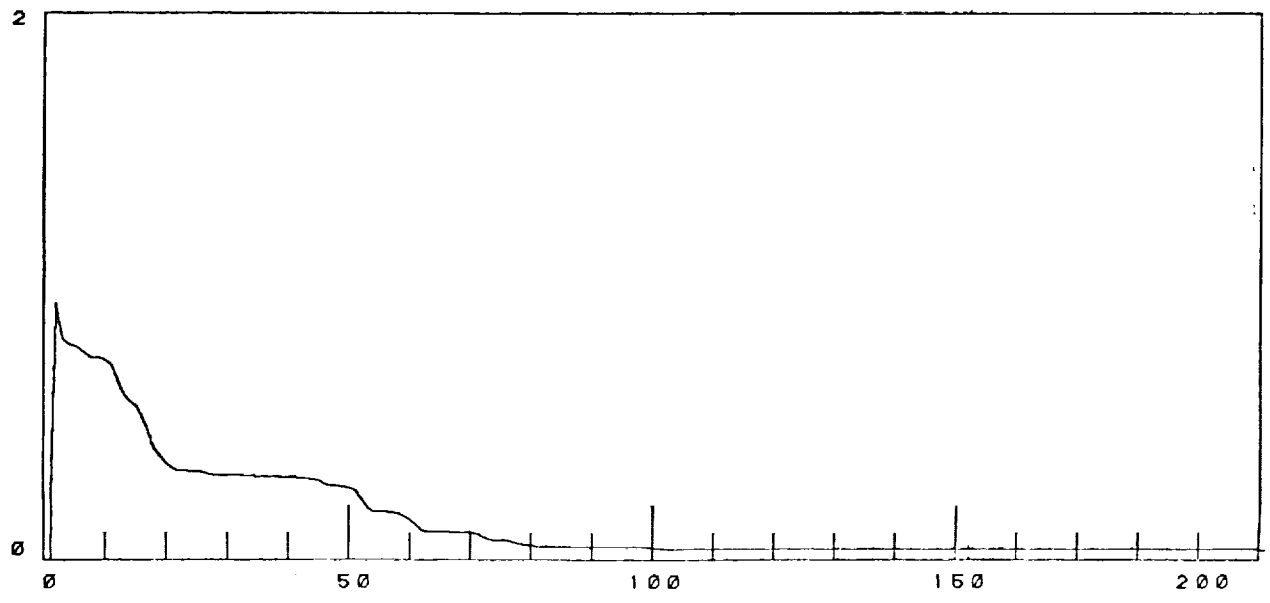
INVERSE IDENTIFICATIO I ERRORS

|——— LEARNING PHASE ———|——— CONTROL PHASE ———|

```
GAIN VECTOR:    0.1000   0.1000   0.1000
CONTROL RELAX:
      1.0000
```

Figure 10A   Learning Curve with Ks Diagonals = 0.1 for (3 x 3) Simulation
(Note Learning and Control Phases).

49

ITERATION	I.D. ERROR	VIBRATION
1	0.00000	0.00000
2	0.94165	2.41634
3	0.80996	4.44880
4	0.79122	6.60944
5	0.78467	7.99706
6	0.77161	8.37584
7	0.75002	7.58645
8	0.74004	5.93930
9	0.73857	4.00408
10	0.73354	4.17732
15	0.56770	3.16234
20	0.36151	2.72247
25	0.32730	13.06231
30	0.31325	2.60947
35	0.30758	5.80914
40	0.30427	4.13753
45	0.29251	11.49648
50	0.26803	2.66334
55	0.17646	3.68004
60	0.14742	2.58204
65	0.10206	7.96703
70	0.09967	4.17401
75	0.07356	3.16856
80	0.05246	2.76308
85	0.04967	13.01733
90	0.04787	2.66917
95	0.04693	5.81383
100	0.04398	3.00000
105	0.04023	0.00180
110	0.04023	0.00000
115	0.04023	0.00000
120	0.04023	0.00000
125	0.04023	0.00000
130	0.04023	0.00000
135	0.04023	0.00000
140	0.04023	0.00000
145	0.04023	0.00000
150	0.04023	0.00000
155	0.04023	0.00000
160	0.04023	0.00000
165	0.04023	0.00000
170	0.04023	0.00000
175	0.04023	0.00000
180	0.04023	0.00000
185	0.04023	0.00000
190	0.04023	0.00000
195	0.04023	0.00000
200	0.04023	0.00000

Figure 10B   Identification Errors and Vibration Level,
Ks Diagonals = 0.1.

50

THE IDENTIFIED INVERSE

```
   0.5563     -0.1683      0.0701
  -0.1833      0.4208     -0.1968
   0.0615     -0.1746      0.5743
```

THE TRUE INVERSE

```
   0.6250     -0.2500      0.1250
  -0.2500      0.5000     -0.2500
   0.1250     -0.2500      0.6250
```

INVERSE INITIAL ESTIMATE

```
   0.0000      0.0000      0.0000
   0.0000      0.0000      0.0000
   0.0000      0.0000      0.0000
```

Figure 10C   Identified, True, and Initial (3 x 3) Inverse Estimate,
Ks Diagonals = 0.1.

51

S E N S E D   V I B R A T I O N

I N V E R S E   I D E N T I F I C A T I O N   E R R O R S

├──── LEARNING PHASE ────┼──── CONTROL PHASE ────┤

GAIN VECTOR: 0.1500   0.1500   0.1500
CONTROL RELAX:
     1.0000

Figure 11A   Learning Curve with Ks Diagonals = 0.15 for (3 x 3) Simulation
(Note Learning and Control Phases).

ITERATION	I.D. ERROR	VIBRATION
1	0.00000	0.00000
2	0.78830	2.41634
3	0.63340	4.44880
4	0.62889	6.60944
5	0.62253	7.99706
6	0.60563	8.37584
7	0.58197	7.58645
8	0.57736	5.93930
9	0.57640	4.00408
10	0.57222	4.17732
15	0.39067	3.16234
20	0.20213	2.72247
25	0.18107	13.06231
30	0.16763	2.60947
35	0.16670	5.80914
40	0.16378	4.13753
45	0.15573	11.49648
50	0.13704	2.66334
55	0.07512	3.68004
60	0.06048	2.58204
65	0.03505	7.96703
70	0.03456	4.17401
75	0.01909	3.16856
80	0.01306	2.76308
85	0.01137	13.01733
90	0.01057	2.66917
95	0.01050	5.81383
100	0.00935	3.00000
105	0.00795	0.00008
110	0.00795	0.00000
115	0.00795	0.00000
120	0.00795	0.00000
125	0.00795	0.00000
130	0.00795	0.00000
135	0.00795	0.00000
140	0.00795	0.00000
145	0.00795	0.00000
150	0.00795	0.00000
155	0.00795	0.00000
160	0.00795	0.00000
165	0.00795	0.00000
170	0.00795	0.00000
175	0.00795	0.00000
180	0.00795	0.00000
185	000795	0.00000
190	0.00795	0.00000
195	0.00795	0.00000
200	0.00795	0.00000

Figure 11B Identification Errors and Vibration Level,
Ks Diagonals = 0.15.

53

THE IDENTIFIED INVERSE

```
   0.6008      -0.2095       0.1004
  -0.2265       0.4607      -0.2261
   0.1025      -0.2124       0.6021
```

THE TRUE INVERSE

```
   0.6250      -0.2500       0.1250
  -0.2500       0.5000      -0.2500
   0.1250      -0.2500       0.6250
```
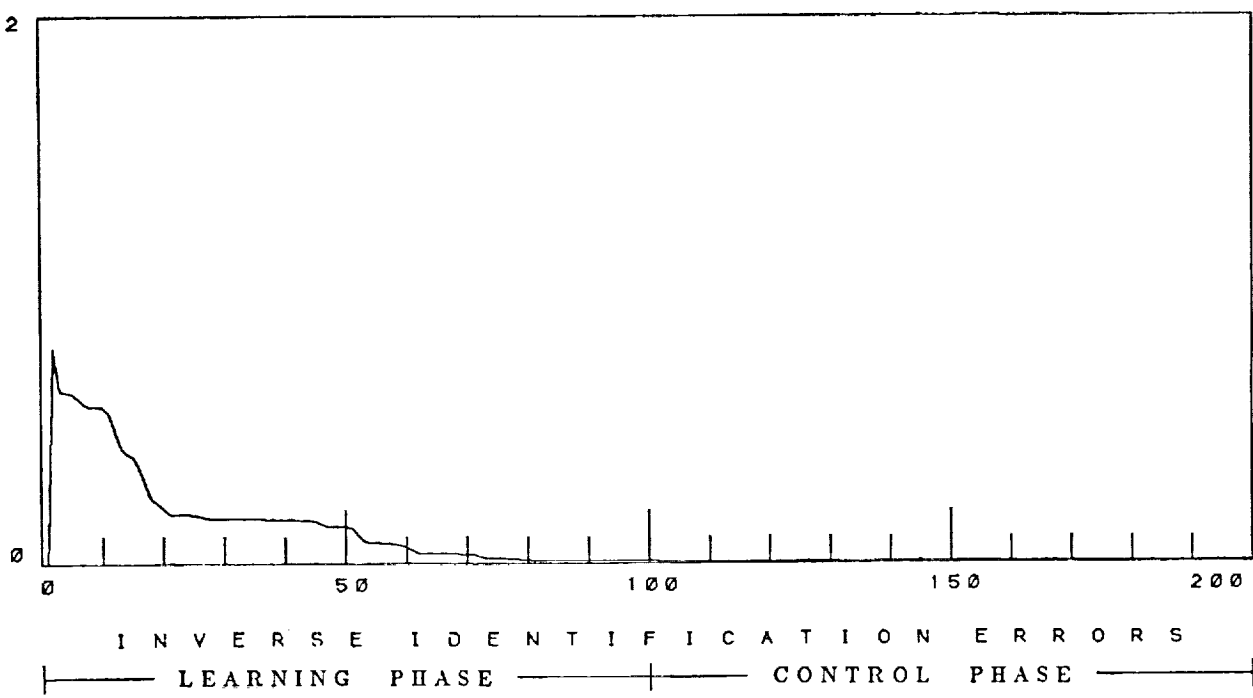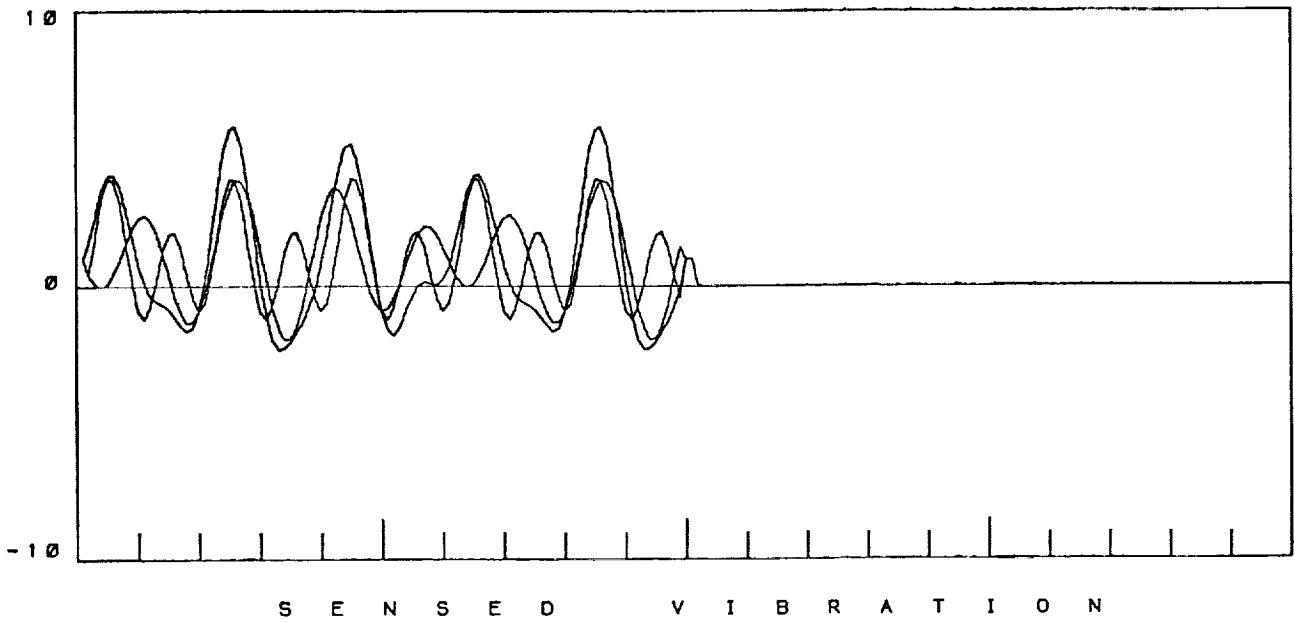
INVERSE INITIAL ESTIMATE

```
   0.0000       0.0000       0.0000
   0.0000       0.0000       0.0000
   0.0000       0.0000       0.0000
```

Figure 11C   Identified, True, and Initial (3 x 3) Inverse Estimate,
Ks Diagonals = 0.15.

54
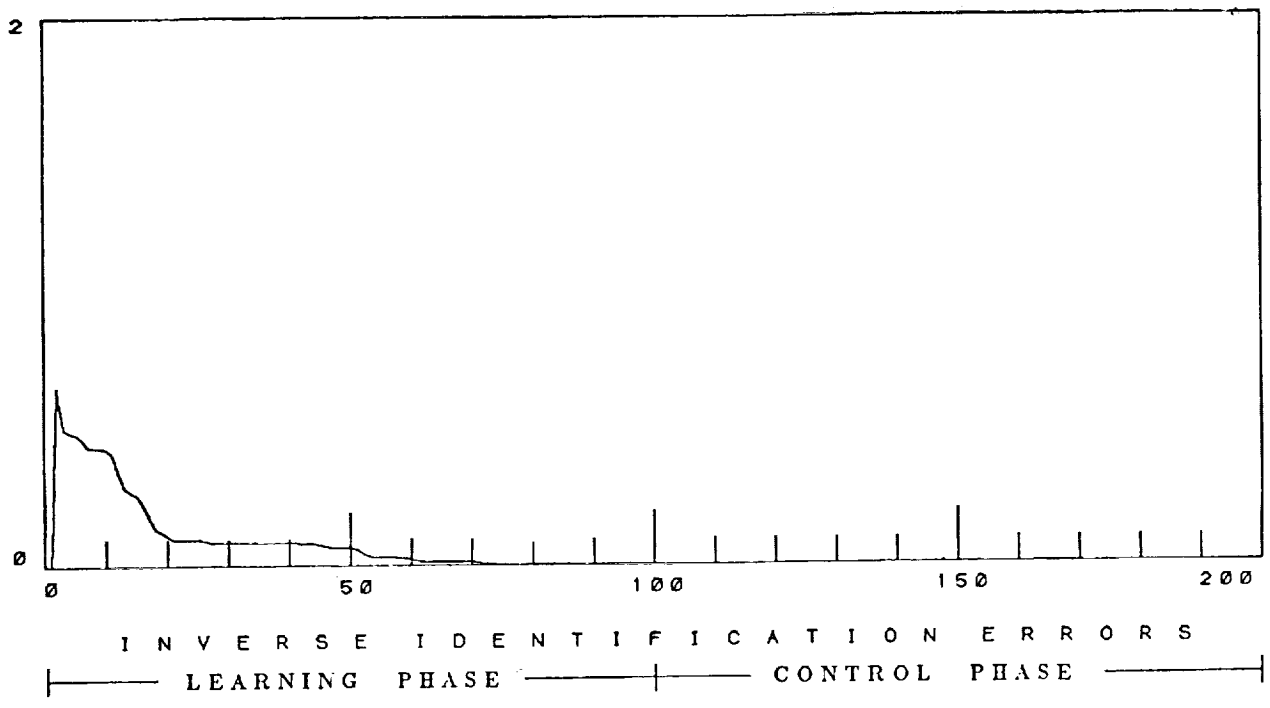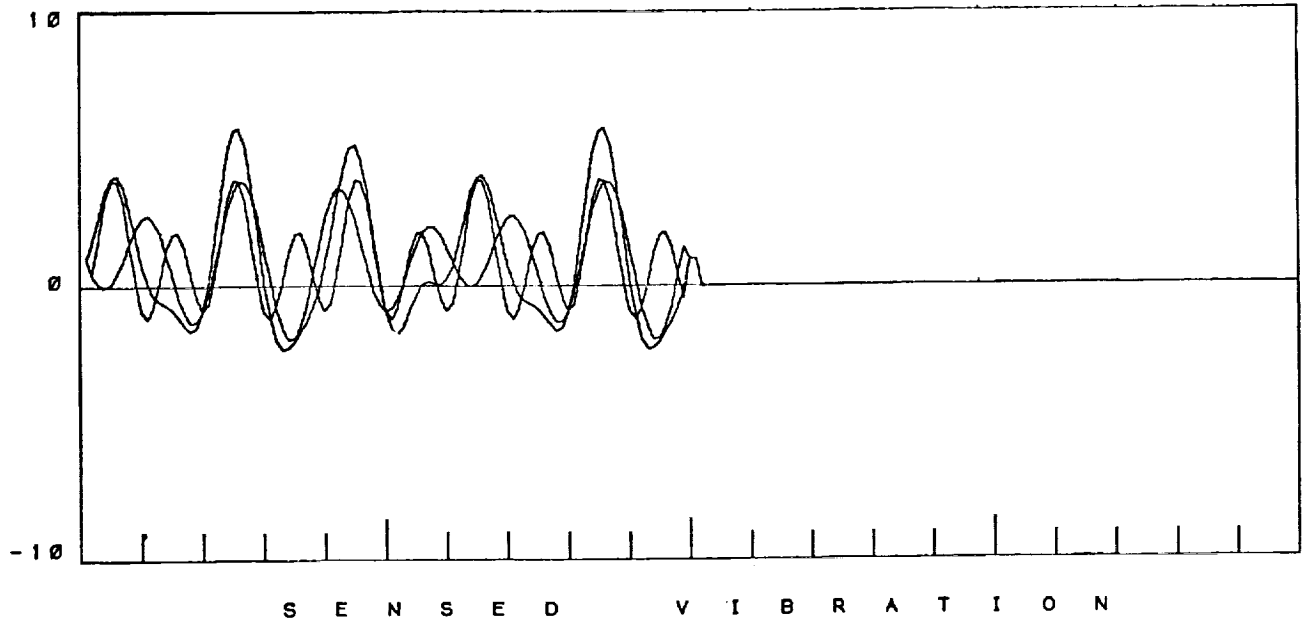
Figure 12A Learning Curve with Ks Diagonals = 0.2 for (3 x 3) Simulation (Note Learning and Control Phases).

ITERATION	I.D. ERROR	VIBRATION
1	0.00000	0.00000
2	0.65634	2.41634
3	0.50652	4.44880
4	0.49325	6.60944
5	0.48798	7.99706
6	0.46850	8.37584
7	0.43972	7.58645
8	0.43746	5.93930
9	0.43640	4.00408
10	0.43350	4.17732
15	0.26057	3.16234
20	0.10964	2.72247
25	0.09593	13.06231
30	0.08587	2.60947
35	0.08489	5.80914
40	0.08321	4.13753
45	0.07819	11.49648
50	0.06528	2.66334
55	0.03039	3.68004
60	0.02344	2.58204
65	0.01208	7.96703
70	0.01189	4.17401
75	0.00452	3.16856
80	0.00317	2.76308
85	0.00251	13.01733
90	0.00224	2.66917
95	0.00222	5.81383
100	0.00195	3.00000
105	0.00151	0.00000
110	0.00151	0.00000
115	0.00151	0.00000
120	0.00151	0.00000
125	0.00151	0.00000
130	0.00151	0.00000
135	0.00151	0.00000
140	0.00151	0.00000
145	0.00151	0.00000
150	0.00151	0.00000
155	0.00151	0.00000
160	0.00151	0.00000
165	0.00151	0.00000
170	0.00151	0.00000
175	0.00151	0.00000
180	0.00151	0.00000
185	0.00151	0.00000
190	0.00151	0.00000
195	0.00151	0.00000
200	0.00151	0.00000

Figure 12B Identification Errors and Vibration Level,
Ks Diagonals = 0.2.

56

THE IDFNTIFIED INVERSE

```
 0.6191      -0.2306       0.1147
-0.2442       0.4809      -0.2398
 0.1193      -0.2312       0.6150
```

THE TRUE INVERSE

```
 0.6250      -0.2500       0.1250
-0.250        0.5000      -0.2500
 0.1250      -0.2500       0.6250
```

INVERSE INITIAL ESTIMATE

```
 0.0000       0.0000       0.0000
 0.0000       0.0000       0.0000
 0.0000       0.0000       0.0000
```

Figure 12C   Identified, True, and Initial (3 x 3) Inverse Estimate,
Ks Diagonals = 0.2.
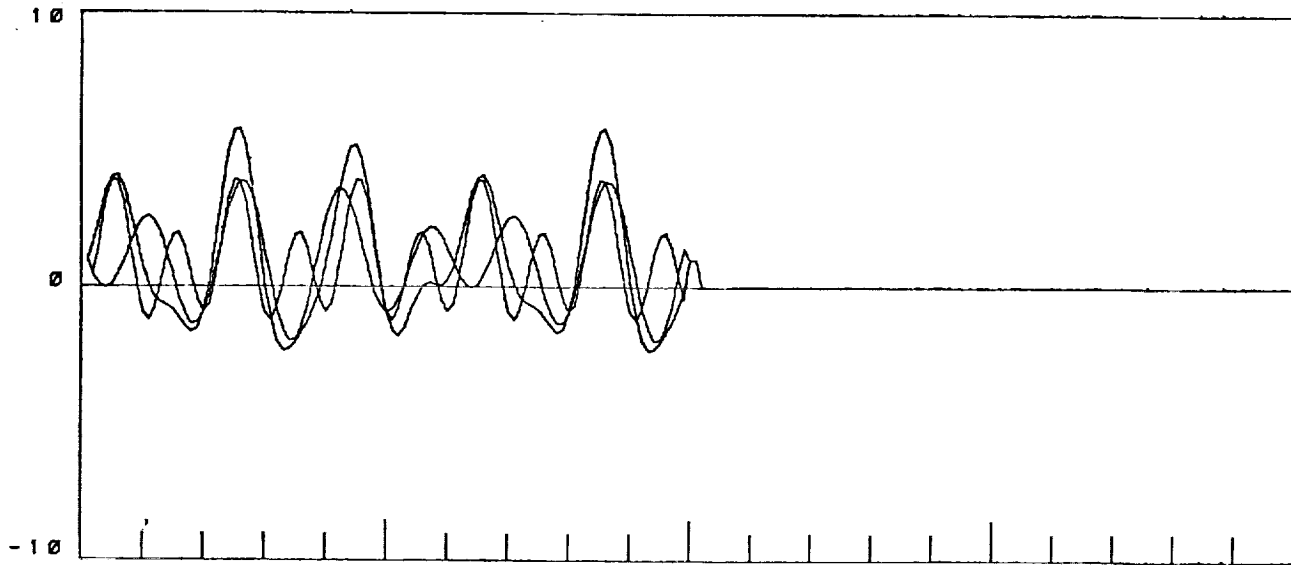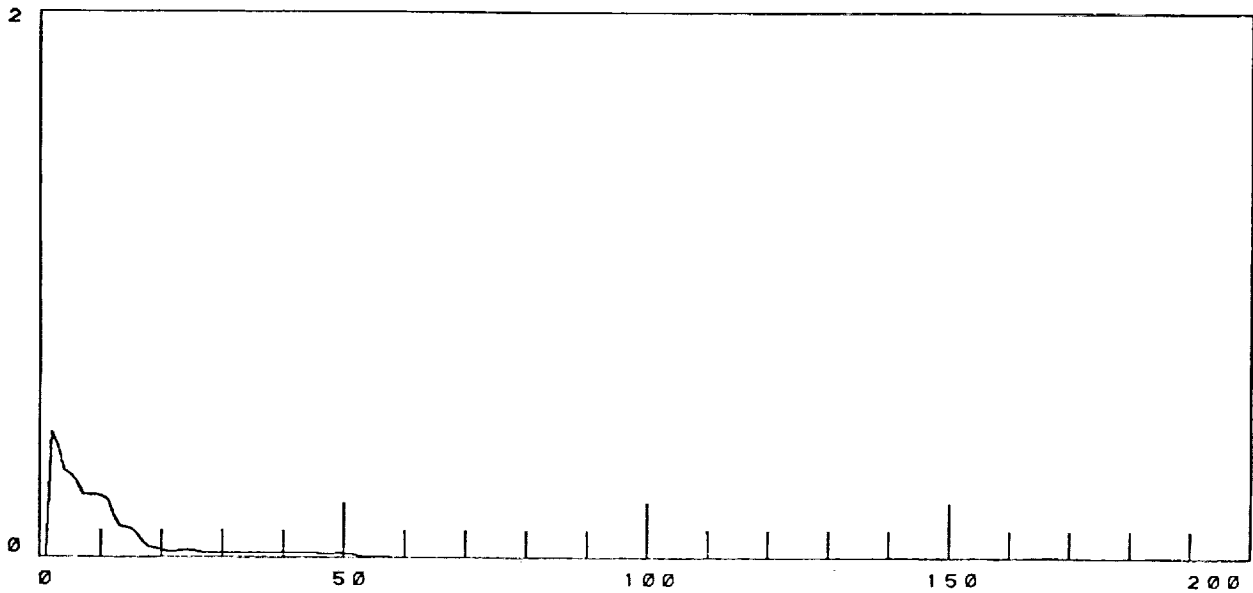
GAIN VECTOR: 0.3000   0.3000   0.3000
CONTROL RELAX:
    1.0000

Figure 13A   Learning Curve with Ks Diagonals = 0.3 for (3 x 3) Simulation
              (Note Learning and Control Phases).

58

ITERATION	I.D. ERROR	VIBRATION
1	0.00000	0.00000
2	0.45657	2.41634
3	0.40161	4.44880
4	0.31746	6.60944
5	0.30090	7.99706
6	0.27725	8.37584
7	0.22549	7.58645
8	0.22529	5.93930
9	0.22546	4.00408
10	0.22430	4.17732
15	0.10265	3.16234
20	0.02622	2.72247
25	0.02252	13.06231
30	0.01812	2.60947
35	0.01766	5.80914
40	0.01743	4.13753
45	0.01604	11.49648
50	0.01346	2.66334
55	0.00261	3.68004
60	0.00136	2.58204
65	0.00088	7.96703
70	0.00078	4.17401
75	0.00010	3.16856
80	0.00008	2.76308
85	0.00006	13.01733
90	0.00005	2.66917
95	0.00004	5.81393
100	0.00005	3.00000
105	0.00004	0.00000
110	0.00004	0.00000
115	0.00004	0.00000
120	0.00004	0.00000
125	0.00004	0.00000
130	0.00004	0.00000
135	0.00004	0.00000
140	0.00004	0.00000
145	0.00004	0.00000
150	0.00004	0.00000
155	0.00004	0.00000
160	0.00004	0.00000
165	0.00004	0.00000
170	0.00004	0.00000
175	0.00004	0.00000
180	0.00004	0.00000
185	0.00004	0.00000
190	0.00004	0.00000
195	0.00004	0.00000
200	0.00004	0.00000

Figure 13B   Identification Errors and Vibration Level, Ks Diagonals = 0.3.

THE IDENTIFIED INVERSE

```
   0.6262      -0.2471      0.1241
  -0.2513       0.4968     -0.2491
   0.1265      -0.2463      0.6239
```

THE TRUE INVERSE

```
   0.6250      -0.2500      0.1250
  -0.2500       0.5000     -0.2500
   0.1250      -0.2500      0.6250
```

INVERSE INITIAL ESTIMATE

```
   0.0000       0.0000      0.0000
   0.0000       0.0000      0.0000
   0.0000       0.0000      0.0000
```

Figure 13C   Identified, True, and Initial (3 x 3) Inverse Estimate,
Ks Diagonals = 0.3.
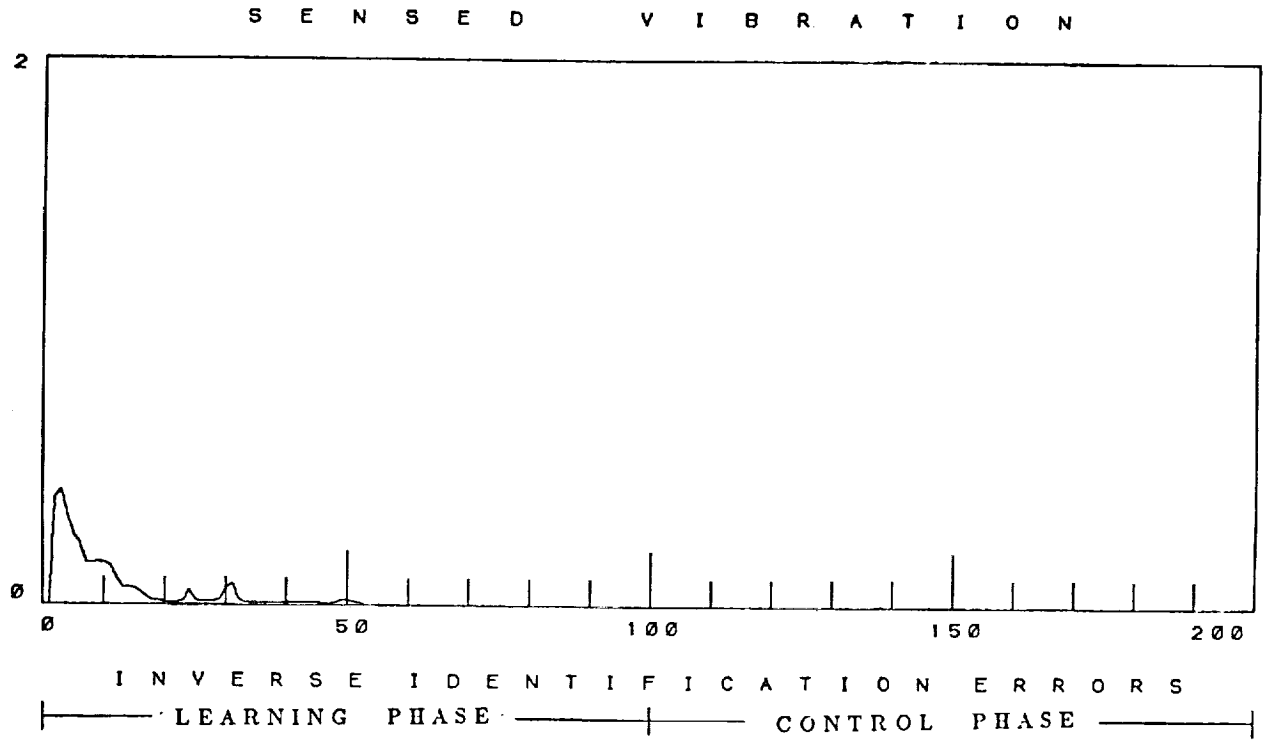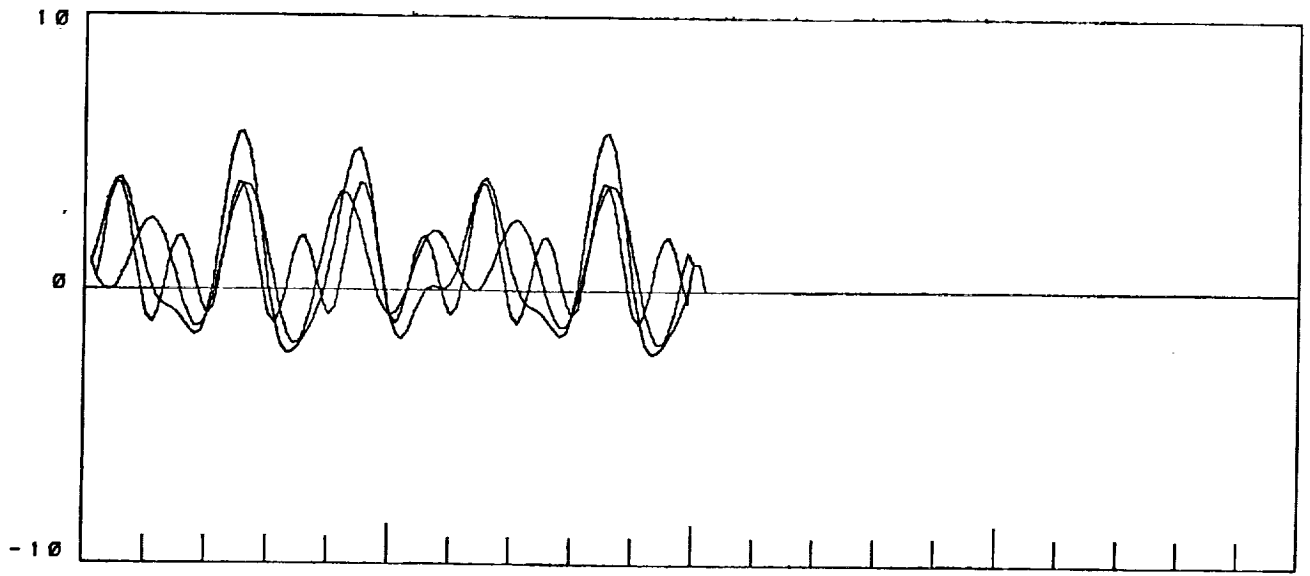
Figure 14   Learning Curve with Ks Diagonals = 0.35 for (3 x 3) Simulation
(Note. Learning and Control Phases).
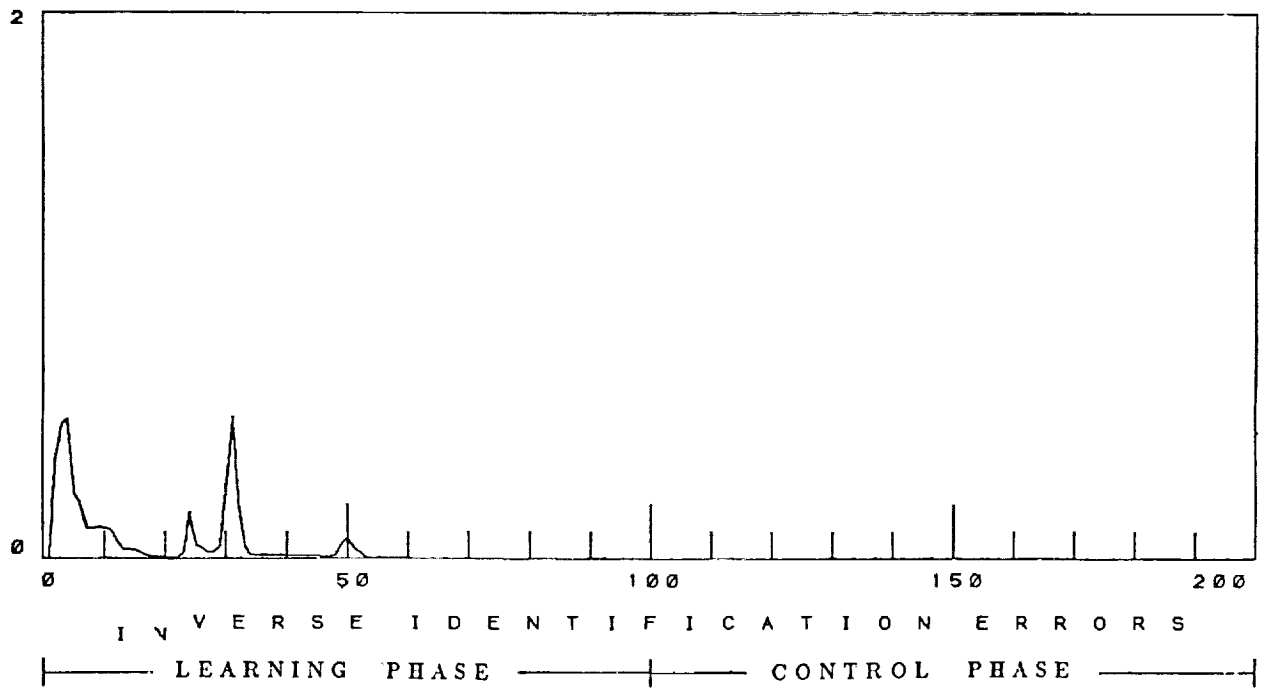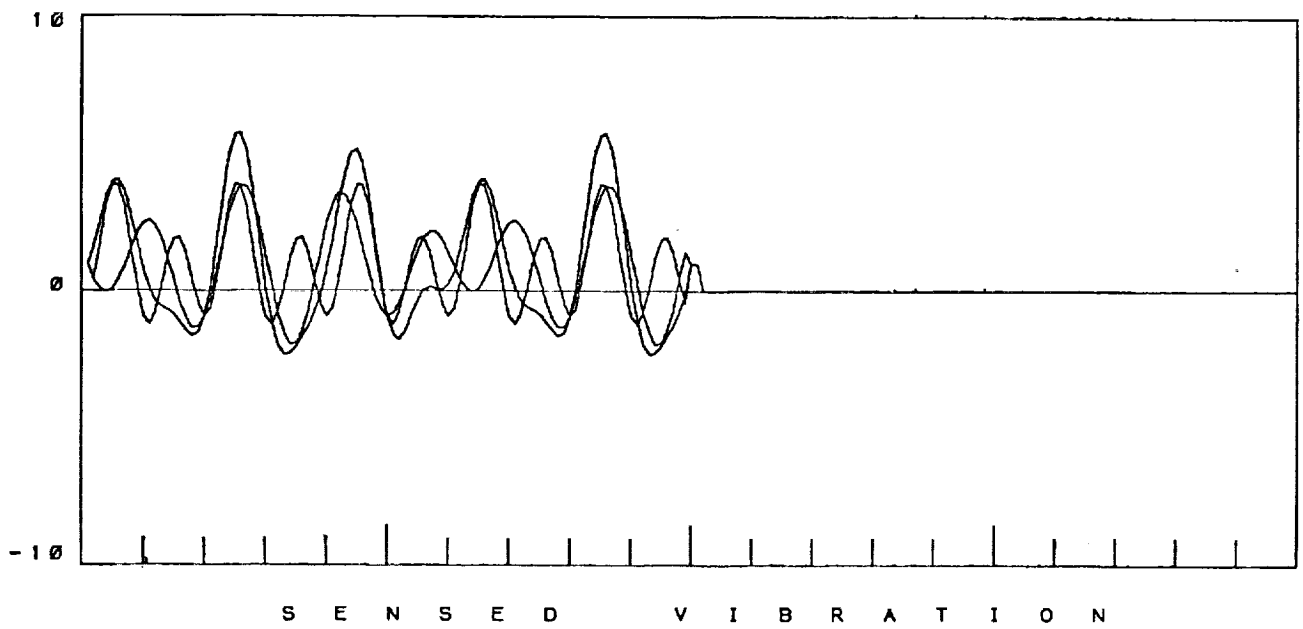
Figure 15   Learning Curve with Ks Diagonals = 0.40 for (3 x 3) Simulation
(Note Learning and Control Phases).

Figure 16A   Learning Curve with Ks Diagonals = 0.45 for (3 x 3) Simulation
(Note Learning and Control Phases).

THE IDENTIFIED INVERSE

0.5143	-0.3477	0.1107
-0.2607	0.4906	-0.2514
0.1551	-0.2235	0.5289

THE TRUE INVERSE

0.6250	-0.2500	0.1250
-0.2500	0.5000	-0.2500
0.1250	-0.2500	0.6250

INVERSE INITIAL ESTIMATE

|		
0.0000	0.0000	0.0000
0.0000	0.0000	0.0000
0.0000	0.0000	0.0000

Figure 16C   Identified, True, and Initial (3 x 3) Inverse Estimate,
Ks Diagonals = 0.45.
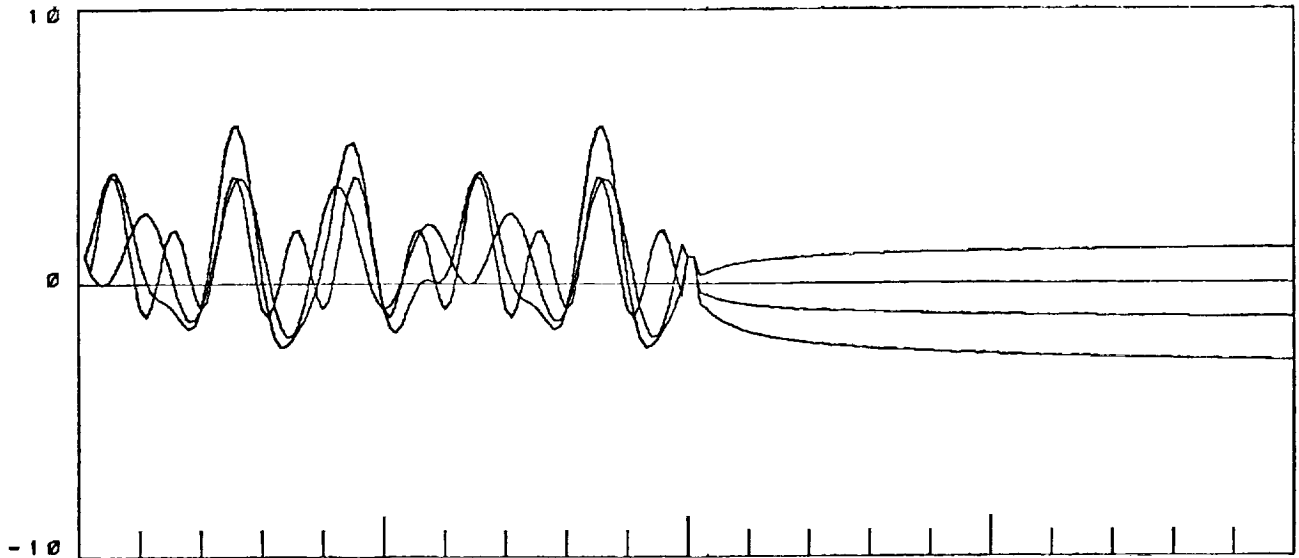
64

SENSED VIBRATION
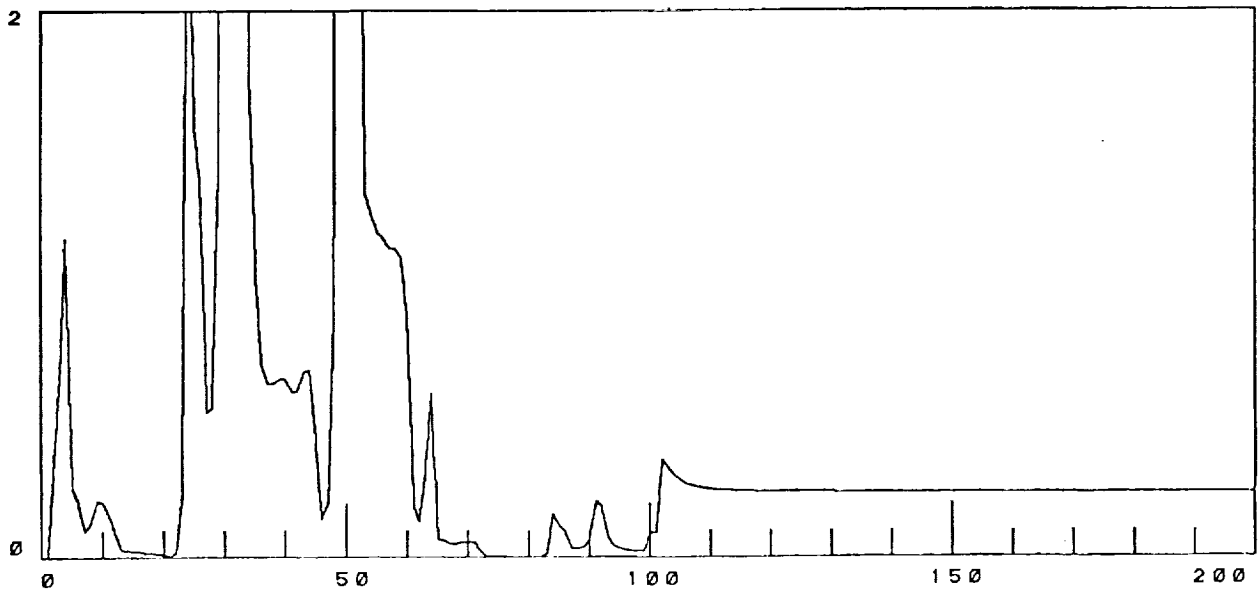
INVERSE IDENTIFICATION ERRORS

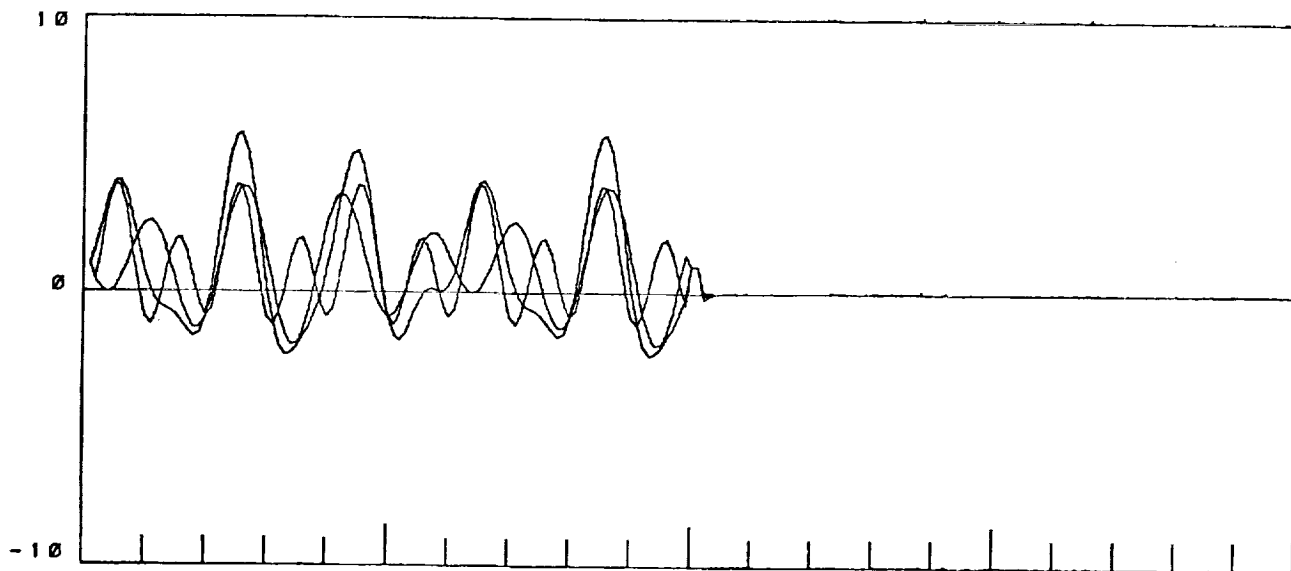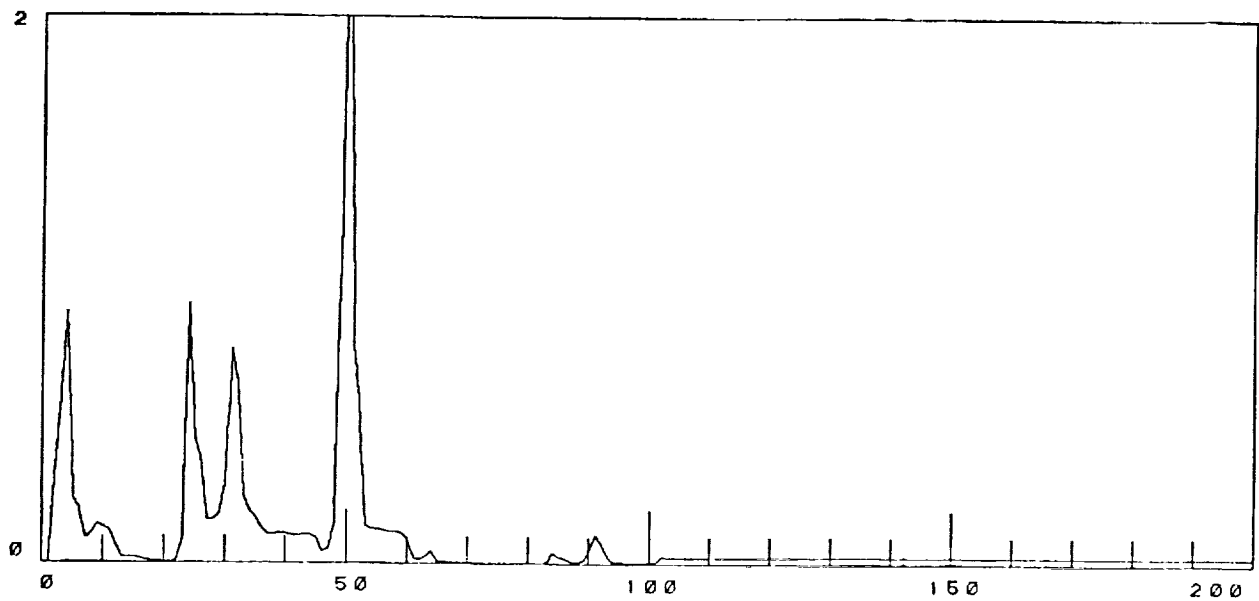LEARNING PHASE ——————|—————— CONTROL PHASE

GAIN VECTOR: 0.4700   0.4700   0.4700
CONTROL RELAX:
    1.0000

Figure 17A   Learning Curve with Ks Diagonals = 0.47 for (3 x 3) Simulation
(Note Learning and Control Phases).

65

ITERATION	I.D. ERROR	VIBRATION
1	0.00000	0.00000
2	0.31329	2.41634
3	0.67837	4.44880
4	1.17067	6.60944
5	0.24943	7.99706
6	0.20252	8.37584
7	0.09812	7.58645
8	0.11914	5.93930
9	0.20665	4.00408
10	0.20425	4.17732
15	0.02433	3.16234
20	0.00955	2.72247
25	1.58514	13.06231
30	10.29409	2.60947
35	1.04530	5.80914
40	0.65607	4.13753
45	0.42915	11.49648
50	25.00018	2.66334
55	1.19192	3.68004
60	0.87958	2.58204
65	0.06783	7.96703
70	0.05677	4.17401
75	0.00261	3.16856
80	0.00036	2.76308
85	0.11338	13.01733
90	0.06291	2.66917
95	0.03490	5.81383
100	0.08947	3.00000
105	0.28406	2.37973
110	0.25045	3.32919
115	0.24333	3.79522
120	0.24062	4.08815
125	0.23925	4.29746
130	0.23845	4.45848
135	0.23793	4.58840
140	0.23757	4.69678
145	0.23731	4.78941
150	0.23711	4.87009
155	0.23695	4.94140
160	0.23683	5.00519
165	0.23673	5.06282
170	0.23665	5.11532
175	0.23658	5.16348
180	0.23652	5.20792
185	0.23646	5.24916
190	0.23542	5.28760
195	0.23538	5.32359
200	0.23534	5.35739

Figure 17B   Identification Errors and Vibration Level,
Ks Diagonals = 0.47.

66

THE IDENTIFIED INVERSE

```
    0.2594      -0.4454       0.1416
   -0.3162       0.4646      -0.2470
    0.3383      -0.1360       0.6153
```

THE TRUE INVERSE

```
    0.6250      -0.2500       0.1250
   -0.2500       0.5000      -0.2500
    0.1250      -0.2500       0.6250
```

INVERSE INITIAL ESTIMATE

```
    0.0000       0.0000       0.0000
    0.0000       0.0000       0.0000
    0.0000       0.0000       0.0000
```

Figure 17C   Identified, True, and Initial (3 x 3) Inverse Estimate,
Ks Diagonals = 0.47.

67

For very low values of K_s the convergence is smooth, but slow. For higher values of K_s, the speed of convergence increases, until it becomes oscillatory at K_s equal 0.40, and unstable for K_s greater than or equal to about 0.45. The results are summarized in tabular form below, and graphically in figure 18.

TABLE 2

Convergence Times and Stability Trends for (3 x 3) Simulation
Starting from Zero Initial Conditions on the Inverse Estimate

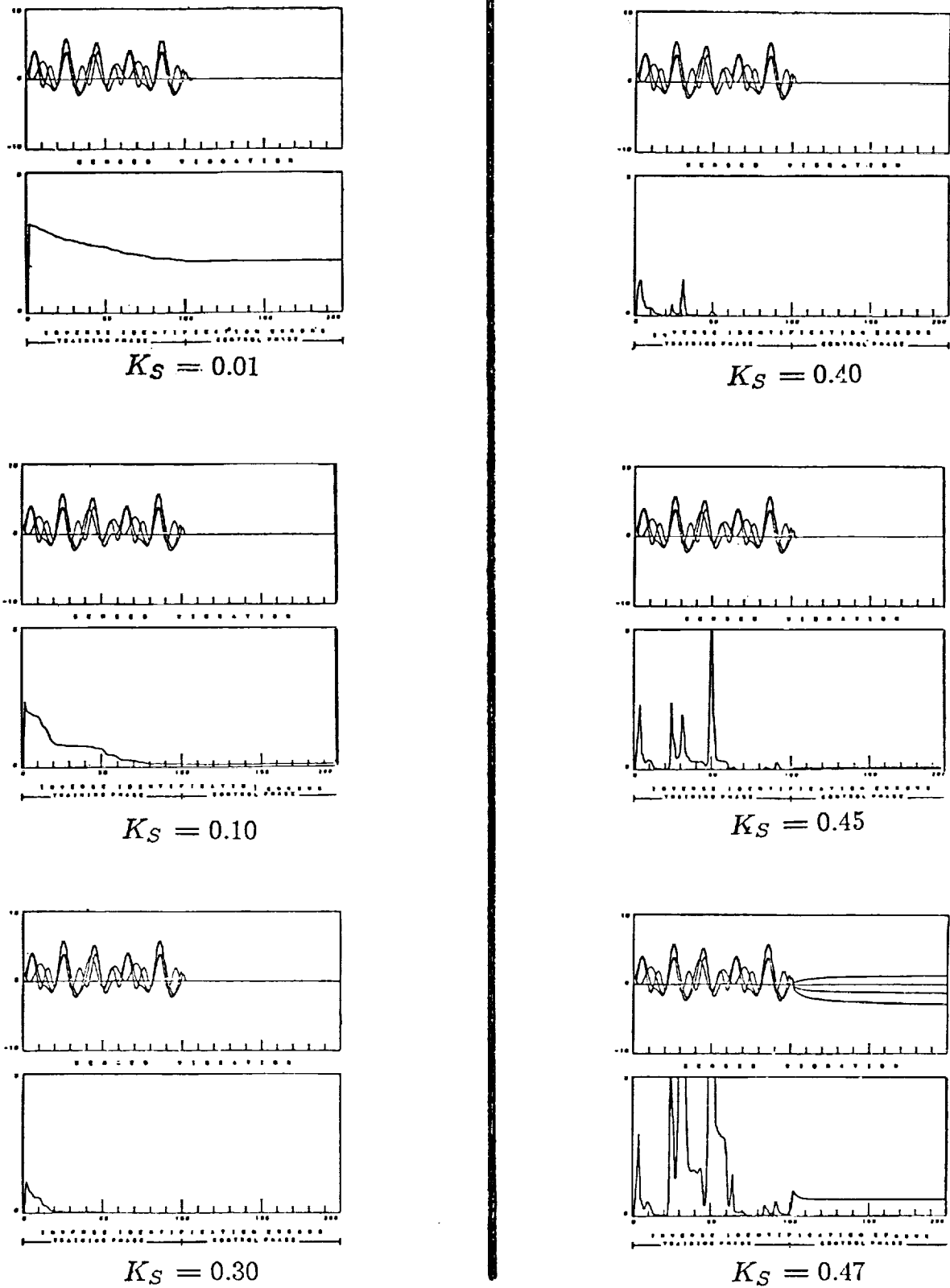| K_s	ITERATION TO CONVERGENCE	STABILITY
-0.01	Greater Than 100	Overdamped Convergence
-0.10	Not Quite After 100 Steps	Overdamped Convergence
-0.15	100	Overdamped Convergence
-0.20	73	Overdamped Convergence
-0.30	60	Critical
-0.35	53	Slightly Underdamped
-0.40	52	Large Oscillations
-0.45	Converged, But Unstable	Large Oscillations
-0.50	Will Not Converge	Unstable

Figure 18   Comparison of Identification Error for Various Ks Diagonal
Element Values.

Since the learning phase pitch commands were *known*, it was possible to compute the signal information matrix. For each iteration, N, of the learning cycle the learning phase pitch commands were,

$$\Theta(N,1) = Sine(N/15.0 + 7.0/15.0)$$
$$\Theta(N,2) = Sine(N/20.0)$$
$$\Theta(N,3) = Sine(N/10.0 - 3.0/30.0)$$

The signal information matrix, $E(\Delta Z \Delta Z^T)$, was then computed by performing the indicated multiplication over an appropriate number of cycles. When this was done, the eigenvalues of this matrix were found to be,

$$\lambda_1 = 0.1734$$

$$\lambda_2 = 0.9935$$

$$\lambda_3 = 2.6219$$

From this information, the theoretical stability limit for the K_s elements was,

$$\frac{1}{\lambda_{max}} = \frac{1}{2.6219} = 0.381$$

or,

$$0 < k_i < 0.381$$

which was in good agreement with the experimentally found convergence limit of about 0.40 . The numbers were not the same because the slower modes had a stabilizing influence on the fastest mode, upon which the stability criteria was based.

More than this, the theoretical learning curves associated with the eigenvalues of the signal information matrix were generated and compared to the experimental learning inverse error. Recalling that the learning curve time constants associated with each normal mode and k_i are predicted by:

$$\tau_p = \frac{1}{2k_i\lambda_p}$$

the normal mode learning time constants are,

$$\tau_1 = \frac{1}{(0.347)k_{s1}}$$

$$\tau_2 = \frac{1}{(1.987)k_{s2}}$$

$$\tau_3 = \frac{1}{(5.244)k_{s3}}$$

Table 3 compares the identification error associated with each mode assuming that the initial inverse estimate square error was 1.31, and that the K_s diagonal elements were all equal to 0.15. From this table, it is seen that the experimentally found learning curve appears to be an average of the learning curves associated with the normal modes. The faster modes can be viewed as being responsible for rapid initial learning, while the slow modes govern final convergence. These modes have been roughly indicated in Figure 19. It appears that the best selection of the K_s elements is, therefore, a compromise between stable and fast convergence.

TABLE 3

Comparison of Experimental and Normal Mode
Predicted Learning (Identification) Error

STEP	$\tau_1 = 20$	$\tau_2 = 3.5$	$\tau_3 = 1.5$	AVERAGE	EXPERIMENTAL
0	1.31	1.31	1.31	1.31	1.31
2	1.22	0.77	0.45	0.81	0.74
4	1.15	0.66	0.11	0.64	0.73
20	0.49	0.02	0.00	0.17	0.24
40	0.18	0.00	0.00	0.06	0.20
60	0.07	0.00	0.00	0.02	0.07
80	0.02	0.00	0.00	0.01	0.02
100	0.01	0.00	0.00	0.00	0.01

$$k_s = -0.30$$

$$T = \begin{bmatrix} 2 & 1 & 0 \\ 1 & 3 & 1 \\ 0 & 1 & 2 \end{bmatrix}$$

$$E(\Delta Z \Delta Z^T)$$

$$\Lambda = \begin{matrix} 0.17 \\ 0.99 \\ 2.62 \end{matrix}$$

$$-0.40 < k_s < 0$$

SUM SQUARE
IDENTIFICATION
ERRORS IN C

τ FAST MODE

τ MODERATE MODE

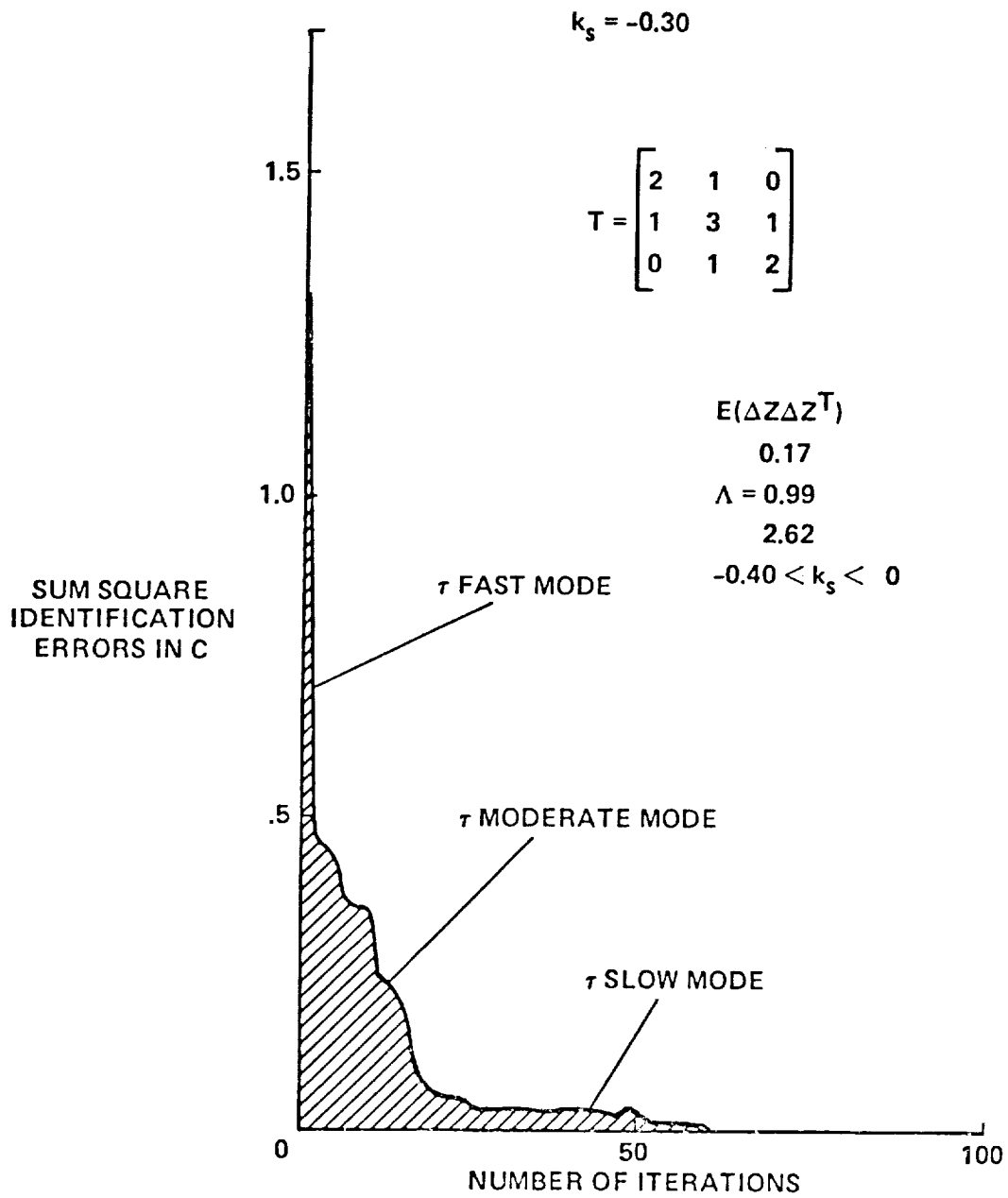τ SLOW MODE

NUMBER OF ITERATIONS

Figure 19.   The Learning Curve of the Adaptation
Process Showing Convergence Modes for
the (3 x 3) Simulation with $K_s = 0.30$

73

6.2

ADAPTIVE INVERSE CONTROL SIMULATION
WITH THE (3 X 3) T MATRIX

Once the inverse matrix identification error is small enough, the vibration control phase may be initiated by using the inverse matrix to generate vibration control commands. For the (3 x 3) simulation, this was done after 100 iterations. This section presents five plots to show the behavior of the (3 x 3) simulation during the control phase. The K_s diagonal elements were chosen to be 0.30, since this value produced the most rapid convergence without oscillations or instabilities about the true solution. For these simulation runs, the uncontrolled vibration vector elements were held constant at 1.0, after the start of the control phase. This simulation represented the simplest case, in which the vibration vector to be minimized was held constant. Figure 20 shows the uncontrolled vibration levels, for no control (or, control relaxation set to zero). Note that *control relaxation* refers to that fraction of the inverse control actually implemented, expressed as a number between zero and one. Figure 21 shows that, even for control relaxation of 0.6, the vibration decreases to near zero in two or three iterations.
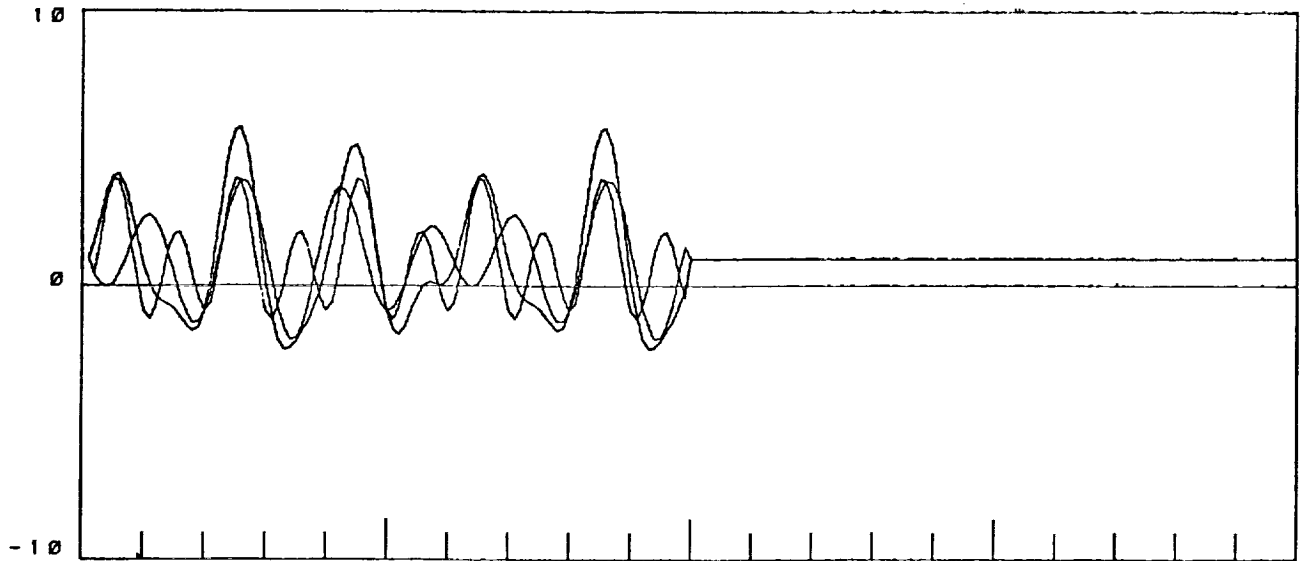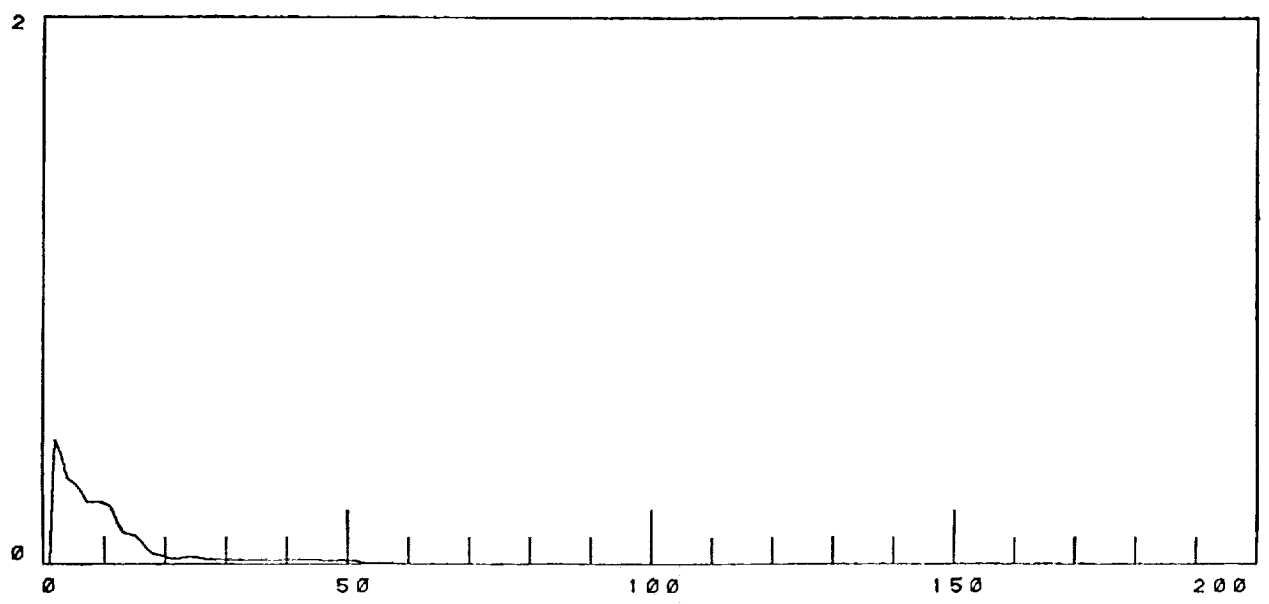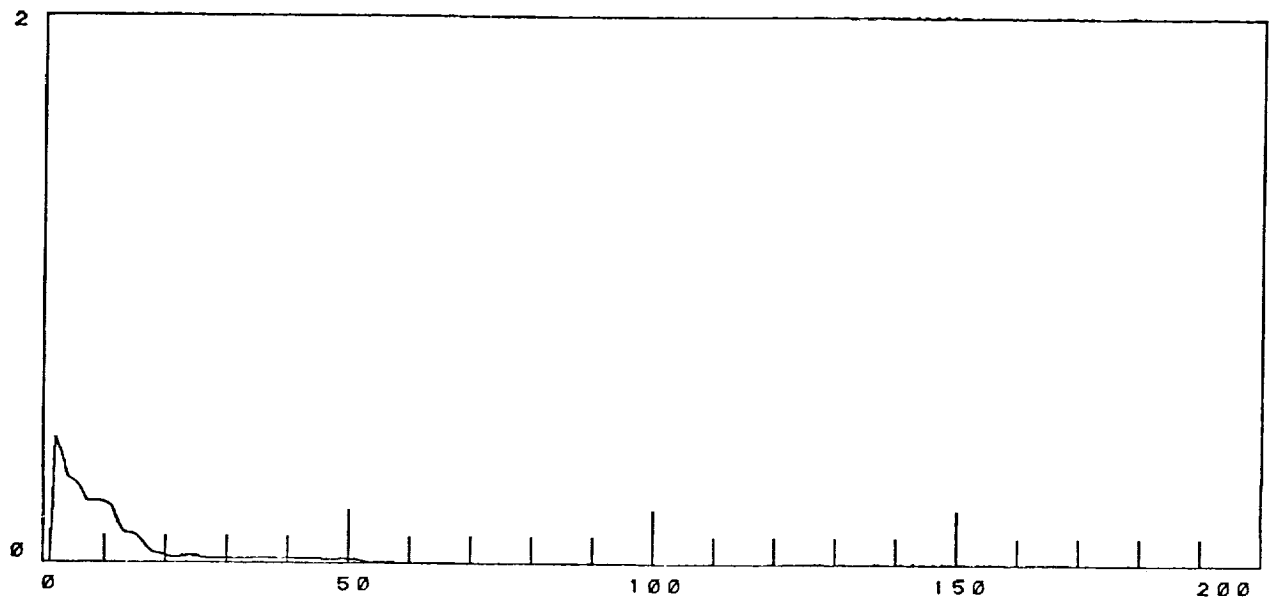
Figure 20A   Uncontrolled Vibration for No Control During the Control
Phase, Ks Diagonals = 0.30.

75

ITERATION	I.D. ERROR	VIBRATION
1	0.00000	0.00000
2	0.45657	2.41634
3	0.40161	4.44880
4	0.31746	6.60944
5	0.30090	7.99706
6	0.27725	8.37584
7	0.22549	7.58645
8	0.22529	5.93930
9	0.22546	4.00408
10	0.22430	4.17732
15	0.10265	3.16234
20	0.02622	2.72247
25	0.02252	13.06231
30	0.01812	2.60947
35	0.01766	5.80914
40	0.01743	4.13753
45	0.01604	11.49648
50	0.01346	2.66334
55	0.00261	3.68004
60	0.00136	2.58204
65	0.00088	7.96703
70	0.00078	4.17401
75	0.00010	3.16856
80	0.00008	2.76308
85	0.00006	13.01733
90	0.00005	2.66917
95	0.00004	5.81383
100	0.00005	3.00000
105	0.00005	3.00000
110	0.00005	3.00000
115	0.00005	3.00000
120	0.00005	3.00000
125	0.00005	3.00000
130	0.00005	3.00000
135	0.00005	3.00000
140	0.00005	3.00000
145	0.00005	3.00000
150	0.0005	3.00000
155	0.00005	3.00000
160	0.00005	3.00000
165	0.00005	3.00000
170	0.00005	3.00000
175	0.00005	3.00000
180	0.00005	3.00000
185	0.00005	3.00000
190	0.00005	3.00000
195	0.0005	3.00000
200	0.00005	3.00000

Figure 20B   Identification Errors and Vibration Level for No Control
Ks Diagonals = 0.30.
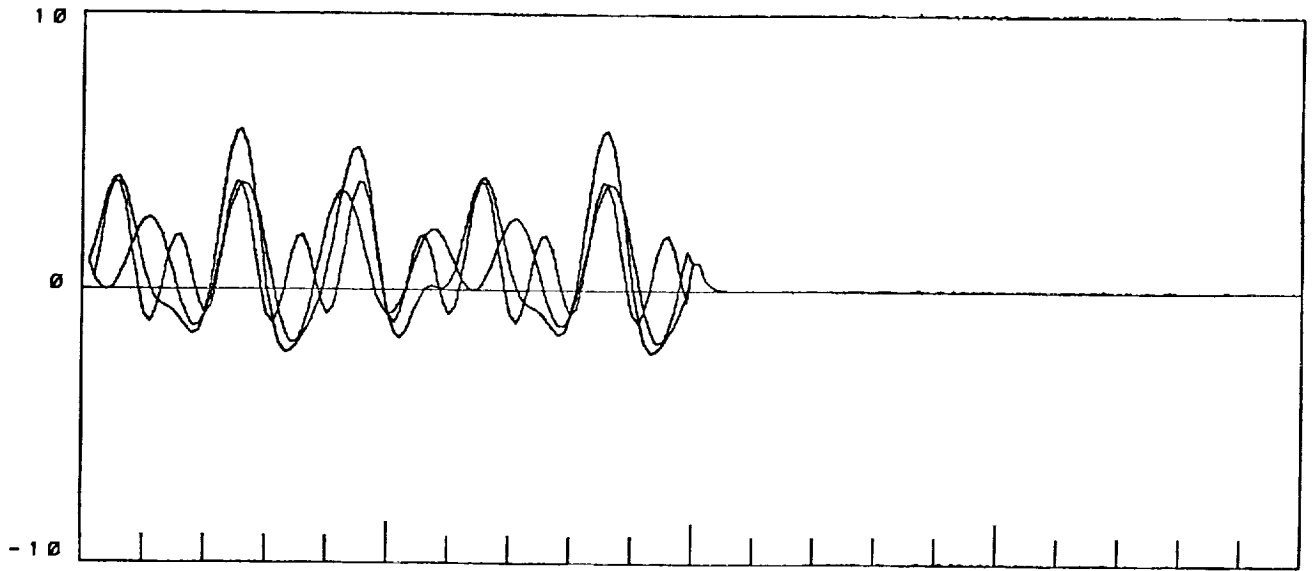
GAIN VECTOR: 0.3000   0.3000   0.3000
CONTROL RELAX:
     0.6000
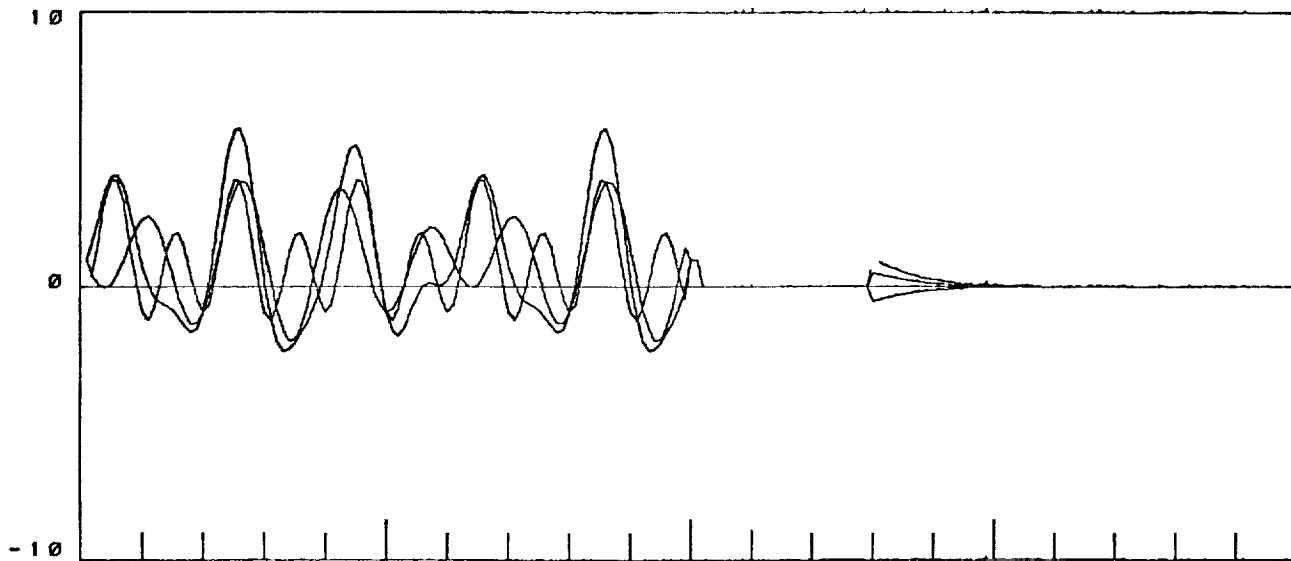
Figure 21A.   Steady State Vibration Reduction in the Control
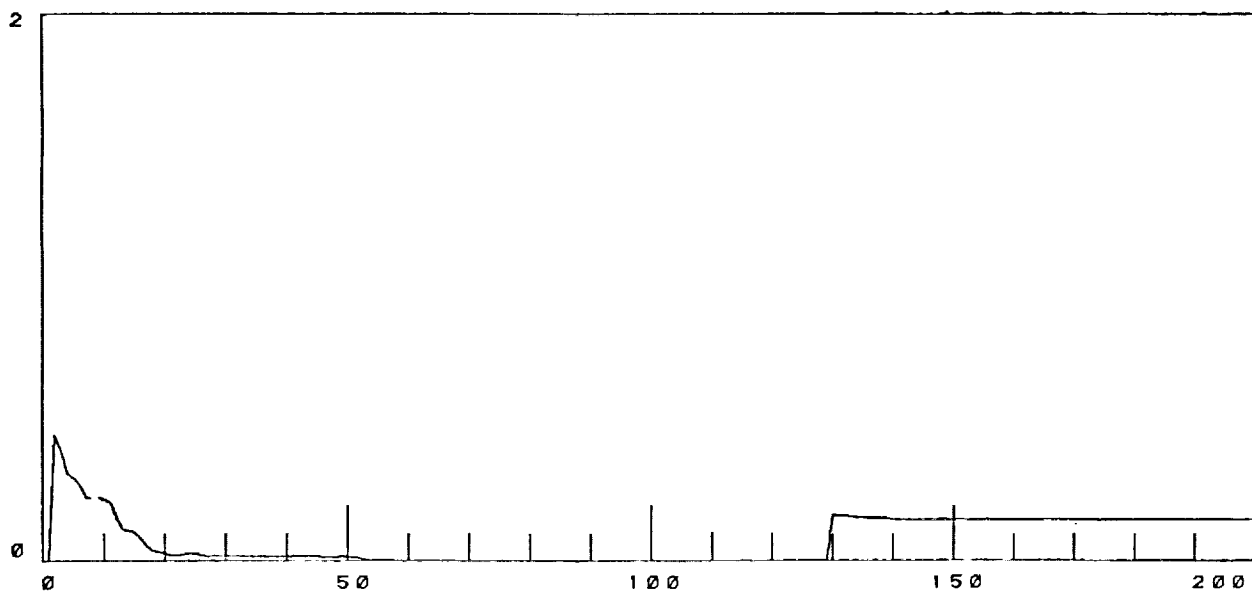   Phase (beginning step 100)

77

ITERATION	I.D. ERROR	VIBRATION
1	0.00000	0.00000
2	0.45657	2.41634
3	0.40161	4.44880
4	0.31746	6.50944
5	0.30090	7.99706
6	0.27725	8.37584
7	0.22549	7.58645
8	0.22529	5.93930
9	0.22546	4.00408
10	0.22430	4.17732
15	0.10265	3.16234
20	0.02622	2.72247
25	0.02252	13.06231
30	0.01812	2.60947
35	0.01766	5.80914
40	0.0743	4.13753
45	0.01604	11.49648
50	0.01346	2.66334
55	0.00261	3.68004
60	0.00135	2.58204
65	0.00088	7.96703
70	0.00078	4.17401
75	0.00010	3.16856
80	0.00008	2.76308
85	0.00006	13.01733
90	0.00005	2.66917
95	0.00004	5.81383
100	0.00005	3.00000
105	0.00003	0.07721
110	0.00003	0.00079
115	0.00003	0.00001
120	0.00003	0.00000
125	0.00003	0.00000
130	0.00003	0.00000
135	0.00003	0.00000
140	0.00003	0.00000
145	0.00003	0.00000
150	0.00003	0.00000
155	0.00003	0.00000
160	0.00003	0.00000
165	0.00003	0.00000
170	0.00003	0.00000
175	0.00003	0.00000
180	0.00003	0.00000
185	0.00003	0.00000
190	0.00003	0.00000
195	0.00003	0.00000
200	0.00003	0.00000

Figure 21B.   Identification Error and Vibration
Level

The next test was to see how well the adaptive inverse controller would track a change in the operating conditions. The first disturbance was a step change in the uncontrolled vibration. Figure 22 shows the effect of changing the uncontrolled vibration at step 130 from $(1.0, 1.0, 1.0)$ to $(2.0, 1.5, 0.5)$. The second disturbance was to change the transfer (T) matrix by 10 and 30 percent while introducing the step in uncontrolled vibration. These results are shown in Figures 23, 24, 25, and 26.

S E N S E D   V I B R A T I O N

I N V E R S E   I D E N T I F I C A T I O N   E R R O R S

├──────── LEARNING   PHASE ────────┼─────── CONTROL   PHASE ───────┤

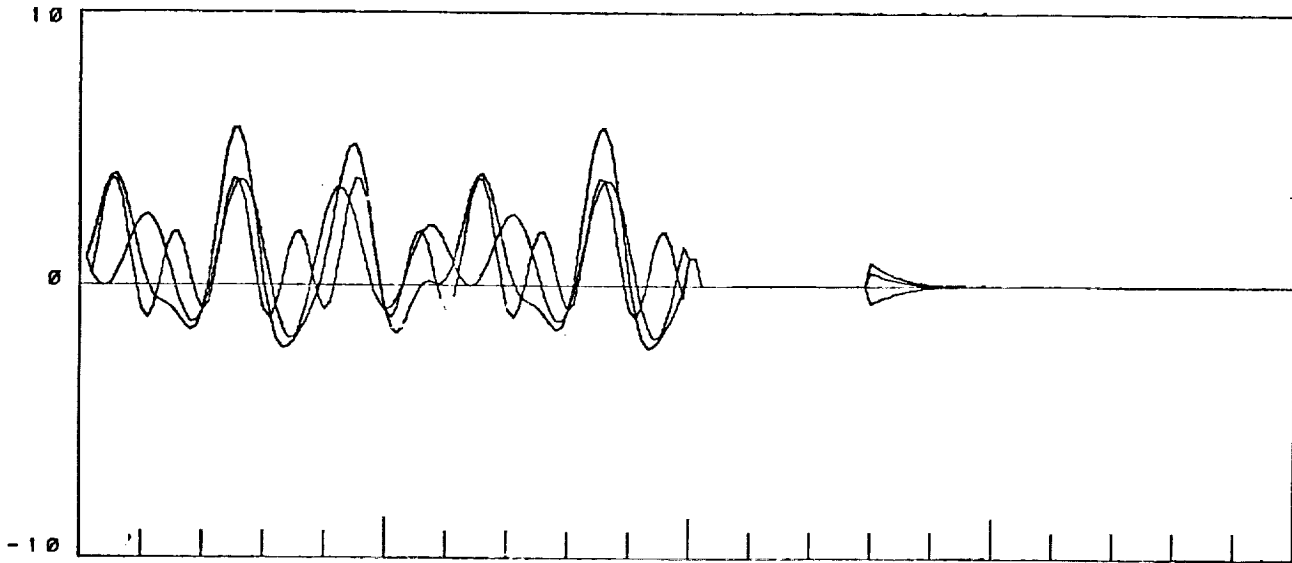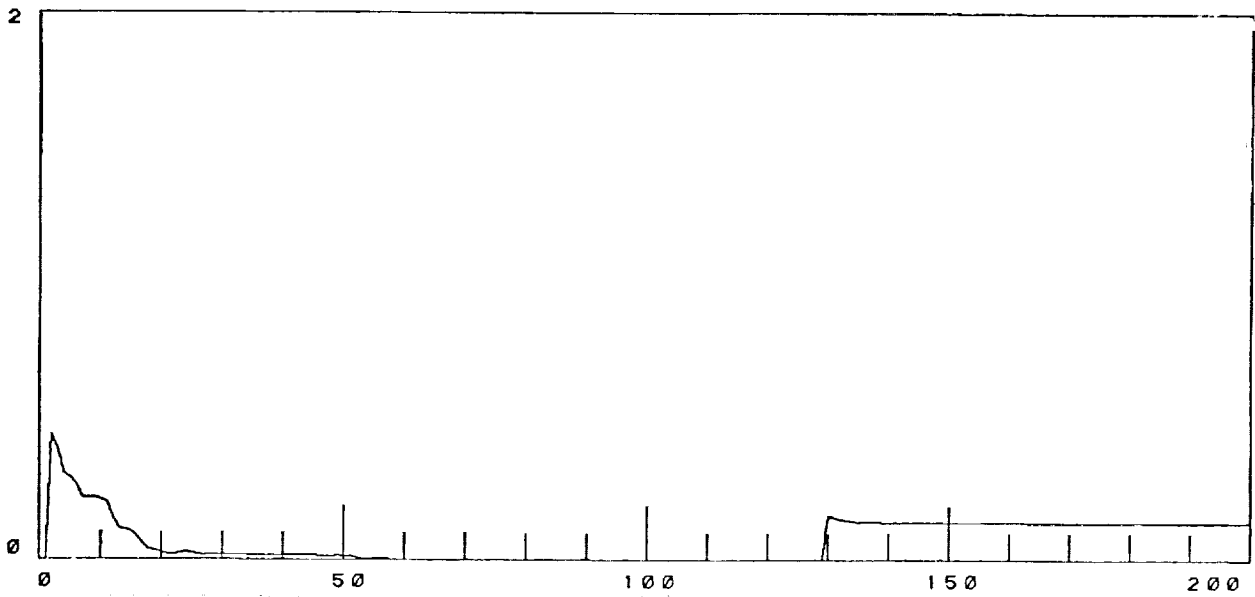GAIN VECTOR: 0.3000   0.3000   0.3000
CONTROL RELAX:
    1.0000

Figure 22A.   Vibration Reduction for Step Change in Uncontrolled Vibration
              After Iteration 130

80

ITERATION	I.D. ERROR	VIBRATION
1	0.00000	0.00000
2	0.45657	2.41634
3	0.40161	4.44880
4	0.31746	6.60944
5	0.30090	7.99706
6	0.27725	8.37584
7	0.22549	7.58645
8	0.22529	6.93930
9	0.22546	4.00408
10	0.22430	4.17732
15	0.10265	3.16234
20	0.02622	2.72247
25	0.02252	13.06231
30	0.01812	2.60947
35	0.01766	5.80914
40	0.01743	4.13753
45	0.01604	11.49648
50	0.01346	2.66334
55	0.00261	3.68004
60	0.00136	2.58204
65	0.00088	7.96703
70	0.00078	4.17401
75	0.00010	3.16856
80	0.00008	2.76308
85	0.00006	13.01733
90	0.00005	2.66917
95	0.00004	5.81383
100	0.00005	3.00000
105	0.00004	0.00000
110	0.00004	0.00000
115	0.00004	0.00000
120	0.00004	0.00000
125	0.00004	0.00000
130	0.16458	2.00000
135	0.15255	1.08630
140	0.14792	0.51074
145	0.14682	0.22880
150	0.14659	0.10137
155	0.14655	0.04482
160	0.14654	0.01980
165	0.14654	0.00875
170	0.14654	0.00387
175	0.14654	0.00171
180	0.14654	0.00075
185	0.14654	0.00033
190	0.14654	0.00015
195	0.14654	0.00007
200	0.14654	0.00003

Figure 22B.   Identification Error and Vibration
Level

81

GAIN VECTOR: 0.3000   0.3000   0.3000
CONTROL RELAX:
     1.0000

Figure 23.   Vibration Reduction for Step Change in Uncontrolled Vibration
              and 10% Change in T Matrix at Step 130

C-2

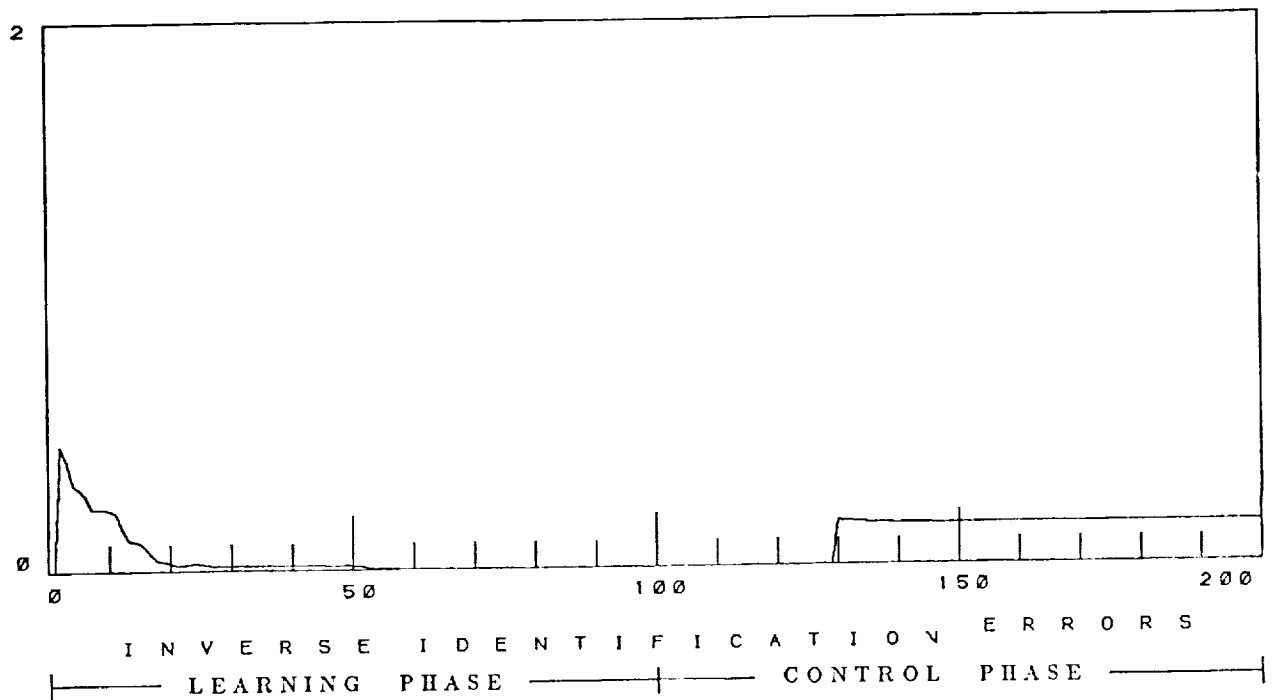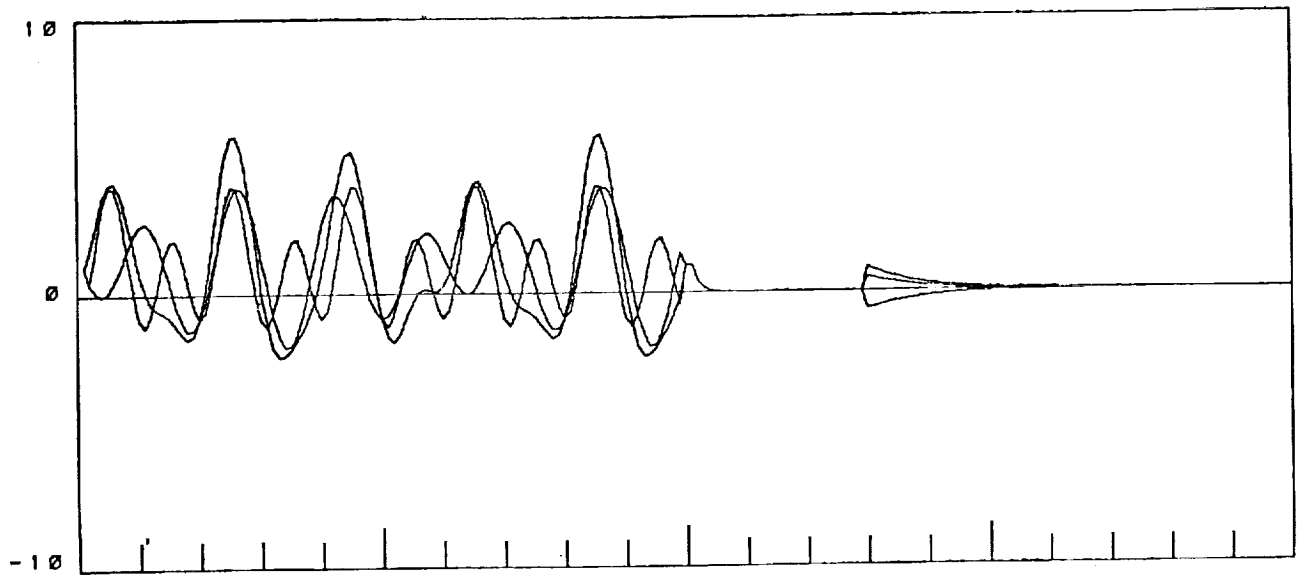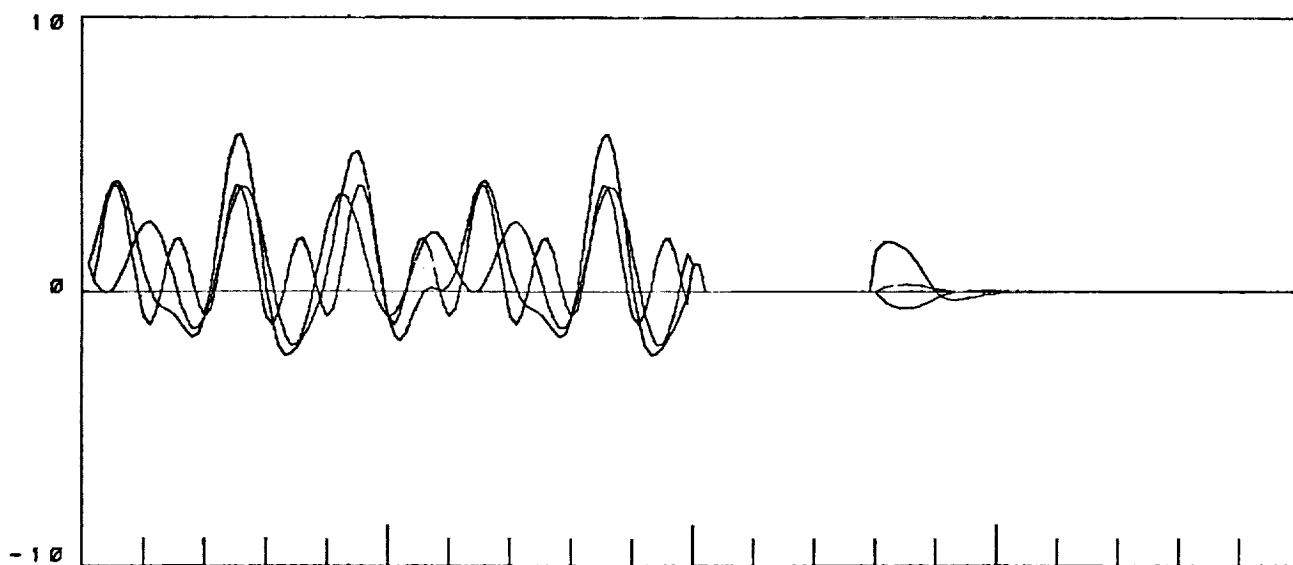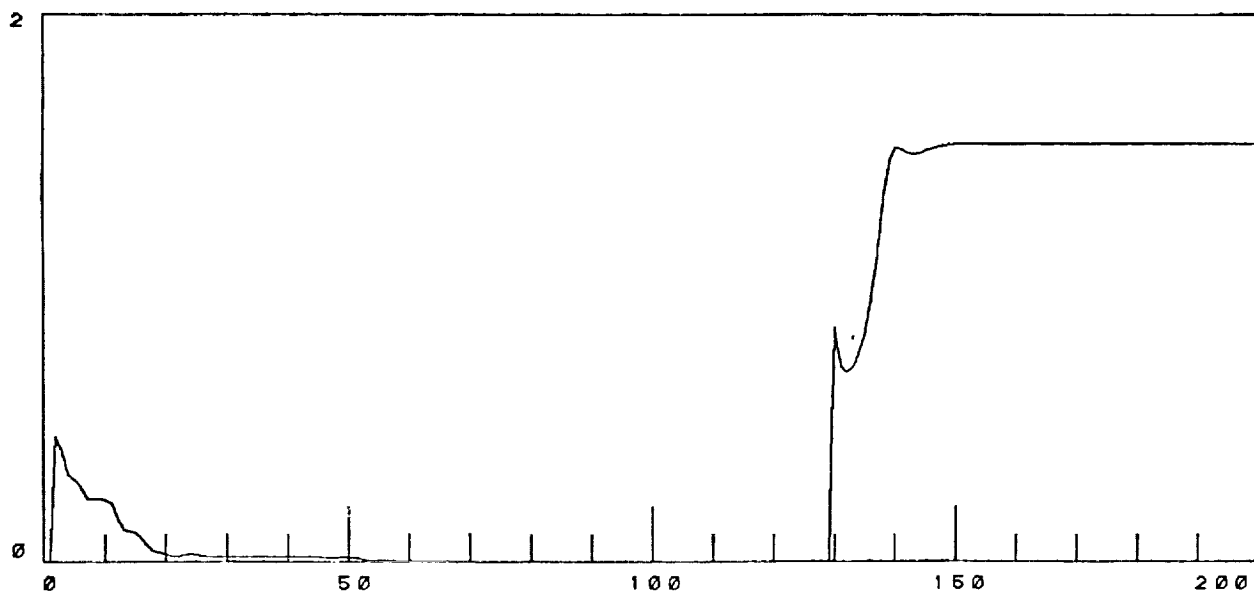S E N S E D   V I B R A T I O N

I N V E R S E   I D E N T I F I C A T I O N   E R R O R S

|———— LEARNING PHASE ————|—— CONTROL PHASE ——|

GAIN VECTOR: 0.3000   0.3000   0.3000
CONTROL RELAX:
     0.6000

Figure 24.   Vibration Reduction for Step Change in Uncontrolled Vibration
              and 10% Change in T Matrix at Step 130. Control Relaxation = 0.60

83

SENSED VIBRATION

INVERSE IDENTIFICATION ERRORS

|———— LEARNING PHASE ————|——— CONTROL PHASE ———|

GAIN VECTOR: 0.3000   0.3000   0.3000
CONTROL RELAX:
     1.0000

Figure 25A.   Vibration Reduction for 10% Step Change in Uncontrolled
               Vibration and 30% Change in T Matrix at Iteration 130

ITERATION	I.D. ERROR	VIBRATION
1	0.00000	0.00000
2	0.45657	2.41634
3	0.40161	4.44880
4	0.31746	6.60944
5	0.30090	7.99706
6	0.27725	8.37584
7	0.22549	7.58645
8	0.22529	6.93930
9	0.22546	4.00408
10	0.22430	4.17732
15	0.10265	3.16234
20	0.02622	2.72247
25	0.02252	13.06231
30	0.01812	2.60947
35	0.01766	6.80914
40	0.01743	4.13753
45	0.01604	11.49648
50	0.01346	2.66334
55	0.00261	3.68004
60	0.00136	2.58204
65	0.00088	7.96703
70	0.00078	4.17401
75	0.00010	3.16856
80	0.00008	2.76308
85	0.00006	13.01733
90	0.00005	2.66917
95	0.00004	6.81383
100	0.00005	3.00000
105	0.00004	0.00000
110	0.00004	0.00000
115	0.00004	0.00000
120	0.00004	0.00000
125	0.00004	0.00000
130	0.85553	1.50000
135	0.84033	2.41593
140	1.51389	033592
145	1.50256	0.25995
150	1.52501	0.07954
155	1.52640	0.00573
160	1.52640	0.00260
165	1.52640	0.00090
170	1.52640	0.00008
175	1.52640	0.00003
180	1.52640	0.00001
185	1.52640	0.00000
190	1.52640	0.00000
195	1.52640	0.00000
200	1.52640	0.00000

Figure 25B. Identification Error and Vibration
Level

85

THE IDENTIFIED INVERSE

```
-0.3416      -0.1973       0.0056
 0.3027       0.4724      -0.1868
-0.3869      -0.2298       0.5764
```

THE TRUE INVERSE
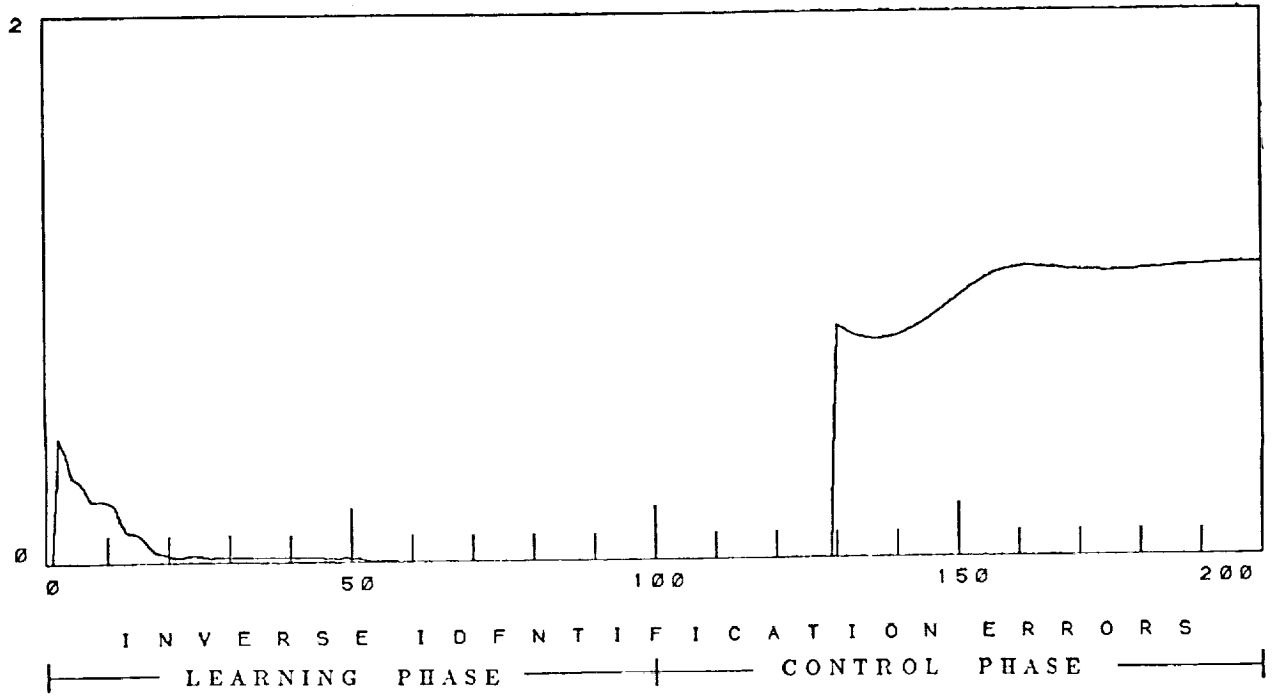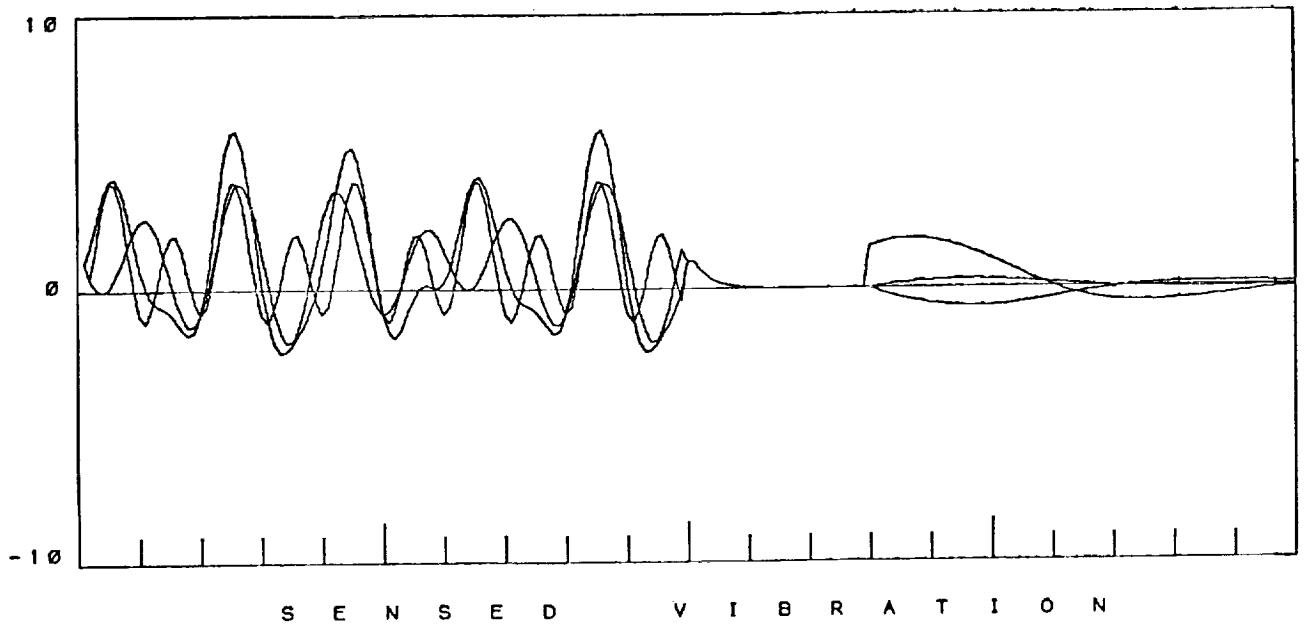
```
 0.6250      -0.2500       0.1250
-0.2500       0.5000      -0.2500
 0.1250      -0.2500       0.6250
```

INVERSE INITIAL ESTIMATE

```
 0.0000       0.0000       0.0000
 0.0000       0.0000       0.0000
 0.0000       0.0000       0.0000
```

Figure 25C. Identified, True, and Initial
             (3x3) Inverse Estimate

86

Figure 26A. Vibration Reduction for 10% Step Change in Uncontrolled Vibration and 30% Change in T Matrix at Iteration 130. Control Relaxation = 0.60

ITERATION	I.D. ERROR	VIBRATION
1	0.00000	0.00000
2	0.45657	2.41634
3	0.40161	4.44880
4	0.31746	6.60944
5	0.30090	7.99706
6	0.27725	8.37584
7	0.22549	7.58645
8	0.22529	5.93930
9	0.22546	4.00408
10	0.22430	4.17732
15	0.10265	3.16234
20	0.02622	2.72247
25	0.02252	13.06231
30	0.01812	2.60947
35	0.01766	5.80914
40	0.01743	4.13753
45	0.01604	11.49648
50	0.01346	2.66334
55	0.00261	3.68004
60	0.00136	2.58204
65	0.00088	7.98733
70	0.00078	4.17401
75	0.00010	3.16856
80	0.00008	2.76308
85	0.00006	13.01733
90	0.00005	2.66917
95	0.00004	5.81383
100	0.00005	3.00000
105	0.00004	0.72215
110	0.00004	0.12171
115	0.00004	0.02051
120	0.00004	0.00346
125	0.00004	0.00058
130	0.85338	1.50008
135	0.80608	2.26976
140	0.81730	2.56034
145	0.87375	2.44955
150	0.95636	1.99762
155	1.02919	1.31291
160	1.06034	0.58116
165	1.05790	0.58452
170	1.04811	0.55340
175	1.04484	0.62896
180	1.04917	0.67296
185	1.05711	0.60456
190	1.06451	0.47088
195	1.06923	0.31345
200	1.07121	0.16385

Figure 26B. Identification Error and Vibration
Level

88

In each case, although the vibration was still nearly eliminated, a steady-state error remained in the identified inverse matrix after the step changes in vibration and T. An error was introduced into the inverse matrix because, although the identification update to the inverse estimate was made proportional to ($\Delta \Theta - C(k)\Delta Z^T$), the change in vibration, ΔZ, did not correspond to the change in cyclic pitch, $\Delta \Theta$, at iteration 130 due to the introduction of a step in the uncontrolled vibration. Hence, the inverse estimator interpreted the error as a result of improper inverse matrix identification, rather than as a change in uncontrolled vibration. After step 130, the changes in pitch correspond to the changes in vibration, and the inverse estimate is recorrected with some residual error.

The reason for the residual steady state identification error can be found by examination of the inverse control law and the inverse update equation:

$$\Delta \Theta_i^* = -C_i^T(k)Z_{measured}$$

$$C_i^T(k+1) = C_i^T(k) + 2k_i\Delta Z(\Delta \Theta_i^* - C_i^T(k)\Delta Z^T)$$

It is seen that if the measured vibration level goes to zero, the commanded change in pitch will also go to zero. This, in turn, causes the change in vibration, ΔZ to go to zero, and thereby makes the inverse update term go to zero. Hence, the inverse estimate is prevented from changing, even though the inverse may be in error. Reaching the optimal control before the inverse can be identified with low error presents problems only in that the controller is more likely to become unstable in the event of a sudden change in the vibration vector. Note that the reason the optimal pitch may be found before the inverse is completely identified is because it may

have been formed by some linear combination of $\Delta\Theta s$ over several iterations.

This line of reasoning suggests that if the control is relaxed, or in other words, if the implemented control is only allowed to be a fraction of the commanded control, the identification might be improved. This was shown in Figures 25 and 26, where a lower steady-state identification error was achieved by reducing the control relaxation from 1.0 to 0.3 . Note that the lower steady state inverse identification error is traded-off there against a slower vibration reduction time. It is evident that control relaxation, as well as the stability gain matrix selection, have an influence on inverse identification.

Many other runs were made with the (3 x 3) simulation, but are not presented here in deference to presenting similar results from the (6 x 6) simulation, to be discussed next.

6.3

ADAPTIVE INVERSE CONTROL SIMULATION
WITH THE (6 X 6) T MATRIX

Unfortunately, no (6 x 6) transfer matrices of the type discussed in Section 3.3 were available from test data. However, another (6 x 6) transfer matrix, representing the 4/Rev response to cyclic pitch oscillations at 2/Rev, 3/Rev, and 4/Rev was available from the test data of Chopra and McCloud, 1981. This matrix (figure 27) was used as if it represented the 4/Rev response to 4/Rev longitudinal, collective, and lateral pitch oscillations. This matrix is less well conditioned than the (3 x 3) matrix, but performs similarly when scaled. By scaling the rows of the matrix, the numerical accuracy of the inverse control technique is improved, in that, the inverse need not contain very small or large numbers. This corresponds to adjusting the input gains on the accelerometer (vibration) input channels. If the vibration signal is not too small, then the transfer matrix terms will not be too small, and the inverse terms too large.

An important feature of the (6 x 6) simulations was that the effect of control relaxation was studied extensively. Figure 28 has been included to give the reader an idea of how the vibration control is influenced by changes in the control relaxation term. For no relaxation (relaxation constant = 1.0), the vibration is alleviated in one step (Figure 28), as expected. Note that as the relaxation constant is made closer to zero, the vibration is reduced at a progressively slower rate. With the control relaxation set to zero, the vibration is uncontrolled, as seen in the last frame. Note that for

91

these figures, the inverse matrix is without error. Hence, these plots form a baseline case in which inverse vibration control is only a function of the control relaxation.

Response harmonics	Control harmonics					
	2 cos	2 sin	3 cos	3 sin	4 cos	4 sin
Vertical acceleration						
4 cos	-15.17	-2.02	18.73	-56.22	102.96	20.05
4 sin	-5.87	-22.50	54.65	17.76	-21.61	67.37
Lateral acceleration						
4 cos	0.73	8.98	-20.52	-2.79	9.34	-8.19
4 sin	-5.52	6.91	2.80	-21.07	20.52	1.93
Longitudinal acceleration						
4 cos	-0.98	0.26	0.05	-2.28	3.89	0.62
4 sin	-0.42	-1.11	2.04	-0.09	-0.22	1.71

Figure 27   Data for a (6 x 6) Transfer Matrix, taken from Controllable Twist Rotor (Chopra and McCloud, 1981).
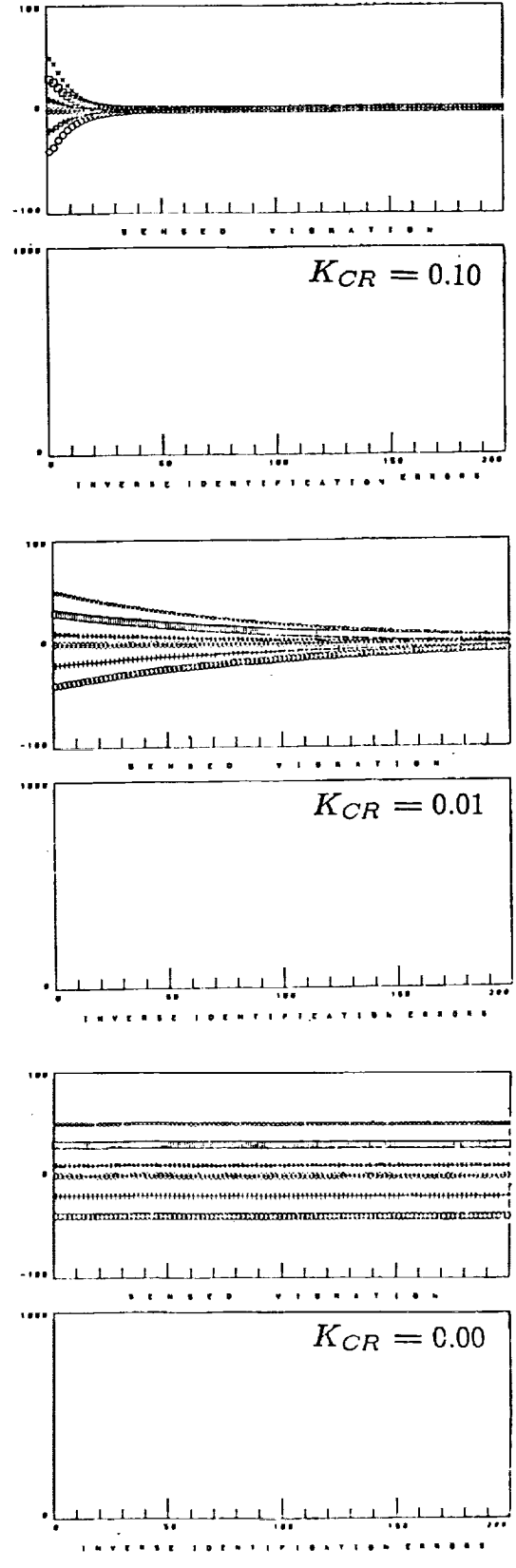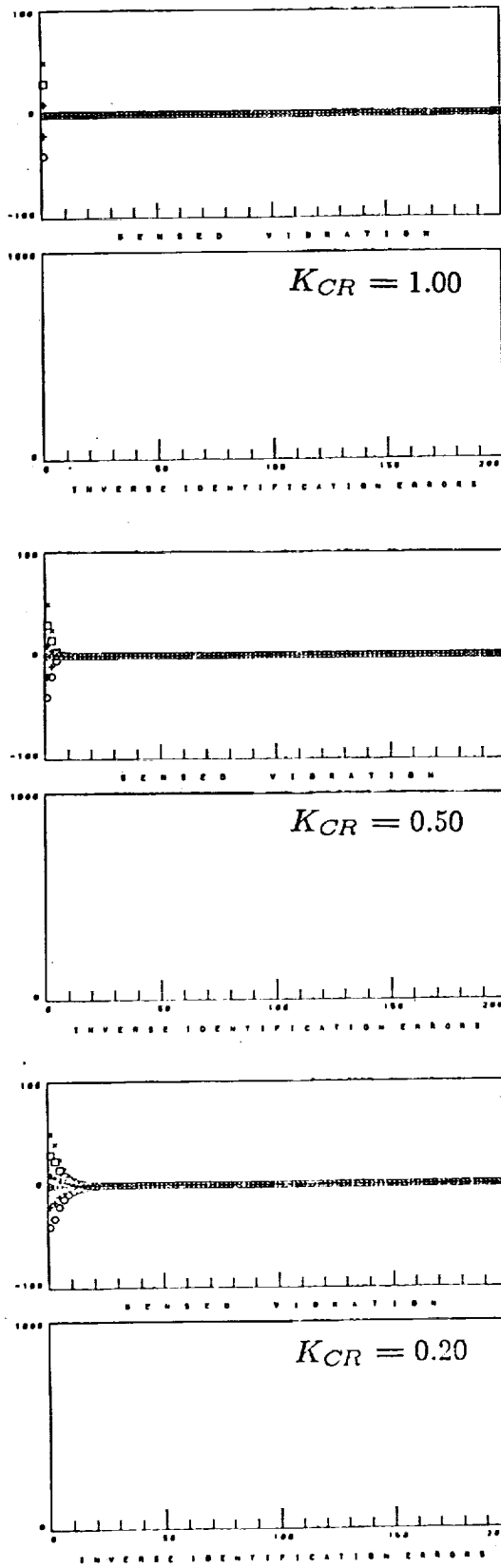
Figure 28   Vibration Control Using Perfect Inverse (6 x 6) Matrix,
Varying the Control Relaxation.

For the (6 x 6) simulation runs, the learning phase concept was not used. The reason for doing this was to simulate the control phase identification dynamics, for which each change in vibration, in essence, formed a new initial condition. The procedure used in the (6 x 6) simulations was to therefore select an initial estimate of the inverse matrix, and then study resulting control phase.

In Figures 29 through 31, the initial estimate of the inverse matrix was selected to be in error by ten percent, and the stability gain matrix, K_s, was selected with all diagonal terms equal to 0.001 . The control relaxation term was then varied from 0.01 in Figure 29, to 1.0 in Figure 31. Figure 30 presents the "Part A" results to conserve space. The effect of using progressively less control relaxation, should be noted. Whereas the inverse is identified well with high control relaxation (figure 29C), the inverse is poorly identified for low control relaxation (figure 31C).
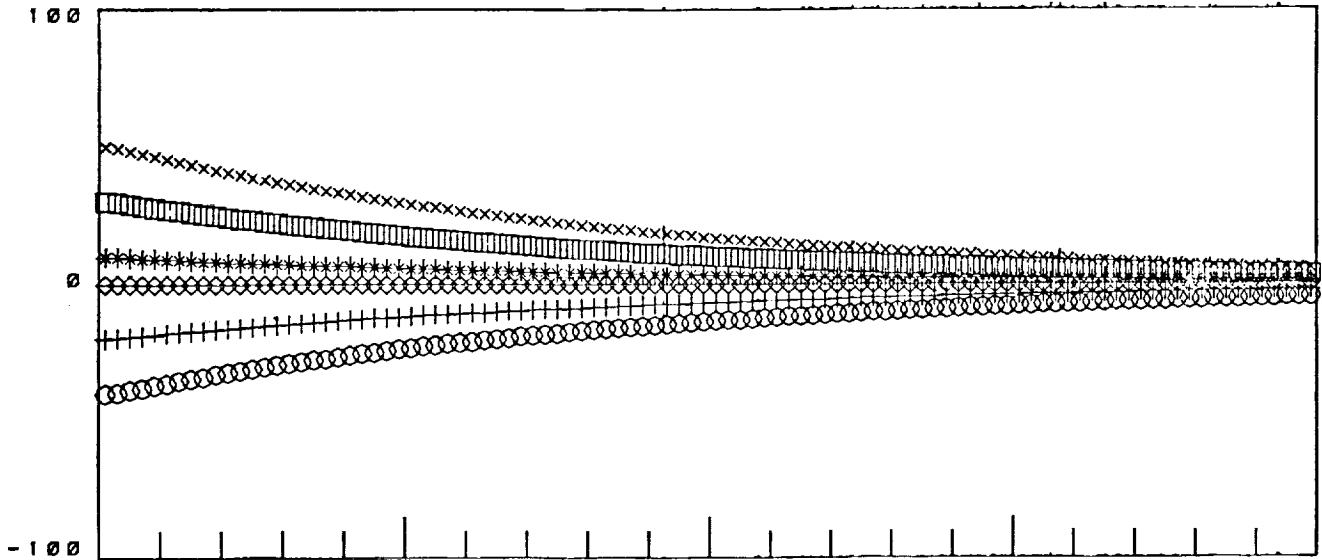
SENSED VIBRATION
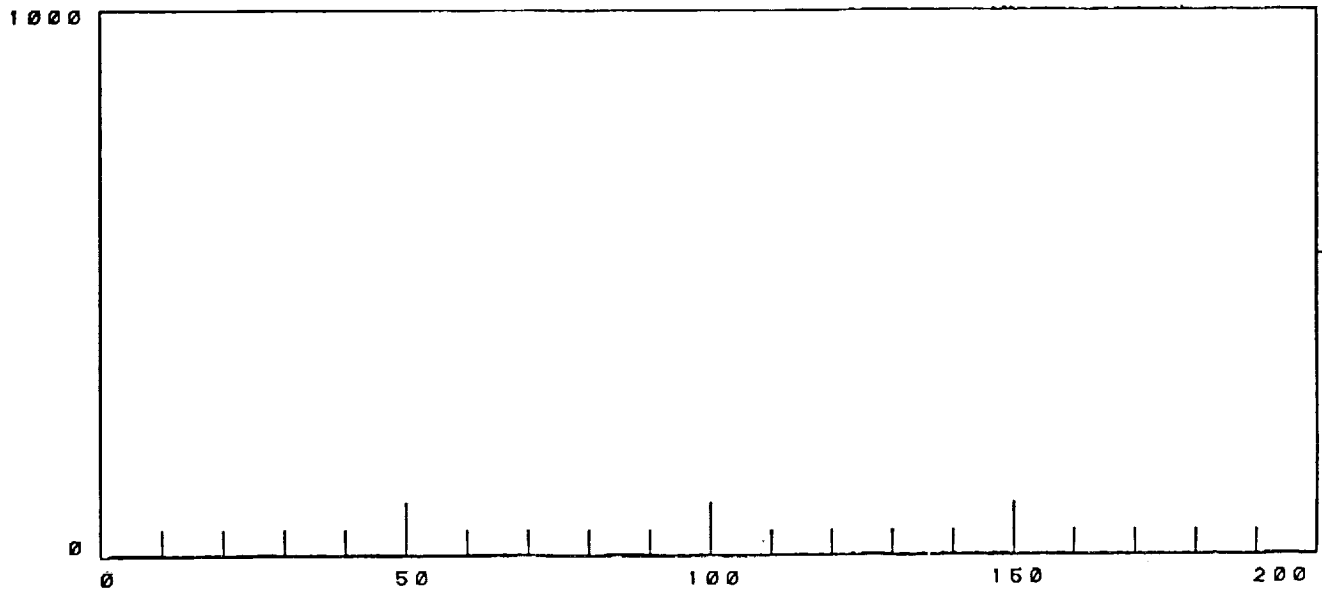
INVERSE IDENTIFICATION ERRORS

GAIN VECTOR: 0.0010 0.0010 0.0010 0.0010 0.0010 0.0010
PERCENT NOISE: CONTROL RELAX:
     0.0000   0.0100

Figure 29A   Vibration Reduction with Ks Diagonals = 0.001, 10 Percent
             Initial Inverse Error, and Control Relaxation of 0.01 for the
             (6 x 6) Quasi-Steady Vibration Control Case.

95

ITERATION	I.D. ERROR	VIBRATION
1	0.00000	0.00000
2	2.70784	150.00000
3	2.70378	148.35011
4	2.69982	146.71857
5	2.69596	145.10516
6	2.69220	143.50956
7	2.68852	141.93190
8	2.68494	140.37164
9	2.68144	138.82872
10	2.67803	137.30290
15	2.66218	129.92390
20	2.64813	122.94457
25	2.63568	116.34277
30	2.62463	110.09769
35	2.61481	104.18973
40	2.60608	98.60040
45	2.59831	93.31223
50	2.59139	88.30882
55	2.58522	83.57457
60	2.57972	79.09496
65	2.57482	74.85612
70	2.57044	70.84521
75	2.56653	67.04943
80	2.56304	63.45761
85	2.55993	60.05850
90	2.55714	56.84174
95	2.55465	53.79759
100	2.55243	50.91656
105	2.55044	48.19007
110	2.54866	45.60971
115	2.54707	43.16770
120	2.54564	40.85641
125	2.54437	38.66905
130	2.54323	36.59890
135	2.54220	34.63960
140	2.54129	32.78524
145	2.54047	31.03025
150	2.53974	29.36914
155	2.53908	27.79709
160	2.53849	26.30927
165	2.53797	24.90096
170	2.53750	23.56819
175	2.53708	22.30666
180	2.53670	21.11275
185	2.53636	19.98269
190	2.53606	18.91321
195	2.53578	17.90096
200	2.53554	16.94279

Figure 29B   Identification Error and Vibration Level for Ks Diagonals = 0.001,
10 Percent Initial Inverse Error, and Control Relaxation of 0.01
for the Quasi-Steady (6 x 6) Vibration Control Case.

96

THE IDENTIFIED INVERSE

9.6789	5.9289	-4.9032	-4.6417	2.7936	-9.2607
-2.7635	0.5850	0.3519	1.9732	-0.8454	0.2848
-1.1708	-0.2741	-0.5716	0.9217	-0.5090	0.2042
-3.6503	-1.4716	1.5917	1.6138	-1.4146	2.8484
-0.2184	-0.2690	0.2909	0.2327	-0.4045	0.4492
1.7612	2.0517	-0.1726	-0.8439	0.6176	1.4833

THE TRUE INVERSE

8.8398	5.4144	-4.4493	-4.2197	2.5233	-8.4514
-2.5172	0.5289	0.3189	1.7938	-0.7666	0.2628
-1.0675	-0.2510	-0.5203	0.8379	-0.4615	0.1881
-3.3315	-1.3456	1.4444	1.4671	-1.2808	2.5999
-0.1997	-0.2452	0.2642	0.2115	-0.3673	0.4093
1.6097	1.8703	-0.1552	-0.7672	0.5580	-1.3553

INVERSE INITIAL ESTIMATE

9.7238	5.9558	-4.8942	-4.6417	2.7756	-9.2965
-2.7689	0.5818	0.3508	1.9732	-0.8433	0.2891
-1.1743	-0.2761	-0.5723	0.9217	-0.5077	0.2069
-3.6646	-1.4802	1.5888	1.6138	-1.4089	2.8599
-0.2197	-0.2697	0.2906	0.2327	-0.4040	0.4502
1.7707	2.0573	-0.1707	-0.8439	0.6138	-1.4908

Figure 29C   Identified, True, and Initial Inverse Matrices for Ks
Diagonals = 0.001, and Control Relaxation of 0.01 .
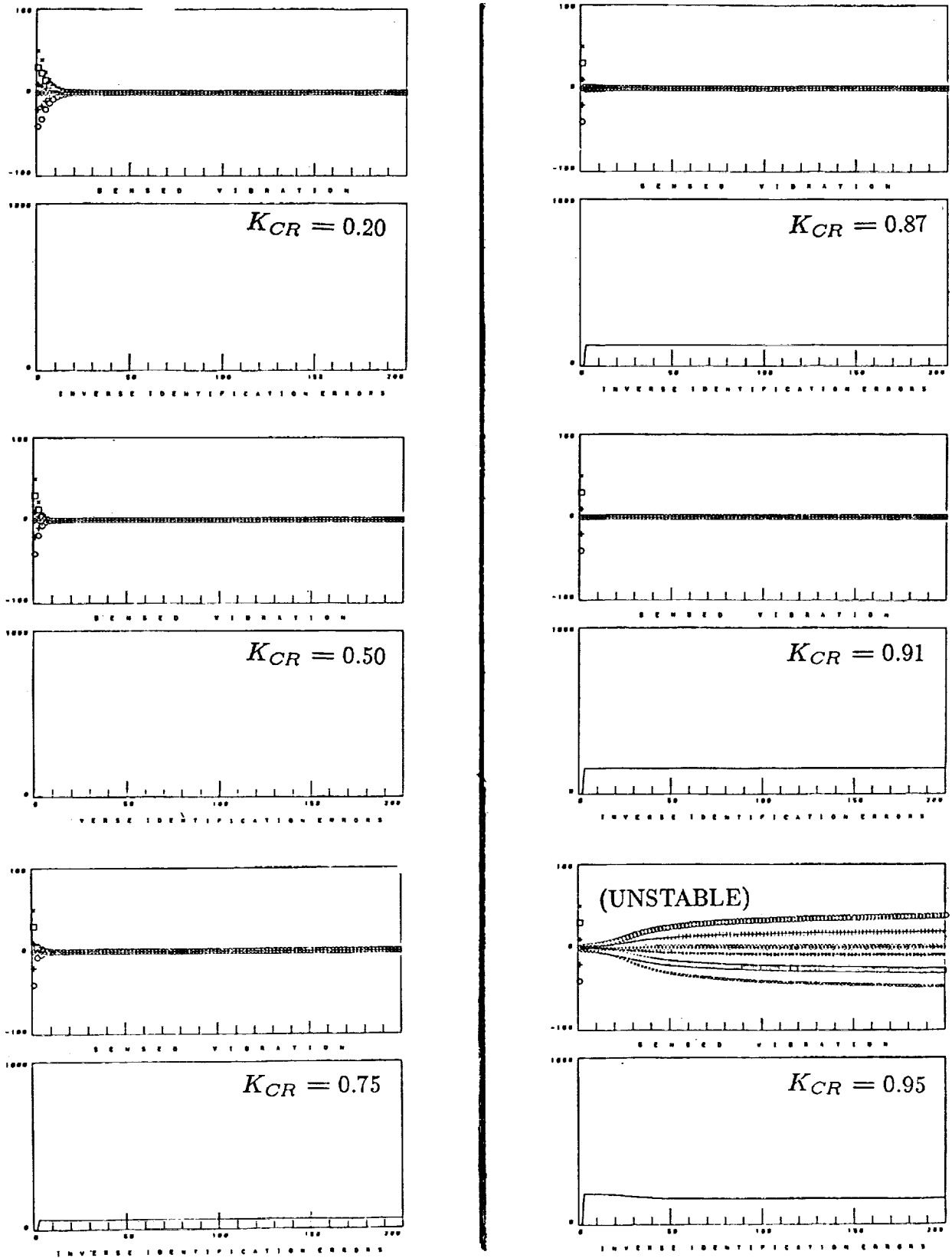
Figure 30   Identification Error and Vibration Reduction, with Ks
Diagonals = 0.001 and 10 Percent Initial (6 x 6) Inverse
Error, for Decreasing Control Relaxation.
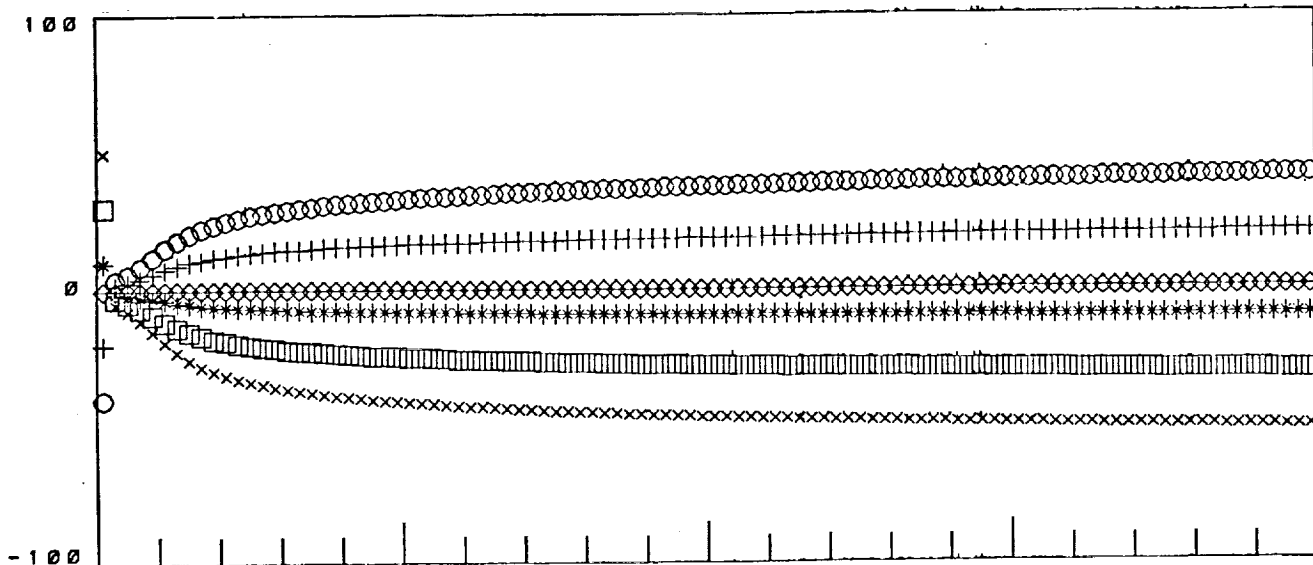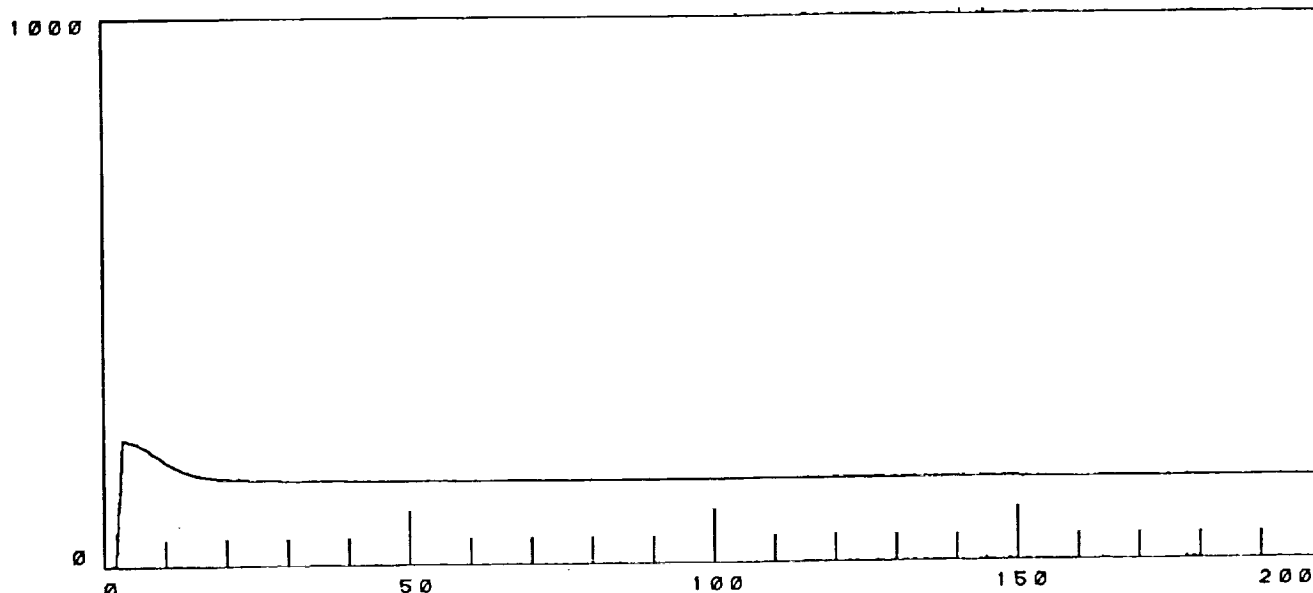
98

GAIN VECTOR: 0.0010 0.0010 0.0010 0.0010 0.0010 0.0010
PERCENT NOISE: CONTROL RELAX:
      0.0000   1.0000

Figure 31A   Vibration Reduction with Ks Diagonals = 0.001, 10 Percent
              Initial Inverse Error, and Control Relaxation of 1.0 for the
              (6 x 6) Quasi-Steady Vibration Control Case.

99

ITERATION	I.D. ERROR	VIBRATION
1	0.00000	0.00000
2	2.70784	150.00000
3	232.56639	15.00130
4	229.86093	18.46545
5	226.06357	22.59613
6	220.97832	27.42004
7	214.58533	32.89534
8	207.16658	38.88514
9	199.31558	45.16114
10	191.75626	51.43977
15	168.75954	76.76307
20	161.41302	91.73647
25	158.54373	101.28940
30	157.13205	108.05312
35	156.32390	113.19624
40	155.81157	117.30265
45	155.46278	120.69724
50	155.21259	123.57596
55	155.02562	126.06726
60	154.88138	128.25635
65	154.76724	130.20509
70	154.67496	131.95773
75	154.59900	133.54858
80	154.53563	135.00261
85	154.48187	136.34044
90	154.43594	137.57875
95	154.39630	138.72968
100	154.36169	139.80482
105	154.33122	140.81235
110	154.30437	141.76059
115	154.28036	142.65500
120	154.25891	143.50166
125	154.23959	144.30458
130	154.22217	145.06790
135	154.20638	145.79559
140	154.19193	146.49034
145	154.17873	147.15757
150	154.16664	147.79152
155	154.15543	148.40242
160	154.14514	148.98965
165	154.13564	149.55470
170	154.12672	150.09917
175	154.11844	150.62462
180	154.11076	151.13202
185	154.10356	151.62227
190	154.09680	152.09695
195	154.09053	152.55644
200	154.08459	153.0235

Figure 31B   Identification Error and Vibration Level for Ks Diagonals = 0.001,
10 Percent Initial Inverse Error, and Control Relaxation of 1.0
for the Quasi-Steady (6 x 6) Vibration Control Case.

100

THE IDENTIFIED INVERSE

1.2253	0.8552	-6.5934	-4.6407	6.1742	-2.4986
-1.7453	1.1960	0.5554	1.9731	-1.2526	-0.5297
-0.5281	0.1116	-0.4431	0.9216	-0.7660	-0.3099
-0.9482	0.1499	2.1320	1.6135	-2.4952	0.6870
0.0184	-0.1268	0.3382	0.2326	-0.4992	0.2598
-0.0153	0.9856	-0.5278	-0.8437	1.3280	-0.0622

THE TRUE INVERSE

8.8398	5.4144	-4.4493	-4.2197	2.5233	-8.4514
-2.5172	0.5289	0.3189	1.7938	-0.7666	0.2628
-1.0675	-0.2510	-0.5203	0.8379	-0.4615	0.1881
-3.3315	-1.3456	1.4444	1.4671	-1.2808	2.5999
-0.1997	-0.2452	0.2642	0.2115	-0.3673	0.4093
1.6097	1.8703	-0.1552	-0.7672	0.5580	-1.3553

INVERSE INITIAL ESTIMATE

9.7238	5.9558	-4.8942	-4.6417	2.7756	-9.2965
-2.7689	0.5818	0.3508	1.9732	-0.8433	0.2891
-1.1743	-0.2761	-0.5723	0.9217	-0.5077	0.2069
-3.6646	-1.4802	1.5888	1.6138	-1.4089	2.8599
-0.2197	-0.2697	0.2906	0.2327	-0.4040	0.4502
1.7707	2.0573	-0.1707	-0.8439	0.6138	-1.4908

Figure 31C   Identified, True, and Initial Inverse Matrices for
Ks Diagonals = 0.001, and Control Relaxation of 1.0 .

101

It is now seen that, unlike the case of using a perfect inverse estimate, with no error, the vibration control and identification may go unstable if the control is not relaxed enough. When the control is very relaxed (relaxation term small), the vibration reduction is smooth and steady. Vibration control improves as the control is relaxed less and less. Identification and control are unstable if the relaxation constant is 0.91 or higher, for the case of ten percent initial error in the inverse matrix. Also note that if the vibration is alleviated too quickly, a steady-state error in the identified inverse matrix persists. As before, the reason for the steady-state error is that once the vibration goes to near zero, the inverse update (or correction) also goes to zero.

The next figure shows the same type of results, with the initial estimate of the inverse again in error by ten percent, but with the diagonals of (K_s) increased to 0.01 . The results are presented in order of decreasing control relaxation.

(STABLE)

$K_{CR} = 0.100$

(MARGINALLY STABLE)

$K_{CR} = 0.287$

(STABLE)

$K_{CR} = 0.200$
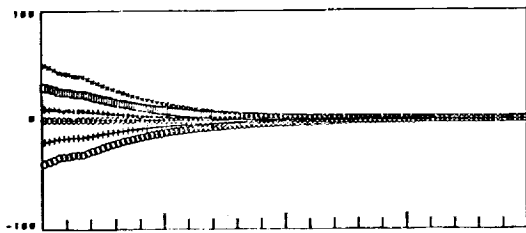
(UNSTABLE)

$K_{CR} = 0.300$

(STABLE)

$K_{CR} = 0.250$
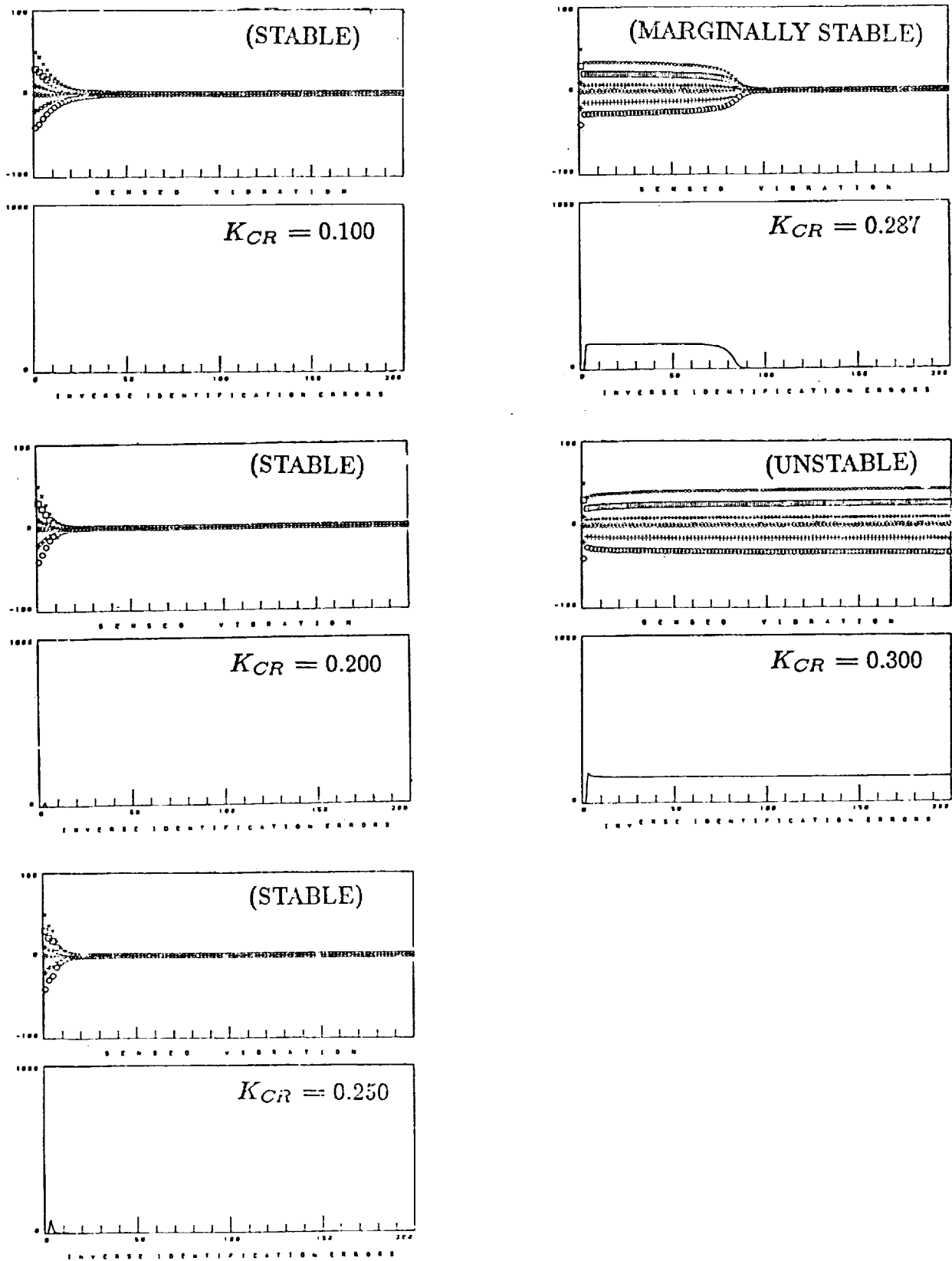
Figure 32   Quasi-Steady Vibration Control with Ks Diagonals = 0.001 and 10 Percent Initial Inverse Error, for Decreasing Control Relaxation.

Note that now even a relaxation term of 0.3 quickly destabilizes the adaptive inverse vibration control method. The boundary value for stable control and identification is where the relaxation term is 0.2870, (Figure 32). Note the interesting convergence pattern when stability is just marginal.

These results indicate that equivalent results are obtained by using a control relaxation of 0.2 with K_s diagonals of 0.001 or by using a control relaxation of 0.25 with K_s equal to 0.01. Note, however, that in the latter case, the system is closer to the unstable control relaxation limit. Furthermore, vibration reduction with K_s equal to 0.01 cannot be made to work as fast as that shown in Figure 30, showing K_s equal to 0.001 with a control relaxation of 0.87.

The next figures show that as the stability gain diagonal elements are increased, the control must be more and more relaxed to achieve stable vibration reduction.
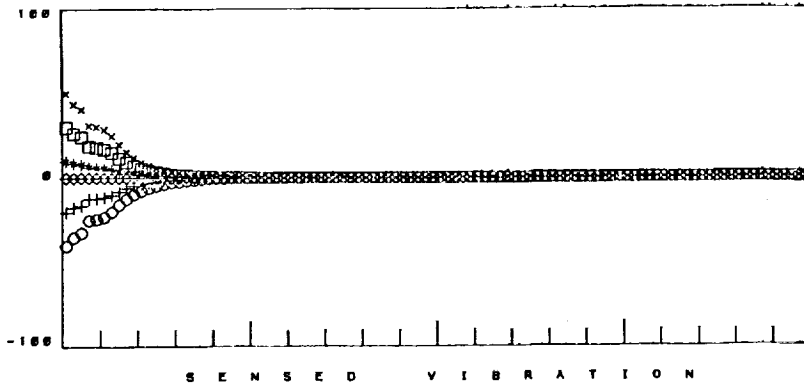
Control Relaxation
0.1155
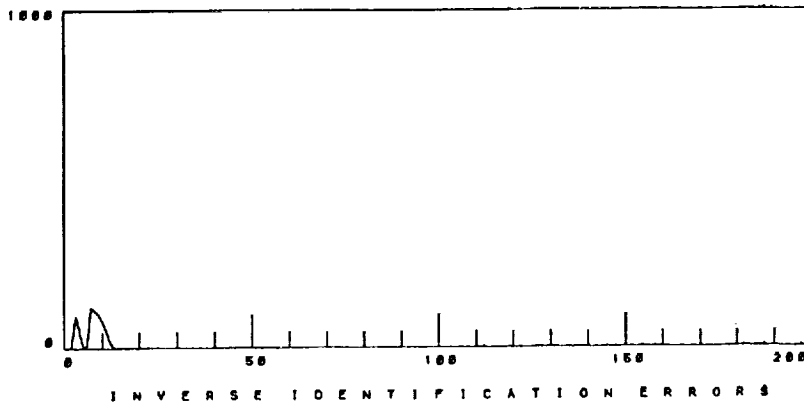
Stable, Good
Identification
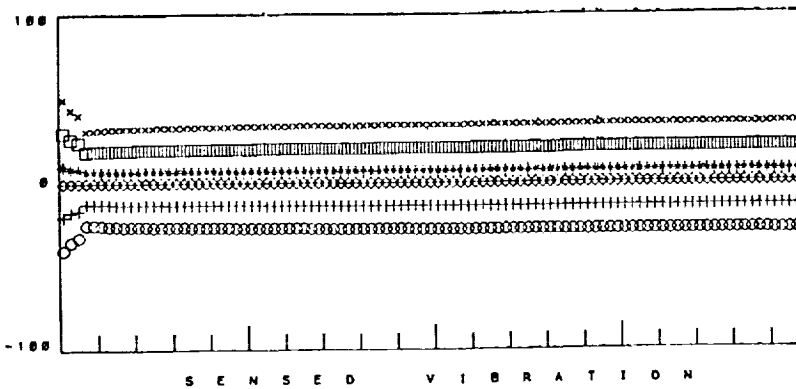
Control Relaxation
0 1156
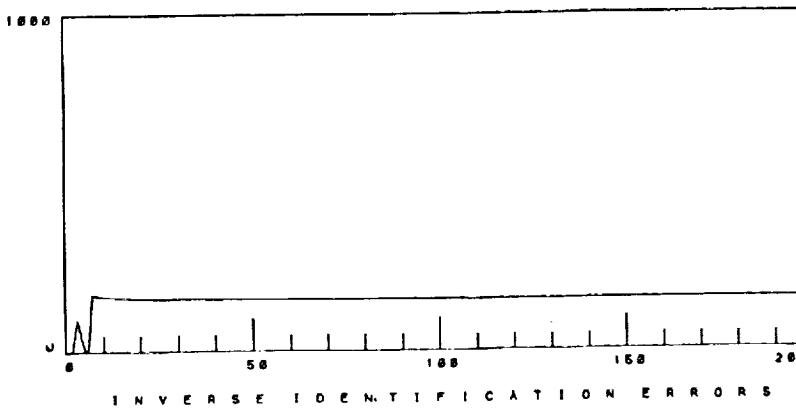
Unstable, Poor
Identification

Figure 33   Quasi-Steady Vibration Control with Ks Diagonals = 0.05
and 10 Percent Initial Inverse Error, for Two Values
of Control Relaxation.

105

Control Relaxation
0.060

Stable
Identfication

Control Relaxation
0.070

Stable
Identfication
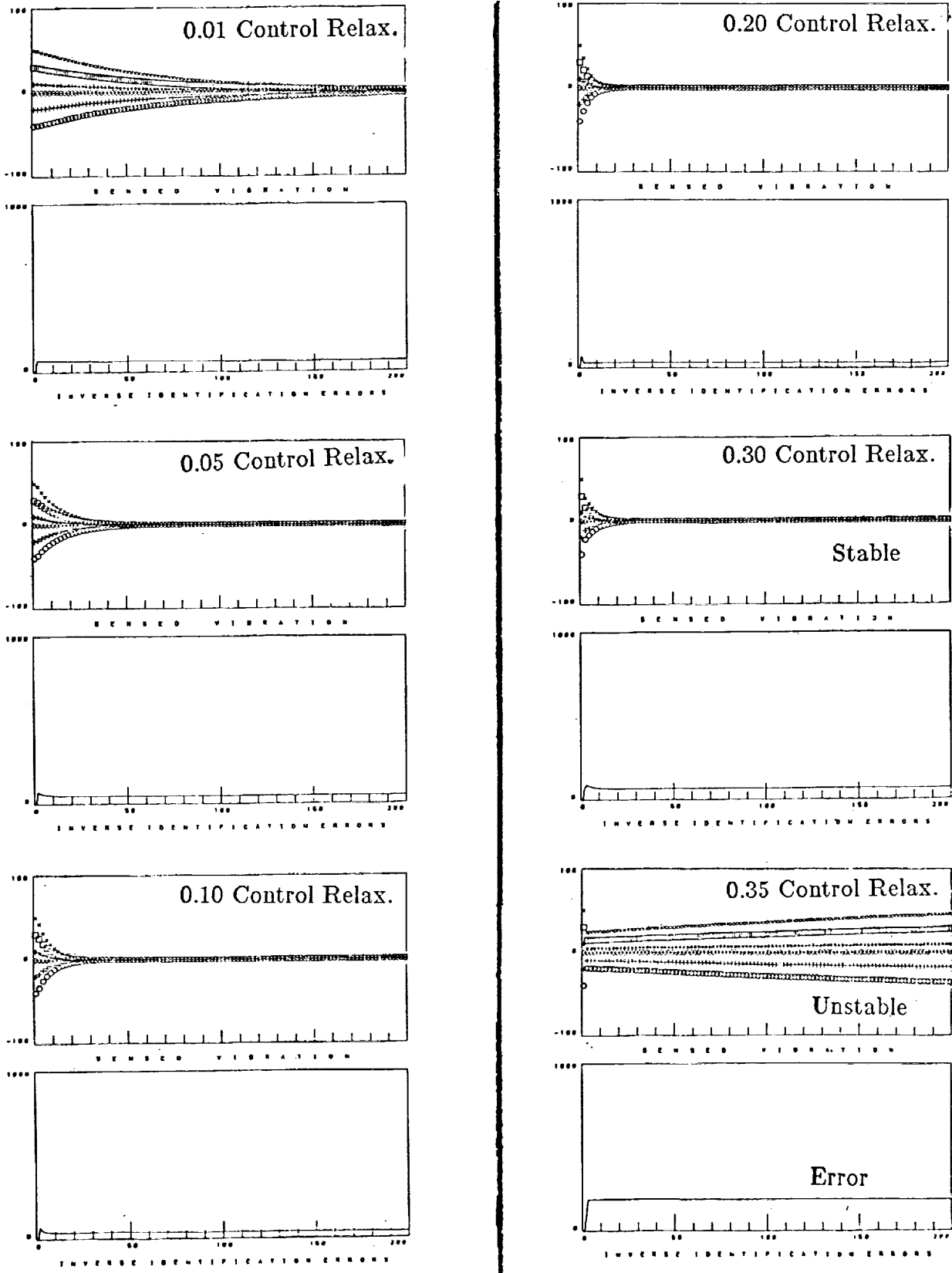
Control Relaxation
0.071

Marginally Stable
Identfication
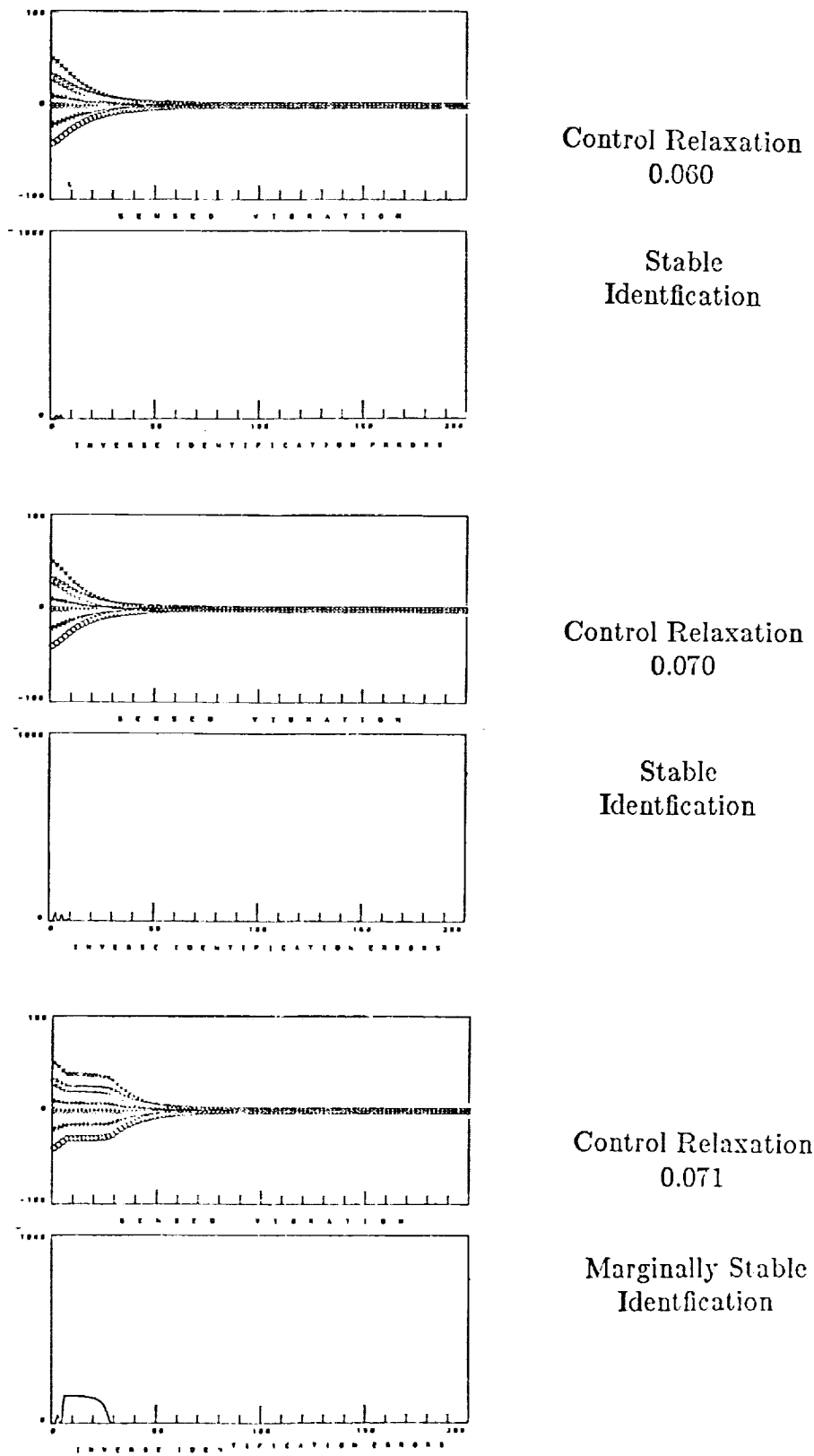
Figure 34   Quasi-Steady Vibration Control with Ks Diagonals = 0.10
and 10 Percent Initial Inverse Error, for Three Values of
Control Relaxation.

$K_S = 0.50$
$K_{CR} = 0.03$

$K_S = 5.0$
$K_{CR} = 0.005$

$K_S = 1.0$
$K_{CR} = 0.01$

$K_S = 5.0$
$K_{CR} = 0.0081$

$K_S = 1.0$
$K_{CR} = 0.02$
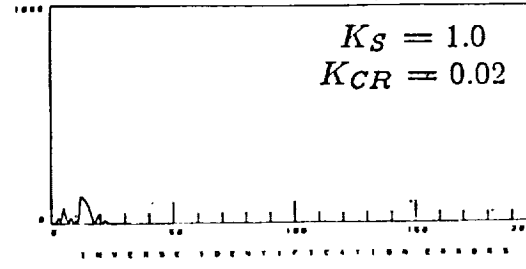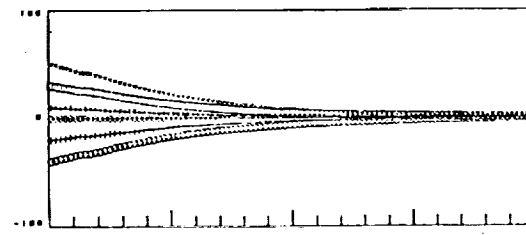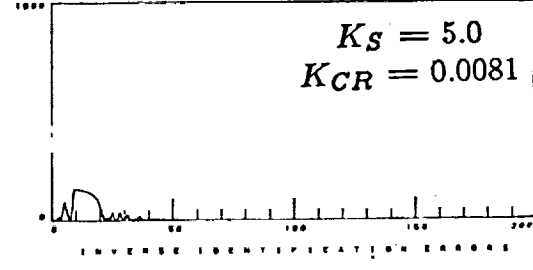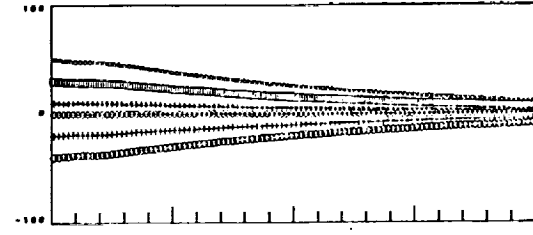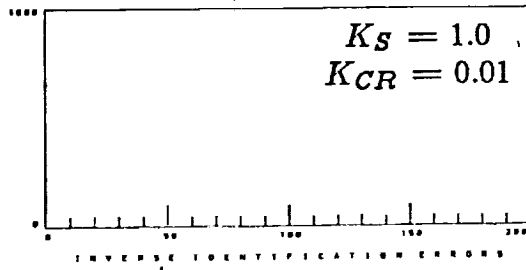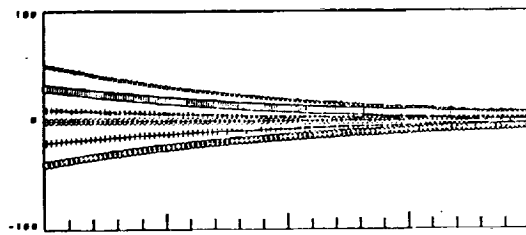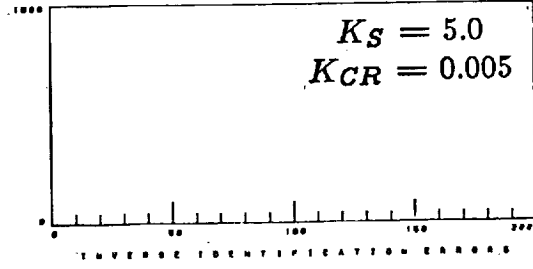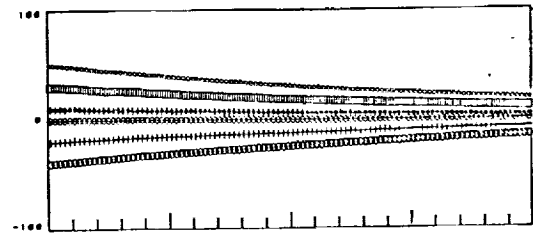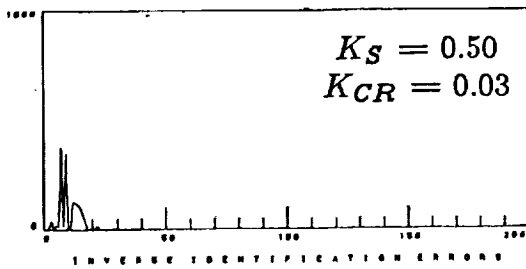
All have about the
Stability.

Figure 35   Vibration Reduction with 10 Percent Initial Inverse Error,
for Five Combinations of Control Relaxation and Ks Diagonals
Having Similar Quasi-Steady Vibration Control Trends.

107

The conclusion is that there are no absolute limits on either the magnitude of the stability gain matrix or the amount of control relaxation. Rather, it is the product of the control relaxation and the stability gain matrix magnitudes that is important. For K_s diagonal elements of 0.05, the relaxation constant must be less than 0.1155 . If the K_s diagonals are 0.1, the relaxation term can be no greater than 0.07. For K_s diagonals of 5.0, the identification is still stable if the control relaxation is less than 0.0081 . These points represent the points of maximum control relaxation which can be tolerated without making the system unstable, and have been plotted in Figure 36. This plot indicates that when the magnitude of the K_s diagonal elements are chosen to be 0.001, or less, the amount of control relaxation need be small (relaxation term large). Higher values of K_s have narrower control relaxation stability regions.

It seems that it is better to choose the diagonal elements or K_s small, and use a small amount of control relaxation, rather than choosing the diagonals of K_s to be large, and having a very narrow range of stable control relaxation values. For example, in figure 33 it is seen that for a K_s of 0.05, that a control relaxation of 0.1155 produces good convergence, whereas control relaxation of 0.1156 produces completely unstable convergence. Moreover, the preceding plots show that when K_s is large, the overall vibration reduction is slower, due to the higher amount of control relaxation needed to achieve stability. Hence, using smaller K_s diagonal elements and less control relaxation appears to make the LMS adaptive inverse control technique more robust.

The following figures present results for the same type of simulation as that done for the above cases, except that the initial estimate of the

inverse is in error by fifty percent, rather than ten percent. For each group of runs, the diagonal elements of the stability gain matrix are held constant, and the relaxation term is varied to explore the stability limits.
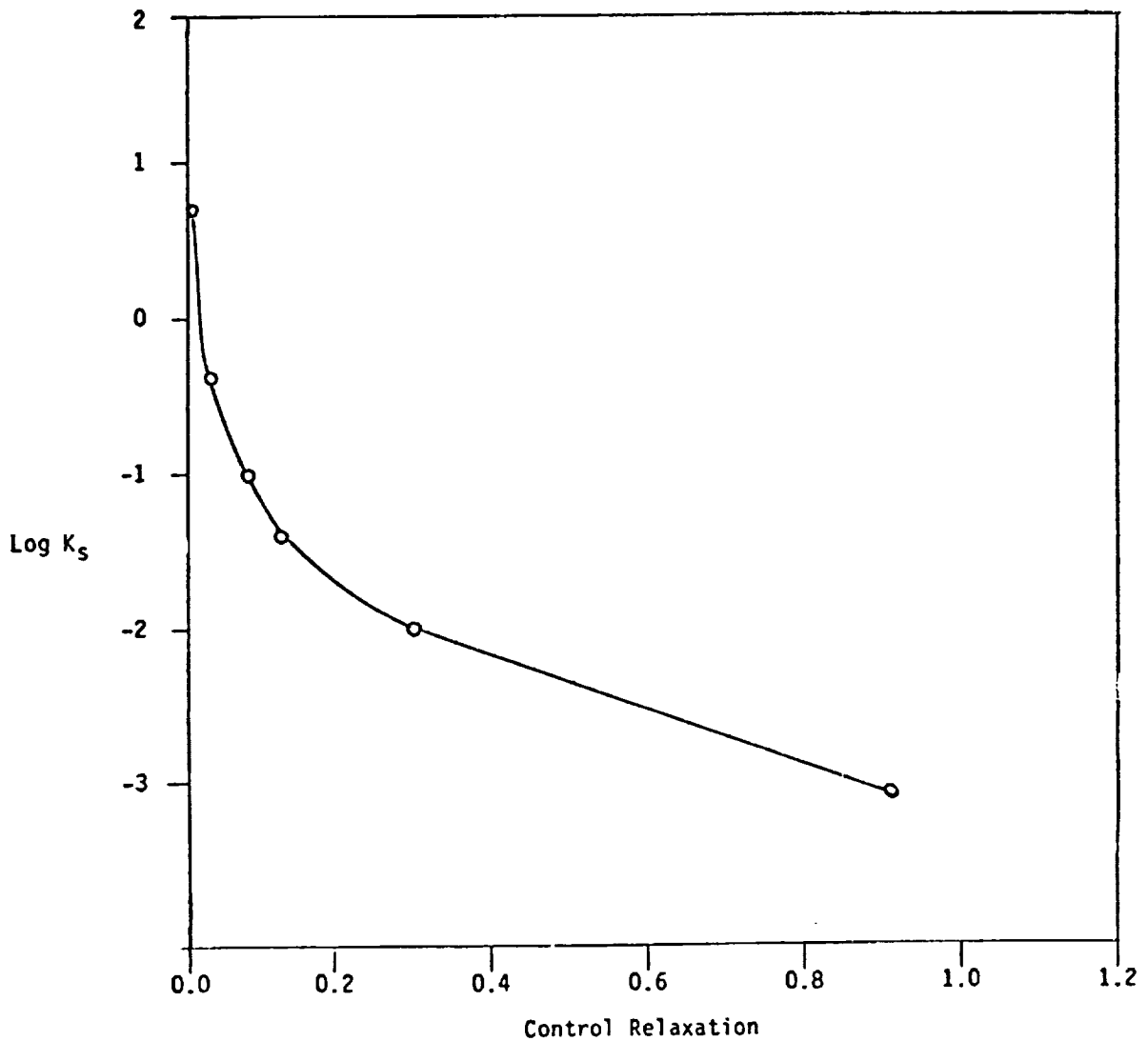
Figure 36   Plot of Adaptive Inverse Control Marginal Stability Points
for the (6 x 6) Simulation for 10 Percent Inverse Error,
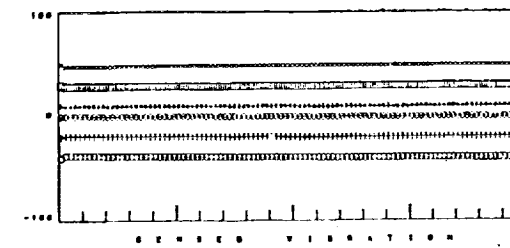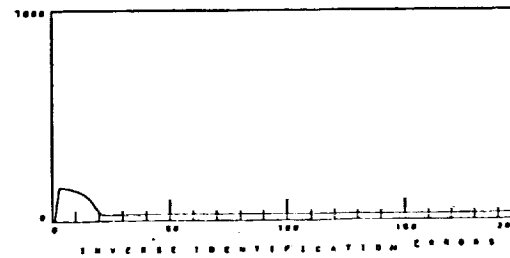Quasi-Steady Vibration Control Cases.

109

Figure 37   Quasi-Steady Vibration Control with Ks Diagonals = 0.001 and
50 Percent Initial Inverse Error, for Decreasing Control
Relaxation.

110

INITIAL INVERSE ESTIMATE

13.2597	8.1216	-6.6739	-6.3295	3.7850	-12.6771
-3.7758	0.7934	0.4783	2.6907	-1.1499	0.3942
-1.6013	-0.3765	-0.7804	1.2569	-0.6923	0.2822
-4.9973	-2.0164	2.1666	2.2006	-1.9212	3.8999
-0.2995	-0.3678	0.3963	0.3173	-0.5509	0.6140
2.4146	2.8055	-0.2328	-1.1508	0.8370	-2.0329

TRUE INVERSE

8.8398	5.4144	-4.4493	-4.2197	2.5233	-8.4514
-2.5172	0.5289	0.3189	1.7938	-0.7666	0.2628
-1.0675	-0.2510	-0.5203	0.8379	-0.4615	0.1881
-3.3315	-1.3456	1.4444	1.4671	-1.2808	2.5999
-0.1997	-0.2452	0.2642	0.2115	-0.3673	0.4093
1.6097	1.8703	-0.1552	-0.7672	0.5580	-1.3553

IDENTIFIED INVERSE, $K_{CR} = 0.20$

9.4268	5.8216	-7.4403	-6.3291	5.3177	-9.6112
-3.3145	1.0702	0.5706	2.6906	-1.3344	0.0252
-1.3100	-0.2017	-0.7222	1.2568	-0.8087	00491
-3.7722	-1.2833	2.4115	2.2005	-2.4111	2.9199
-0.1922	-0.3034	0.4178	0.3172	-0.5939	0.5281
1.6091	2.3221	-0.3938	-1.1507	1.1591	-1.3887

IDENTIFIED INVERSE, $K_{CR} = 0.35$

1.6619	1.1622	-8.9928	-6.3283	8.4230	-3.3999
-2.3798	1.6310	0.7575	2.6906	-1.7082	-0.7224
-0.7198	0.1524	-0.6042	1.2568	-1.0447	-0.4229
-1.2903	0.2050	2.9078	2.2003	-3.4036	0.9347
0.0252	-0.1729	0.4612	0.3172	-0.6808	0.3542
-0.0226	1.3430	-0.7201	-1.1505	1.8117	-0.0834

Figure 38   Comparison of Initial, True, and Identified Inverses for 50 Percent Initial Inverse Error, but Different Control Relaxation Values.

111
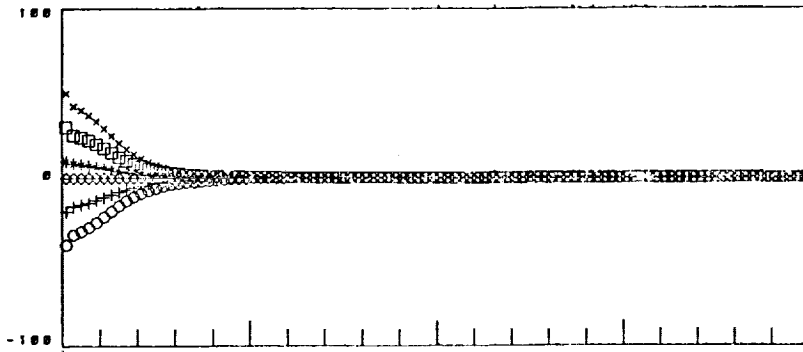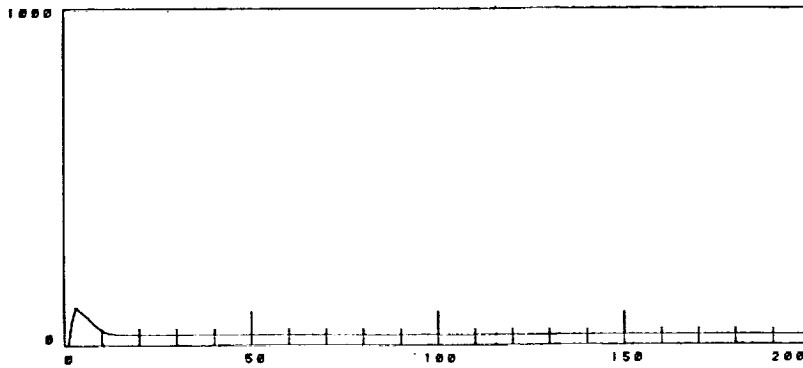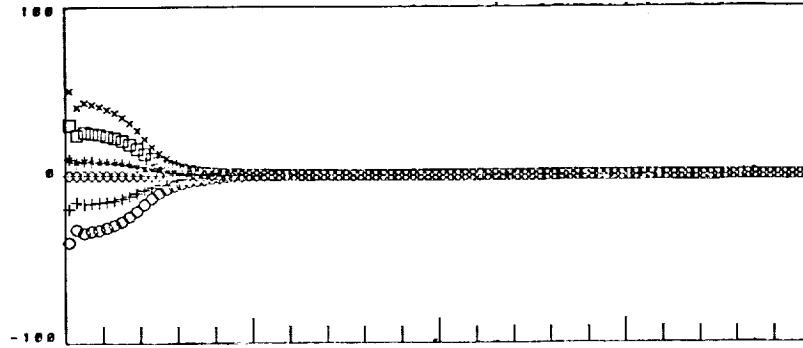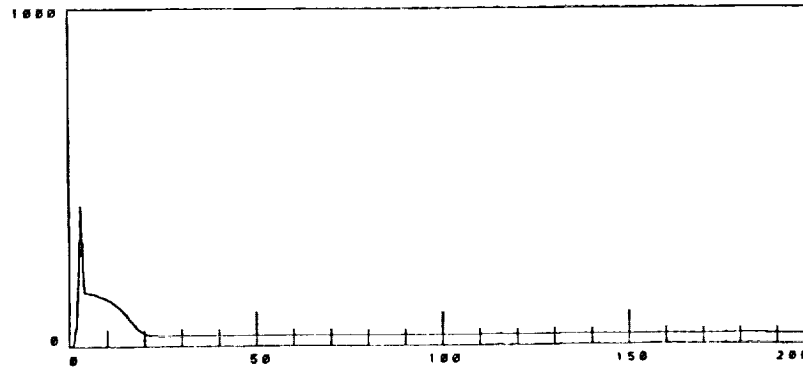
Control Relaxation
0.10

Control Relaxation
0.13

Figure 39   Quasi-Steady Vibration Control with Ks Diagonals = 0.01 and
50 Percent Initial Inverse Error, for Two Values of Control
Relaxation.
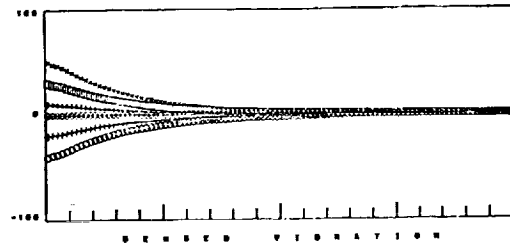
Stable

Control Relaxation
0.030
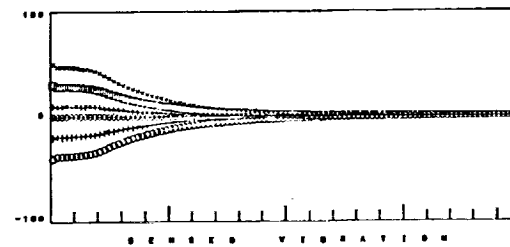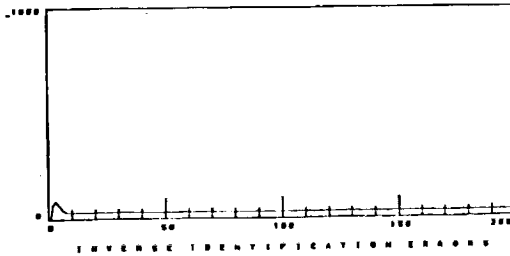
Marginally Stable

Control Relaxation
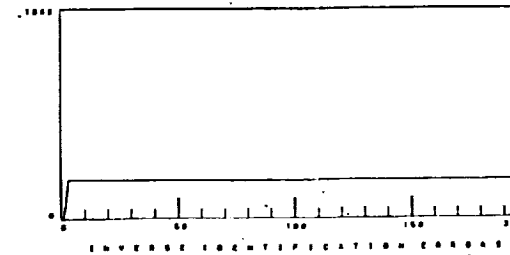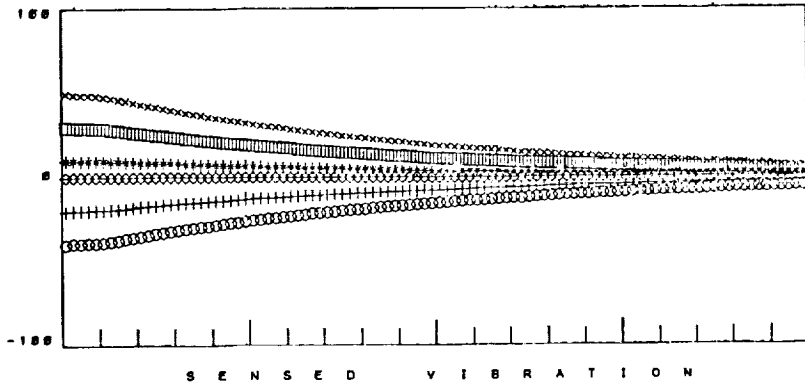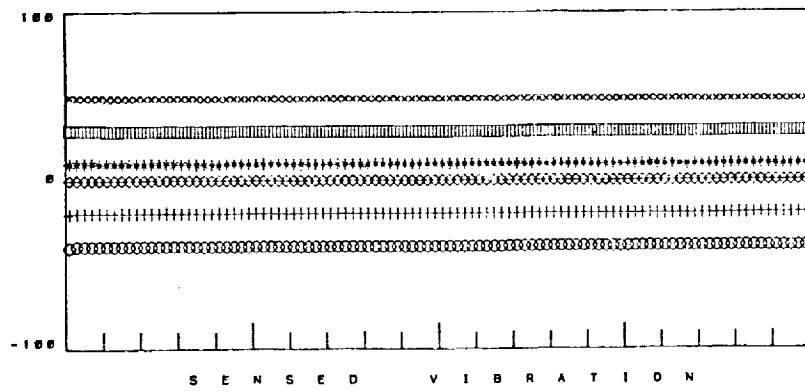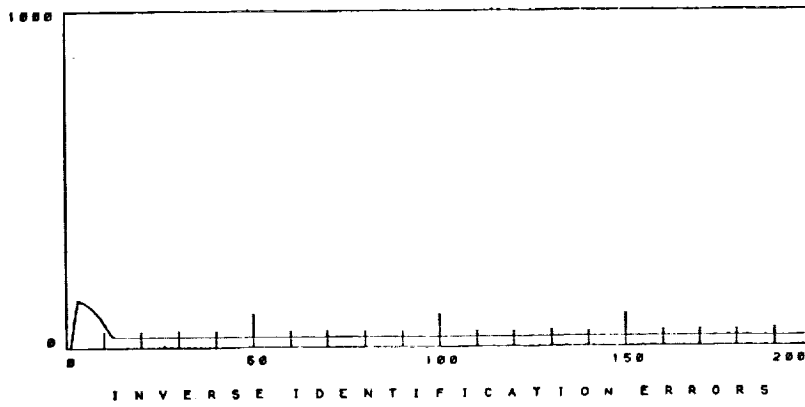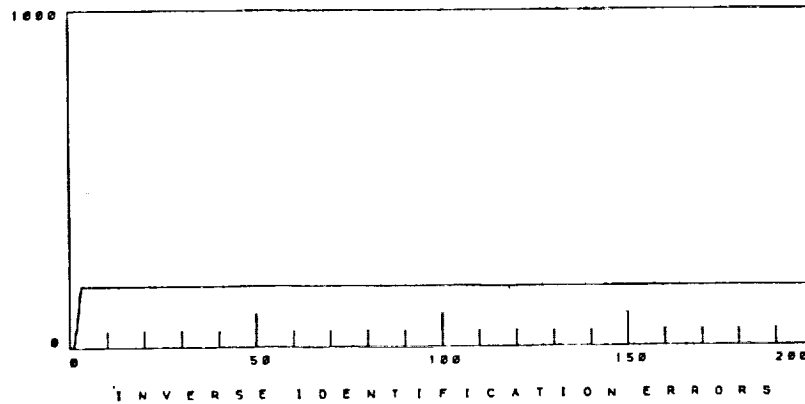0.034

Unstable

Control Relaxation
0.035

Figure 40   Quasi-Steady Vibration Control with Ks Diagonals = 0.10 and
50 Percent Initial Inverse Error, for Decreasing Control
Relaxation.

113

Marginally Stable
Control Relaxation
0.0105

Unstable
Control Relaxation
0.0110

Figure 41   Quasi-Steady Vibration Control with Ks Diagonals = 1.0 and
50 Percent Initial Inverse Error, for Two Values of
Control Relaxation.

INITIAL INVERSE ESTIMATE

13.2597	8.1216	-6.6739	-6.3295	3.7850	-12.6771
-3.7758	0.7934	0.4783	2.6907	-1.1499	0.3942
-1.5013	-0.3765	-0.7804	1.2569	-0.6923	0.2822
-4.9973	-2.0184	2.1666	2.2006	-1.9212	3.8999
-0.2995	-0.3678	0.3963	0.3173	-0.5509	0.6140
2.4146	2.8055	-0.2328	-1.1508	0.8370	-2.0329

TRUE INVERSE

8.8398	5.4144	-4.4493	-4.2197	2.5233	-8.4514
-2.5172	0.5289	0.3189	1.7938	-0.7666	0.2628
-1.0675	-0.2510	-0.5203	0.8379	-0.4615	0.1881
-3.3315	-1.3456	1.4444	1.4671	-1.2808	2.5999
-0.1997	-0.2452	0.2642	0.2115	-0.3673	0.4093
1.5097	1.8703	-0.1552	-0.7672	0.5580	-1.3553

IDENTIFIED INVERSE, $K_{CR} = 0.0105$

9.4052	5.8066	-7.4426	-6.3255	5.3233	-9.5972
-3.3119	1.0720	0.5709	2.6902	-1.3350	0.0235
-1.3083	-0.2006	-0.7220	1.2565	-0.8092	0.0481
-3.7653	-1.2784	2.4123	2.1994	-2.4129	2.9155
-0.1916	-0.3030	0.4178	0.317	-0.5940	0.5277
1.6046	2.3190	-0.3943	-1.1500	1.1603	-1.3857

IDENTIFIED INVERSE, $K_{CR} = 0.0110$

1.7597	1.2204	-8.9727	-6.3274	8.3831	-3.4791
-2.3917	1.6240	0.7550	2.6904	-1.7033	-0.7129
-0.7273	0.1480	-0.6057	1.2567	-1.0417	-0.4169
-1.3216	0.1874	2.9013	2.2000	-3.3909	0.9600
0.0224	-0.1746	0.4607	0.3172	-0.6797	0.3564
-0.0021	1.3552	-0.7159	-1.1504	1.8033	-0.1001

Figure 42   Comparison of Initial, True, and Identified Inverses for 50 Percent Initial Inverse Error, but Different Control Relaxation Values.

115

Again, it is found that as the diagonal terms of K_s are increased, the control must be more and more relaxed to obtain stable convergence. Moreover, it is seen that the relaxation limits become smaller as K_s becomes larger. The points of neutral stability have been plotted in Figure 43. In some cases, the relaxation must be so low that it is doubtful that the controller would be capable of functioning in an adaptive fashion. Whereas the (3 x 3) simulation had little trouble adapting the inverse estimate from all zeros, the higher order simulation evidenced troublesome identification if the initial inverse estimate was too far from the true inverse values. Hence, vibration control performance is compromised if the a plant inverse is too far away from the current estimate.

Figures 44, 45, and 46 plot the minimum identification error for three values of K_s as a function of control relaxation. It is seen that the LMS estimator is more tolerant to various control relaxation values if the stability gain magnitude is kept small. For high K_s values, only a very narrow region of control relaxation values will be even marginally stable.
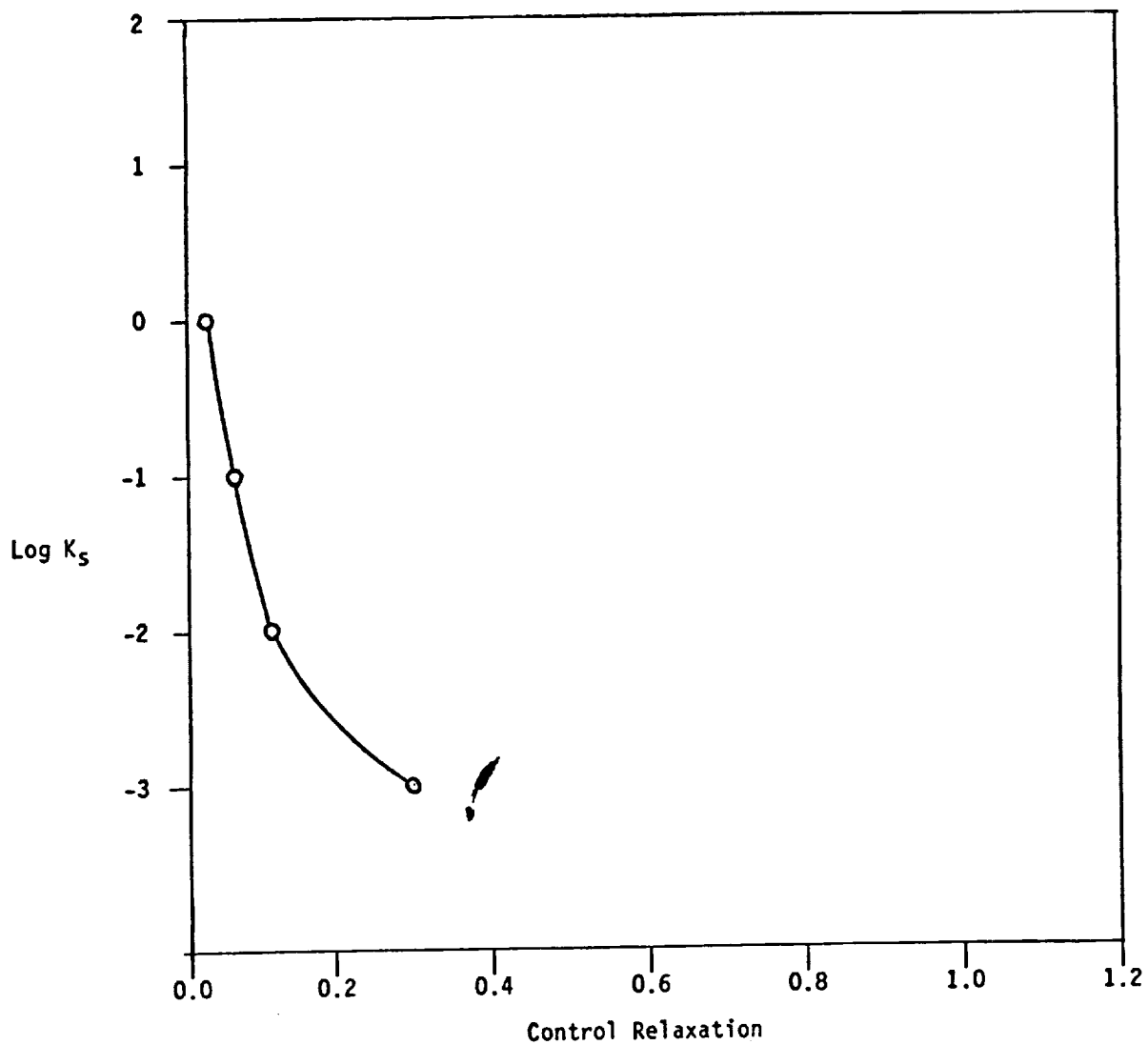
Figure 43 Plot of Adaptive Inverse Control Marginal Stability Points
for 50 Percent Initial Inverse Error, for the
Quasi-Steady (6 x 6) Simulation.

117
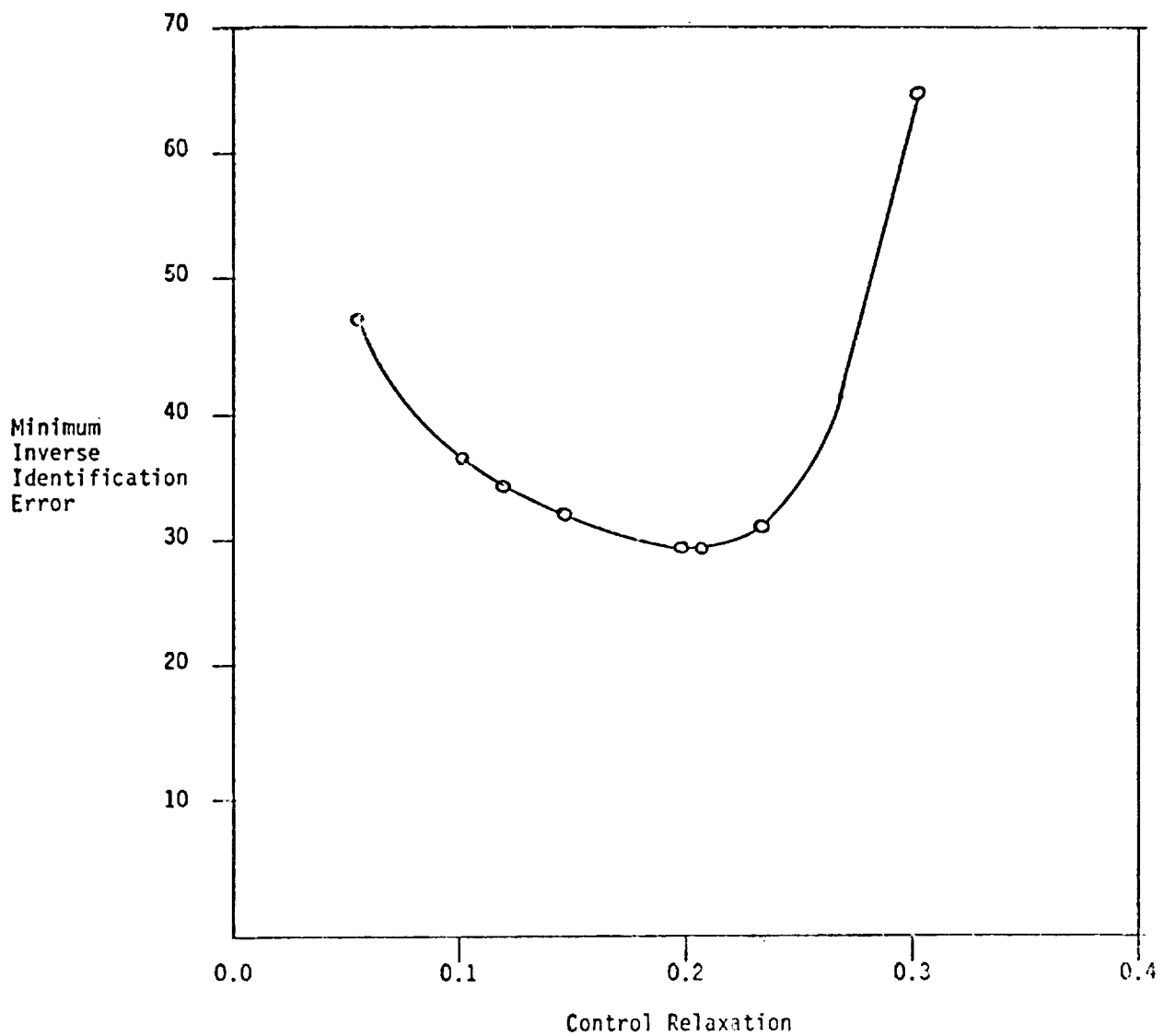
Figure 44   Plot of Minimum Inverse Identification Error in (6 x 6) Matrix
for Ks = 0.001, as a Function of Control Relaxation.
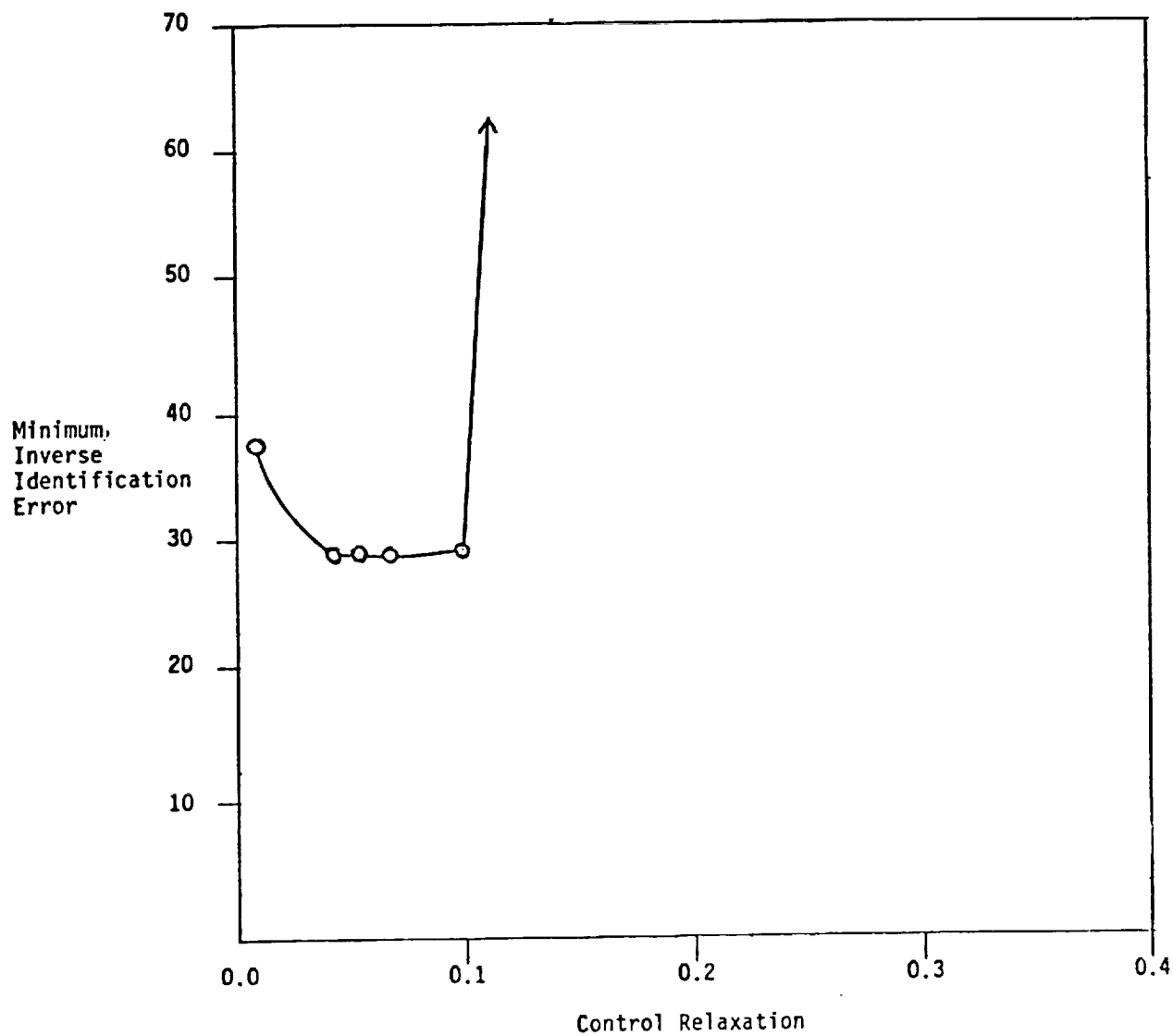
Figure 45   Plot of Minimum Inverse Identification Error in (6 x 6) Matrix
for Ks = 0.01, as a Function of Control Relaxation.
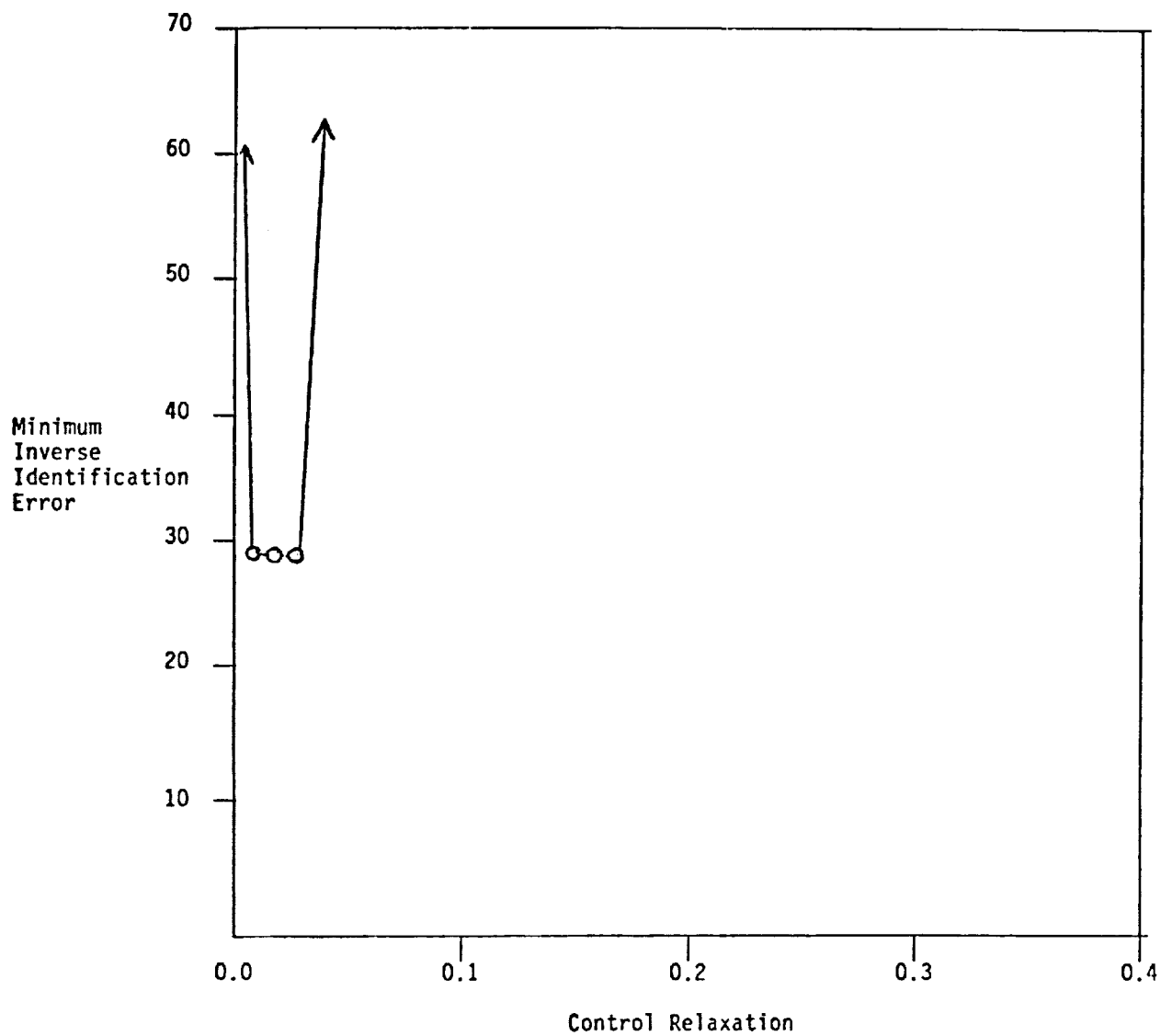
Figure 46   Plot of Minimum Inverse Identification Error in (6 x 6) Matrix
for Ks = 0.10, as a Function of Control Relaxation.

EFFECTS OF MEASUREMENT NOISE ON
LMS ADAPTIVE INVERSE CONTROL

In actual implementation of the extended LMS algorithm to control helicopter vibration, it is reasonable to expect some measurement noise (or FFT conversion) errors on the sensed vibration vector. Simulation studies with the (6 x 6) matrix were therefore made to determine the effect of noise on the performance of the LMS adaptive inverse control method. To do this, white noise was added to the sensed vibration vector representing the Fourier coefficients of the accelerometer signals.

The following figure demonstrates perfect inverse control in the presence of 1, 5, 10, and 20 percent white measurement noise. For these simulation runs, the initial inverse estimate contained no error and was not allowed to change (K_s = *zero*). The vibration is seen to be reduced to zero to within the tolerances permitted by the measurement noise. This figure is intended to serve as baseline comparison case which represents ideal inverse control using a perfect inverse and white measurement noise only.
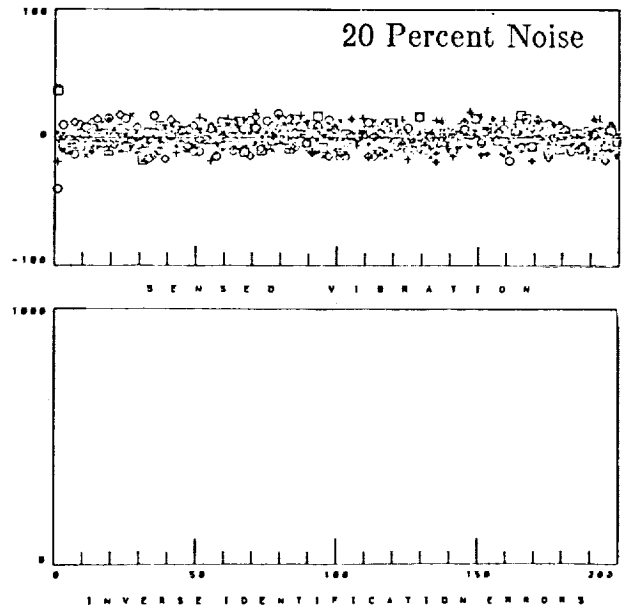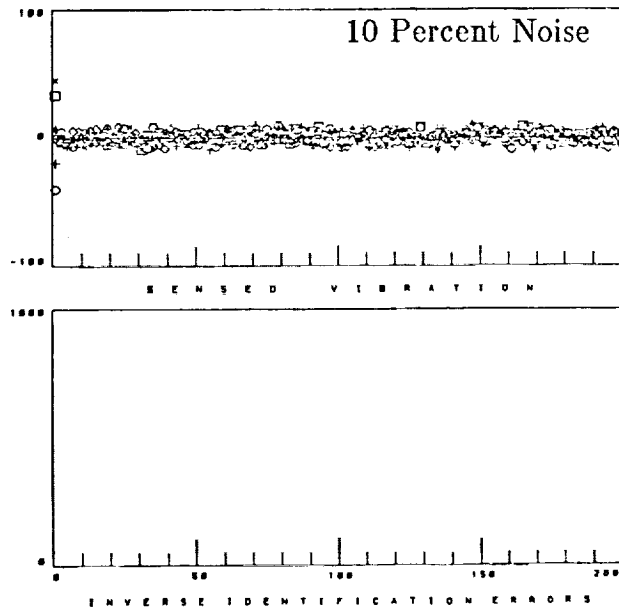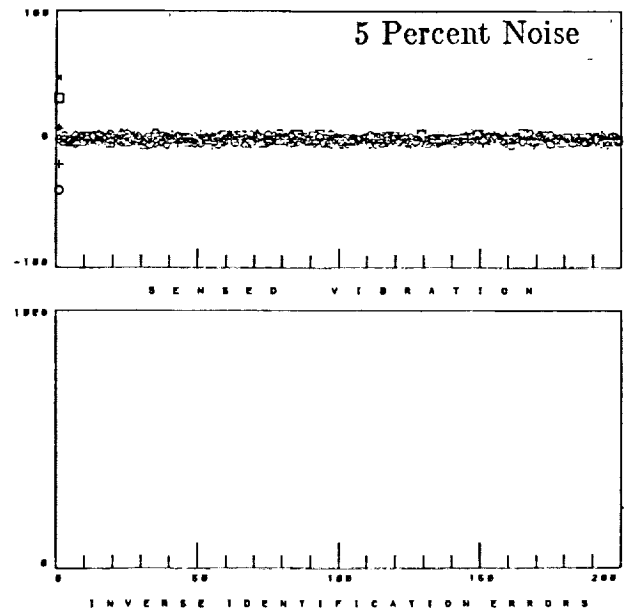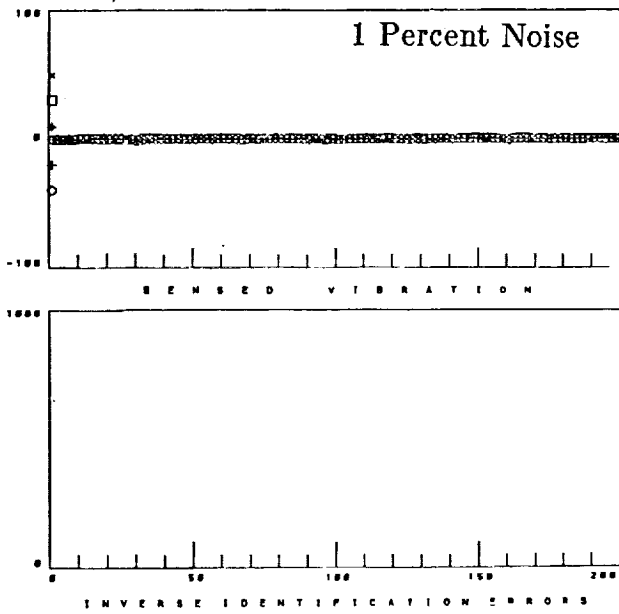
Figure 47   Perfect Inverse Control in the Presence of 1, 5, 10, and 20 Percent
White Measurement Noise for the (6 x 6)
Quasi-Steady Vibration Control Case.

122

The first question to be raised was whether or not the adaptive inverse control method was stable in the presence of white measurement noise. The answer, somewhat surprisingly, was that the method was not stable for even the most benign cases of sensor noise. Figure 48 illustrates that even for one percent measurement noise, and a $K_s = 0.001$ that the convergence process is unstable. The vibration appears to have been controlled well here, but examination of the digital record following the plot shows that the inverse identification error is growing with the number of iterations. Figure 49 shows that when the noise level is increased to five percent, the inverse identification error grows rapidly. Similar results are seen in Figure 50, where the noise has been left at one percent, but the stability matrix diagonals increased from 0.001 to 0.01 . Finally, in Figure 51 the identification process has been made very unstable with five percent noise and K_s equal to 0.01.
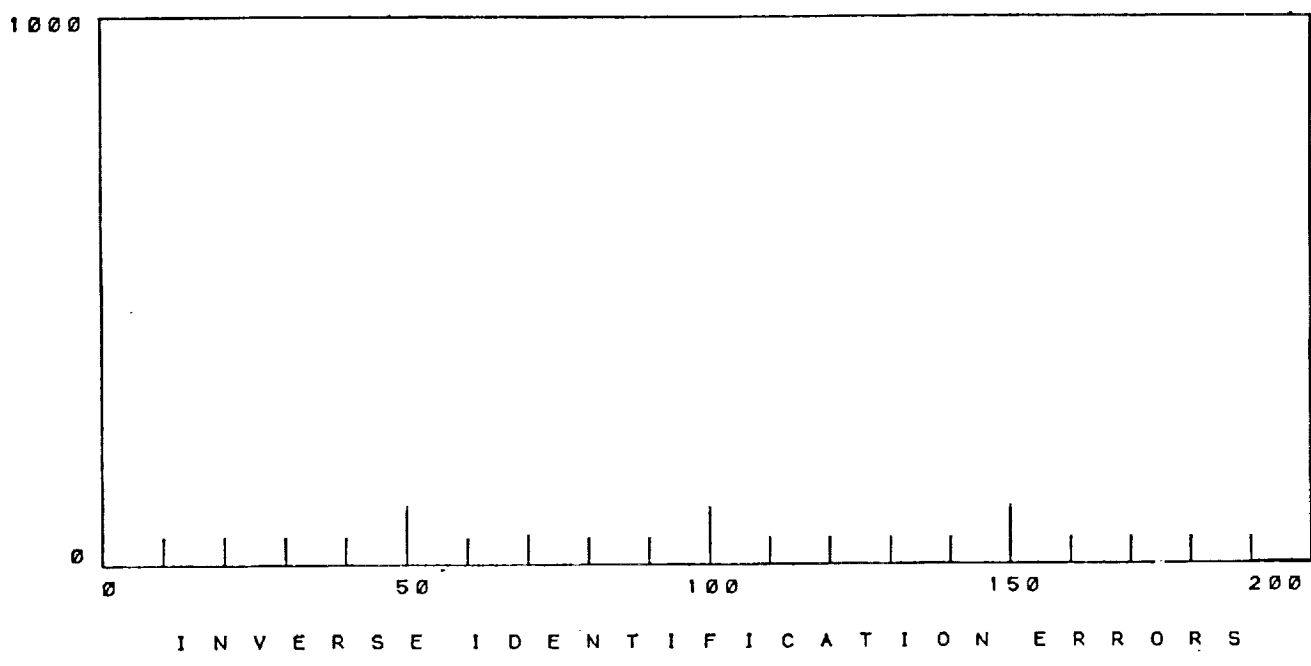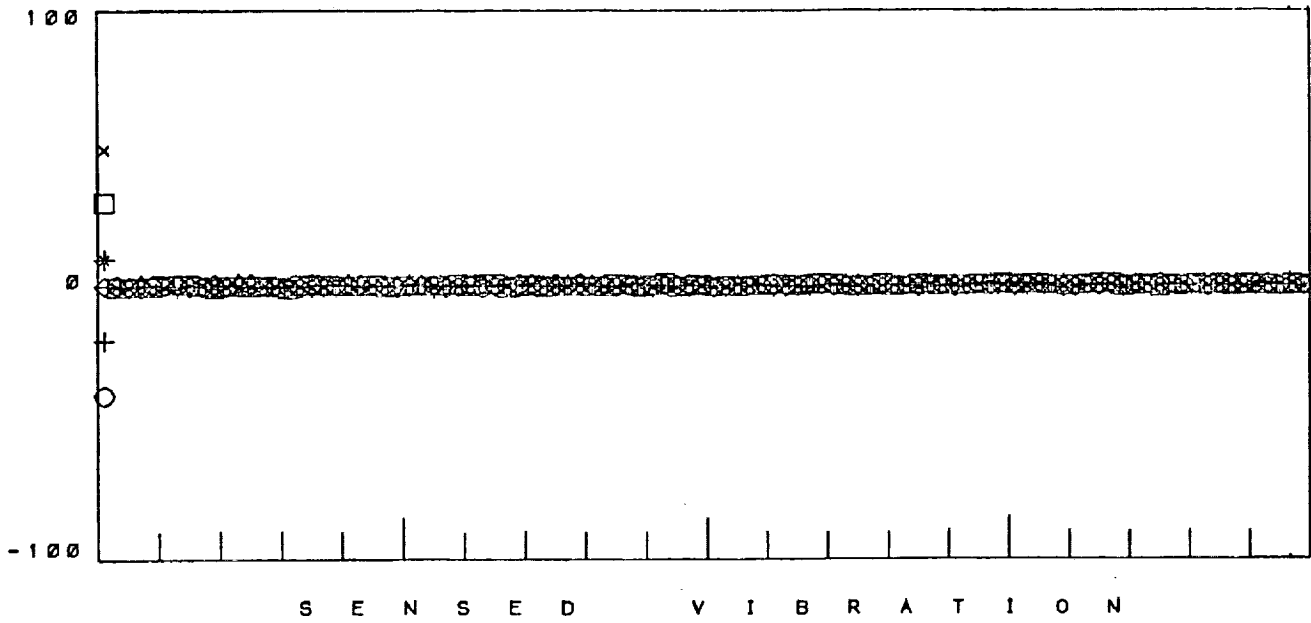
Figure 48A LMS Adaptive Inverse Identification Error and Vibration
Control with No Initial Inverse Error, and No Control
Relaxation with 1 Percent White Measurement Noise.

124

ITERATION	I.D. ERROR	VIBRATION
0	0.00000	0.00100
5	0.19499	2.24554
10	0.23230	2.52320
15	0.27613	2.15161
20	0.32952	1.75795
25	0.35224	1.61314
30	0.40595	2.35051
35	0.50009	2.43958
40	0.49889	1.50817
45	0.52570	1.02994
50	0.53991	1.71510
55	0.58883	2.21527
60	0.66305	2.38938
65	0.67575	2.10325
70	0.69195	2.10687
75	0.71217	1.94504
80	0.86533	2.67723
85	0.91436	1.82457
90	0.95557	2.00340
95	1.06328	1.81098
100	1.10730	1.83546
105	1.36762	1.49405
110	1.42337	0.91990
115	1.46276	1.85342
120	1.50280	1.18123
125	1.55111	2.07368
130	1.60391	1.69420
135	1.67410	2.92733
140	1.76640	2.34431
145	1.77887	2.41710
150	1.81204	1.77316
155	2.02498	1.81796
160	2.04512	1.69420
165	2.22504	1.85189
170	2.33659	1.05650
175	2.40258	2.34517
180	2.40726	2.26187
185	2.42944	1.31942
190	2.48207	1.97092
195	2.63194	2.42080
200	2.72100	1.43121

Figure 48B   Identification Error and Vibration Level with Perfect Inverse, Ks Diagonals = 0.001, and 1 Percent White Measurement Noise.

THE IDENTIFIED INVERSE

```
   7.8792      4.9291     -4.0428     -3.8597      2.3756     -7.6000
  -2.3141      0.4749      0.2995      1.6096     -0.6596      0.2922
  -0.9399     -0.2096     -0.4644      0.7609     -0.4144      0.1717
  -2.9950     -1.2220      1.3181      1.3386     -1.1733      2.3582
  -0.1751     -0.2222      0.2412      0.1970     -0.3394      0.3670
   1.3908      1.6886     -0.1522     -0.7115      0.5274     -1.1948
```

THE TRUE INVERSE

```
   8.8398      5.4144     -4.4493     -4.2197      2.5233     -8.4514
  -2.5172      0.5289      0.3189      1.7938     -0.7666      0.2628
  -1.0675     -0.2510     -0.5203      0.8379     -0.4615      0.1881
  -3.3315     -1.3456      1.4444      1.4671     -1.2808      2.5999
  -0.1997     -0.2452      0.2642      0.2115     -0.3673      0.4093
   1.6097      1.8703     -0.1552     -0.7672      0.5580     -1.3553
```

INVERSE INITIAL ESTIMATE

```
   8.8398      5.4144     -4.4493     -4.2197      2.5233     -8.4514
  -2.5172      0.5289      0.3189      1.7938     -0.7666      0.2628
  -1.0675     -0.2510     -0.5203      0.8379     -0.4615      0.1881
  -3.3315     -1.3456      1.4444      1.4671     -1.2808      2.5999
  -0.1997     -0.2452      0.2642      0.2115     -0.3673      0.4093
   1.6097      1.8703     -0.1552     -0.7672      0.5580     -1.3553
```

Figure 48C   Comparison of Identified, True, and Initial Inverse Matrices for 1 Percent Measurement Noise Showing Divergence from Perfect Initial Conditions on Inverse.
Ks Diagonals = 0.001, Contr. Relax. = 1.0 .
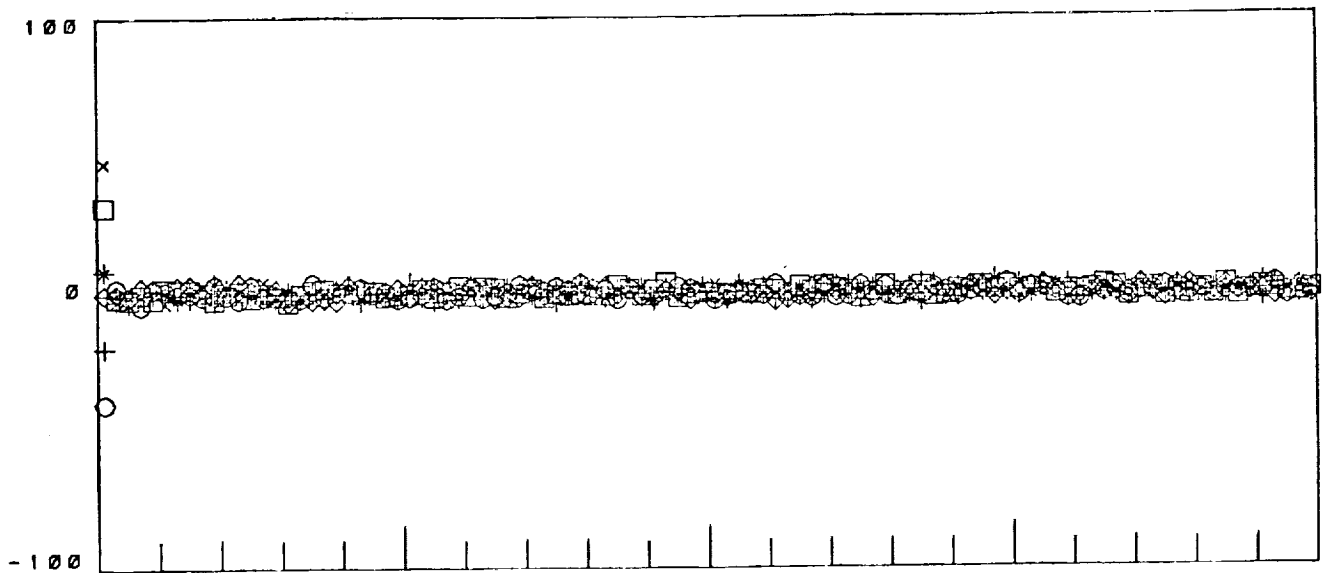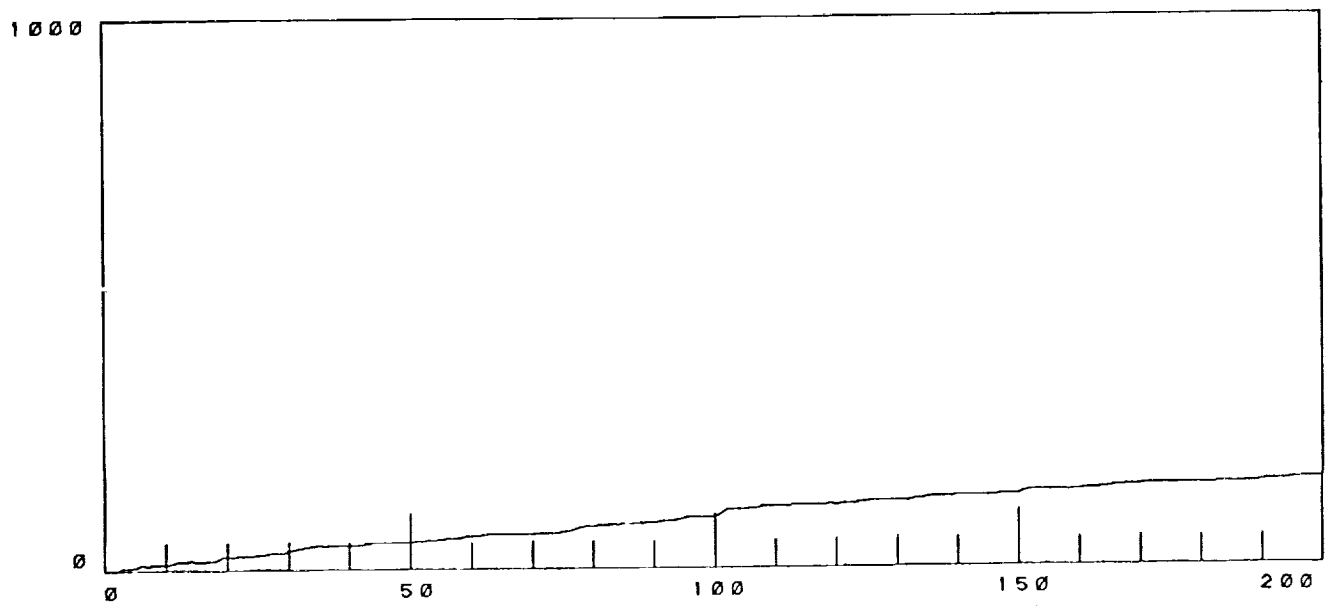
126

Figure 49 LMS Adaptive Inverse Identification Error and Vibration
Control with No Initial Inverse Error, Ks Diagonals = 0.001,
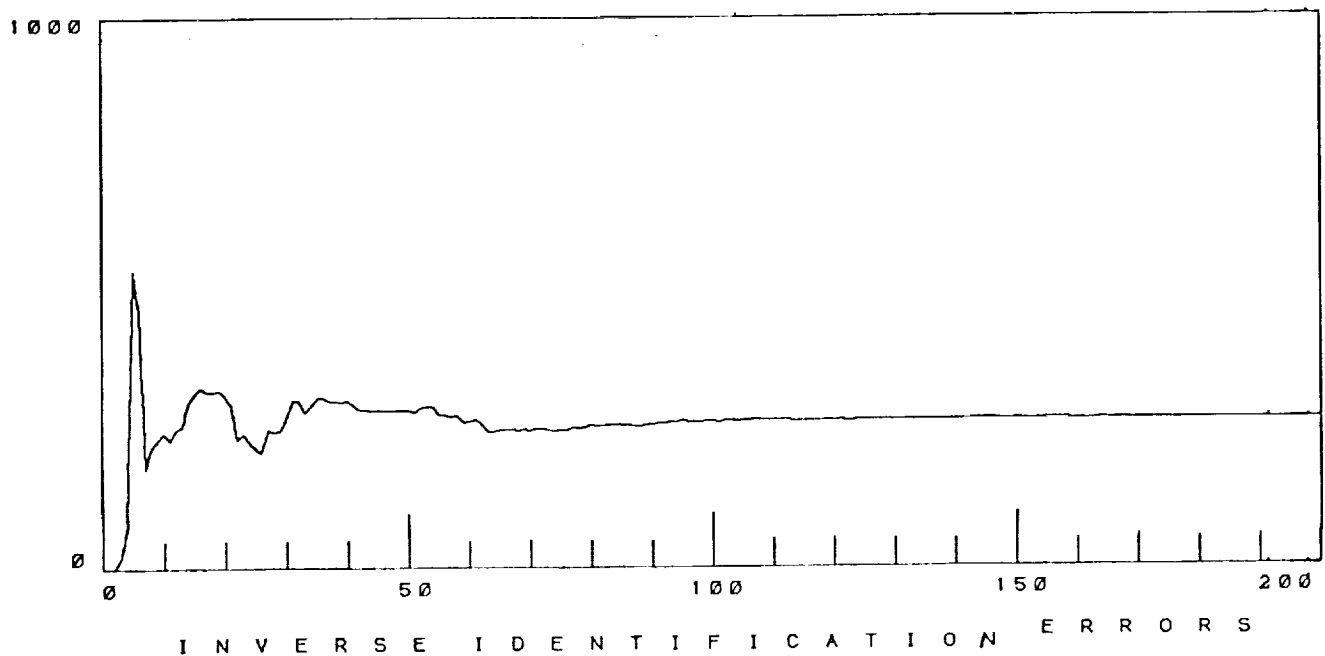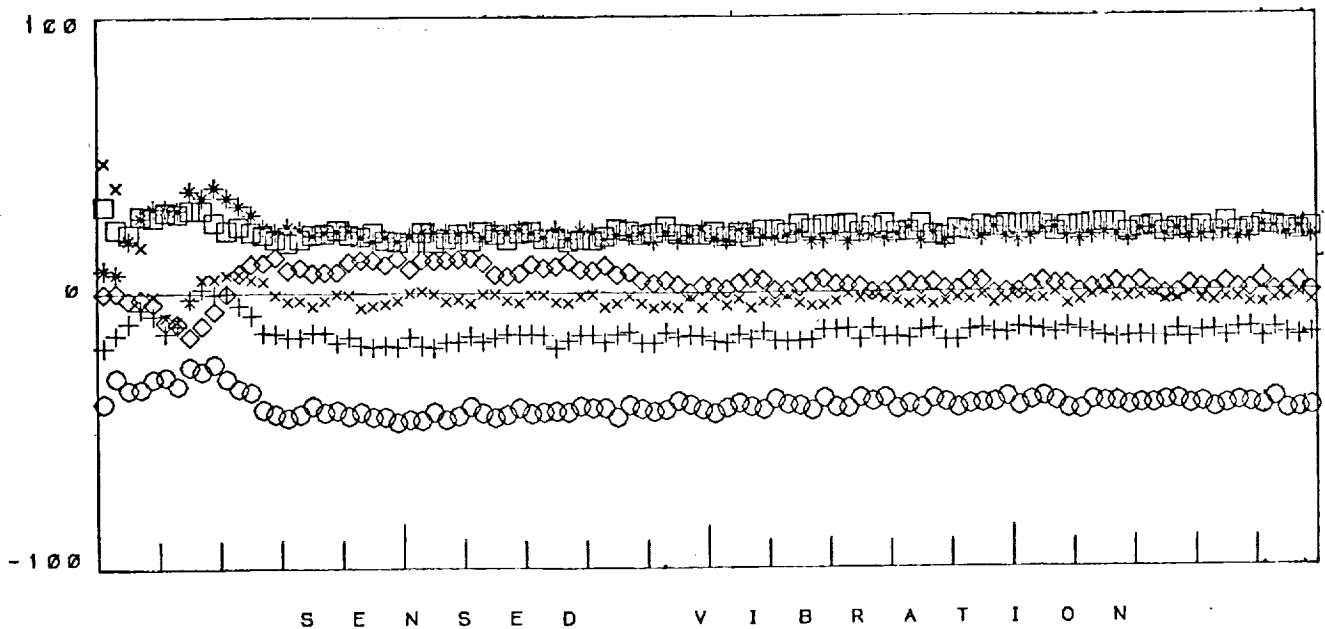and 5 Percent Measurement Noise.
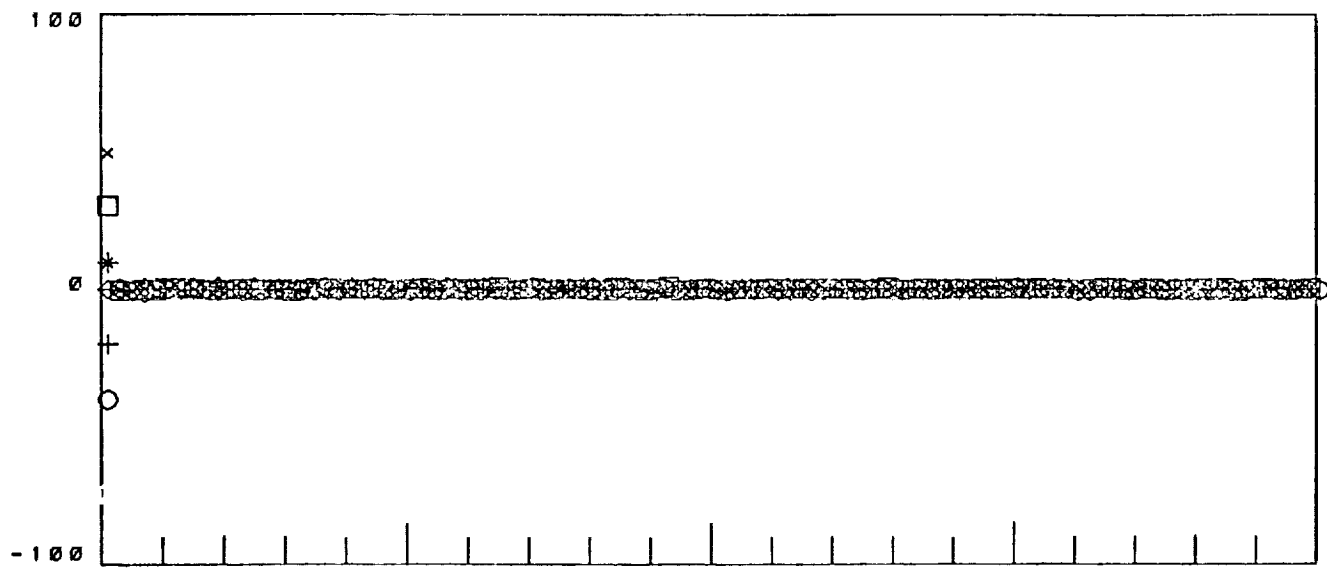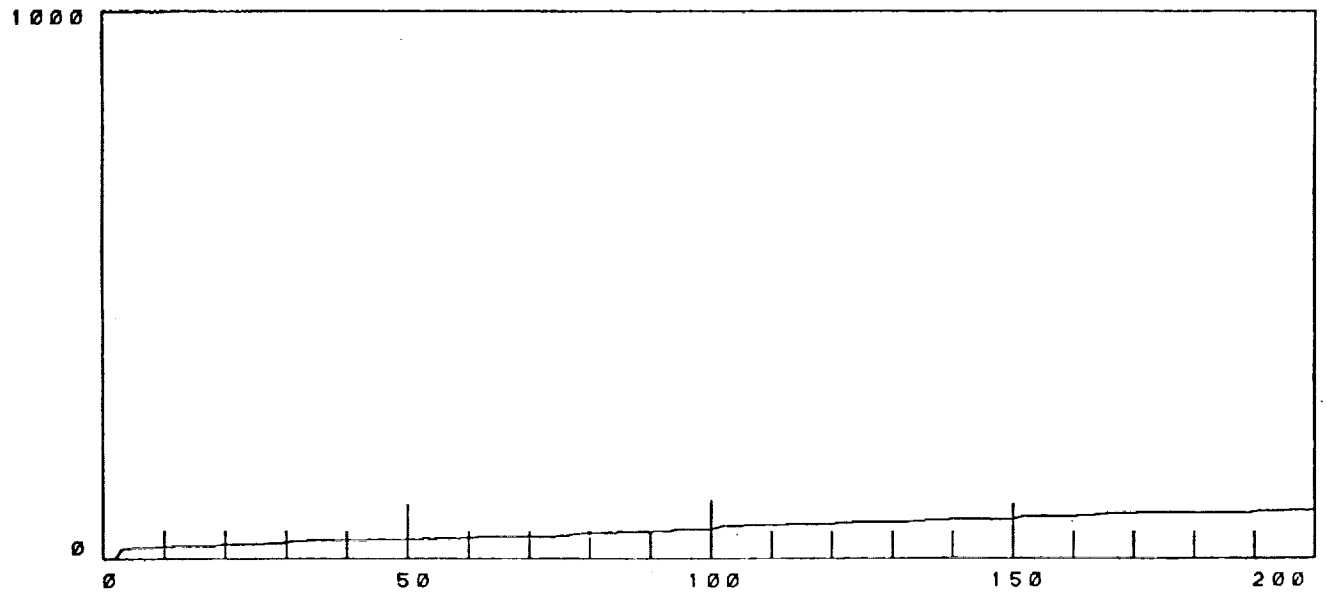
127

Figure 50   LMS Adaptive Inverse Identification Error and Vibration
Control with No Initial Inverse Error, Ks Diagonals = 0.01,
and 1 Percent Measurement Noise.

128

Figure 51A LMS Adaptive Inverse Identification Error and Vibration
Control with No Initial Inverse Error, Ks Diagonals = 0.01,
and 5 Percent Measurement Noise.

129

-0.0005	0.0042	0.0011	-0.0009	0.0031	0.0012
0.0003	-0.0022	-0.0006	0.0005	-0.0016	-0.0006
0.0001	-0.0013	-0.0004	0.0003	-0.0009	-0.0003
0.0002	-0.0015	-0.0004	0.0003	-0.0010	-0.0004
0.0000	-0.0003	-0.0001	0.0001	-0.0002	-0.0001
-0.0002	0.0013	0.0004	-0.0003	0.0010	0.0004

THE TRUE INVERSE

8.8398	5.4144	-4.4493	-4.2197	2.5233	-8.4514
-2.5172	0.5289	0.3189	1.7938	-0.7666	0.2628
-1.0675	-0.2510	-0.5203	0.8379	-0.4615	0.1881
-3.3315	-1.3456	1.4444	1.4671	-1.2808	2.5999
-0.1997	-0.2452	0.2642	0.2115	-0.3673	0.4093
1.6097	1.8703	-0.1552	-0.7672	0.5580	-1.3553

INVERSE INITIAL ESTIMATE

8.8398	5.4144	-4.4493	-4.2197	2.5233	-8.4514
-2.5172	0.5289	0.3189	1.7938	-0.7666	0.2628
-1.0675	-0.2510	-0.5203	0.8379	-0.4615	0.1881
-3.3315	-1.3456	1.4444	1.4671	-1.2808	2.599
-0.1997	-0.2452	0.2642	0.2115	-0.3673	0.4093
1.6097	1.8703	-0.1552	-0.7672	0.5580	-1.3553

Figure 51C Comparison of Identified, True, and Initial Inverse Matrices
for 5 Percent Measurement Noise Showing Divergence from
Perfect Initial Conditions on Inverse.
Ks Diagonals = 0.01, Contr. Relax. = 0.20 .

The interesting feature to note is that the identification error reaches a plateau with increasing iteration number. If the identified inverse is examined at the end of run, it is found that it has all elements nearly equal to zero (Figure 51C). This explains the plateau region of the identification error. The added noise has corrupted the association between the changes in measured vibration and applied changes in cyclic pitch control. Hence, a matrix of zeros is found as an indication of no identified association.

To further explore the effects of noise, simulation runs were conducted in which the initial inverse estimate was in error by ten percent, and a step change in the uncontrolled vibration was introduced at iteration 100. Figure 52 shows the uncontrolled vibration case for no adaptive inverse control and inverse control of the vibration with the K_s diagonals equal to 0.001, and a 0.1 control relaxation. In both cases, no measurement noise was introduced. After the step change in uncontrolled vibration, the new vibration vector was quickly minimized in a few iterations.

With one percent white measurement noise, the adaptive inverse control technique appeared to be successful in terms of controlling the vibration and converging to the true inverse after the step disturbance (Figure 53). However, for 5 percent measurement noise, the control system was spectacularly unstable. Note the large increase in the inverse estimate error at iteration 100, produced by adding a step in vibration. This error resulted from the change in vibration being unrelated to the change in pitch at the same iteration.
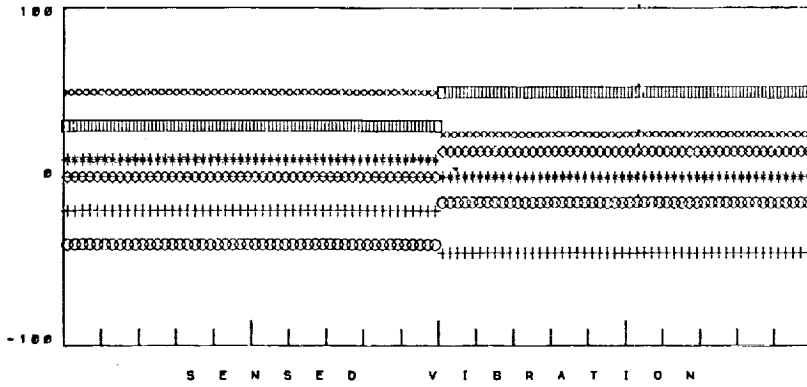
No Control
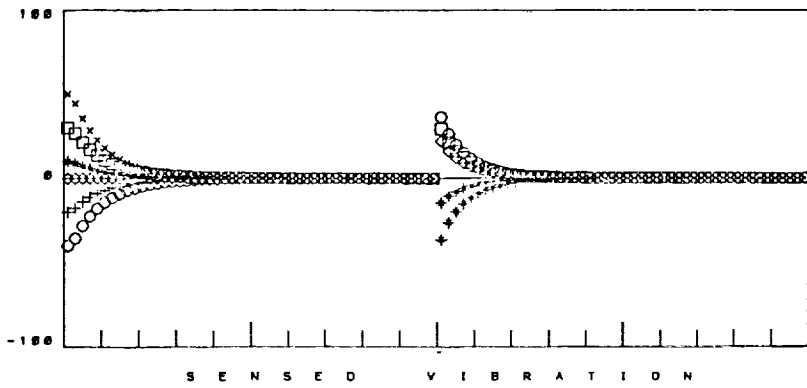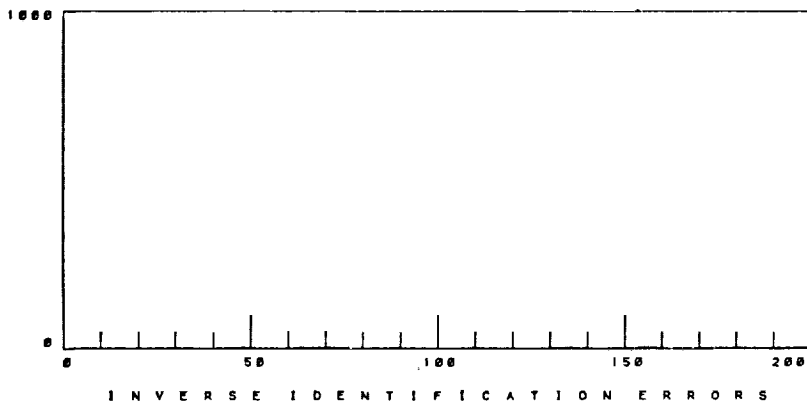
Control Relaxation
0.10

Ideal Control of
Vibration Step with
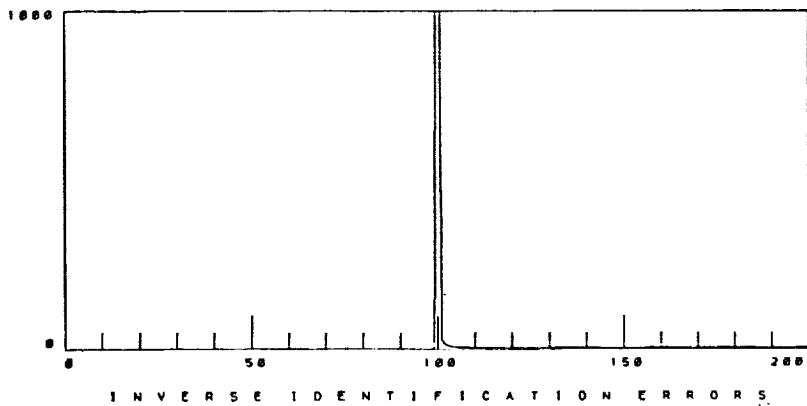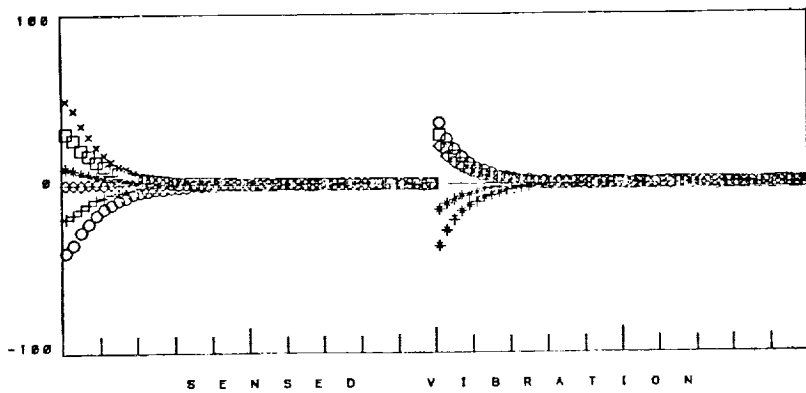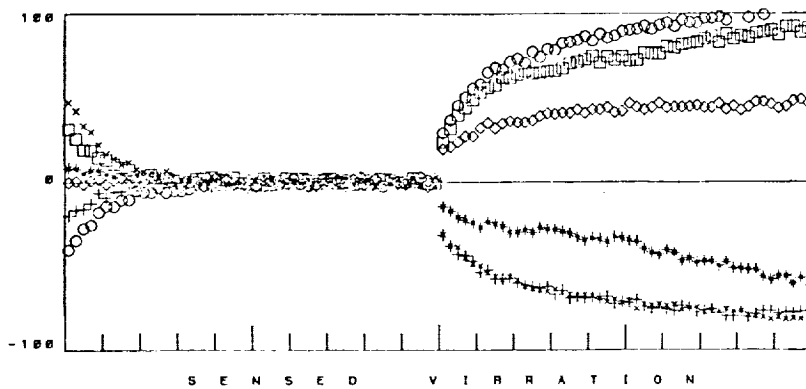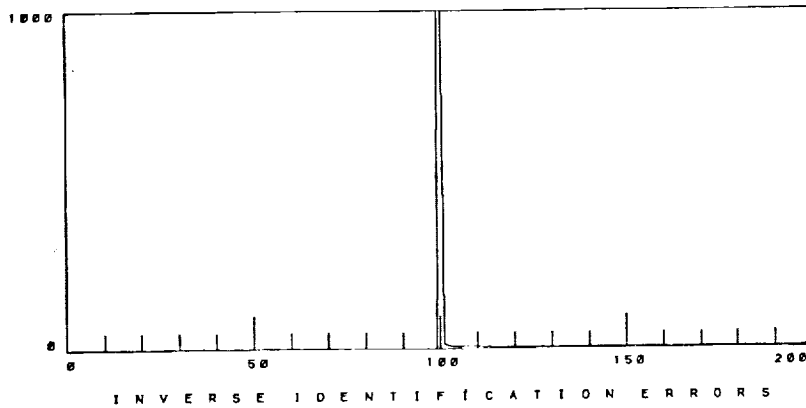No Measurement Noise

Figure 52   Uncontrolled and Controlled Vibration for No Measurement
Noise, No Initial Inverse Error, and Control Relaxations of
0.00 (Top) and 0.10 (Bottom).   132

Good Control of
Vibration Step with
1 Percent Noise

S E N S E D   V I B R A T I O N

I N V E R S E   I D E N T I F I C A T I O N   E R R O R S

Unstable Control of
Vibration Step with
5 Percent Noise

S E N S E D   V I B R A T I O N

I N V E R S E   I D E N T I F I C A T I O N   E R R O R S
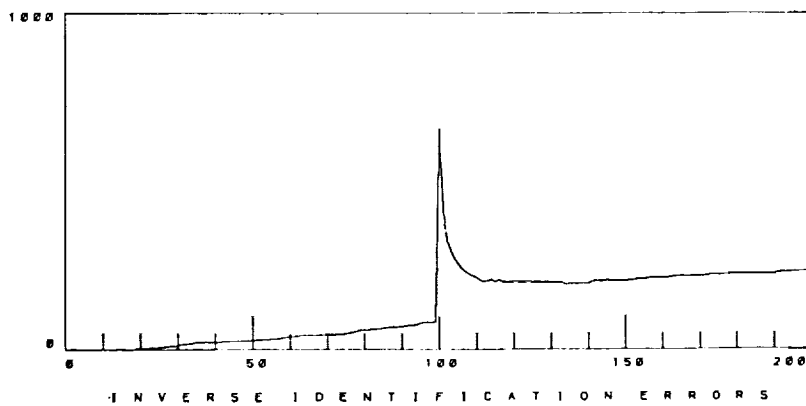
Figure 53   LMS Adaptive Inverse Control of Vibration Step Change at Step
100 with Ks Diagonals = 0.001 and 0.10 Control Relaxation,
for 1 (Top) and 5 (Bottom) Percent Meas. Noise.

The first thought which came to mind was to reduce the stability gain constant K_s (or the relaxation constant) so that the estimator would not track the noise disturbances. As seen in figure 54, this approach seemed to work. K_s was reduced to 0.0001, and the vibration appeared at first glance to have been controlled successfully. However, when the digital record was examined more closely (figure 54B), it was seen that the identification error was still increasing. Hence, reducing the magnitude of the stability gain elements only retarded the onset of the impending identification instability. A very low K_s also made the extended LMS algorithm less responsive to changes in the operating conditions.

The effect of relaxing the control was shown (Figure 55) to have even more disastrous consequences. The reason for the even more unstable behavior is that when the control step size was reduced, the noise at each step was made greater relative to the true change in vibration associated with each change in the cyclic pitch vector. Hence, by increasing the control relaxation, the signal to noise ratio was further degraded.
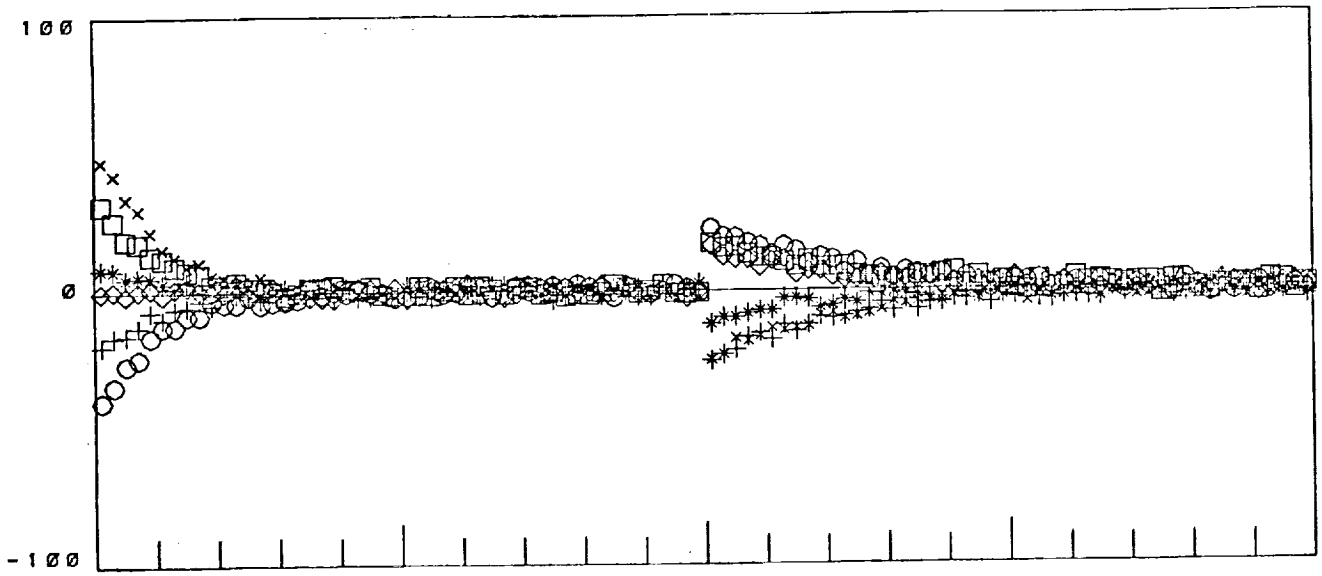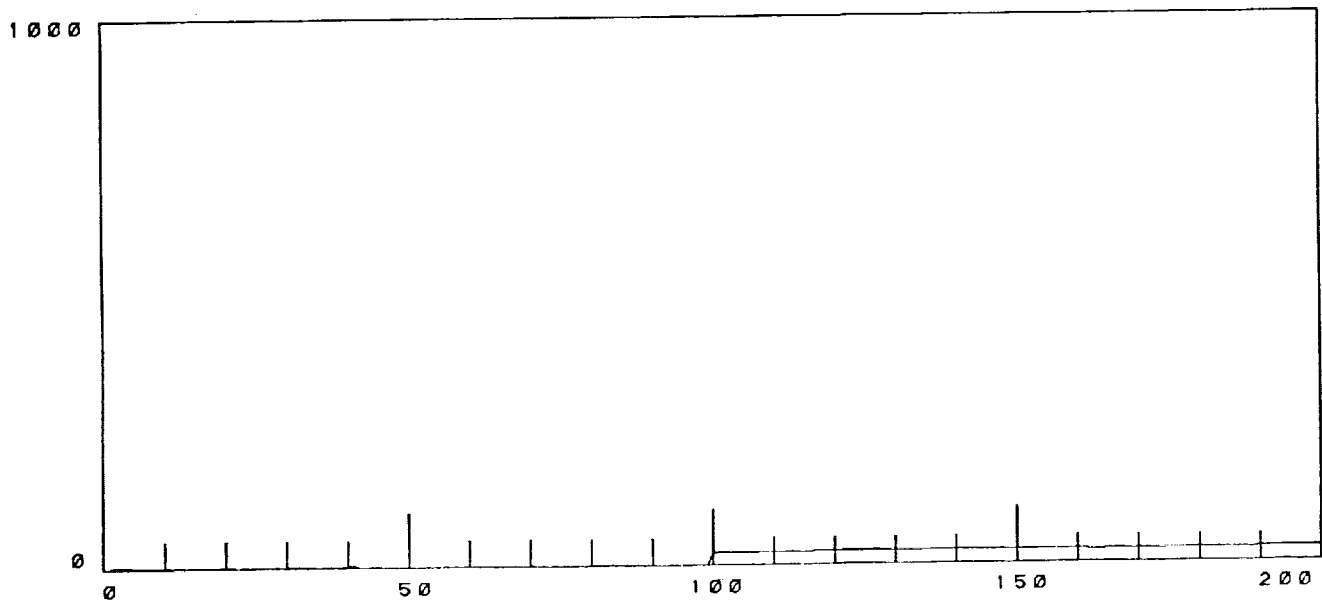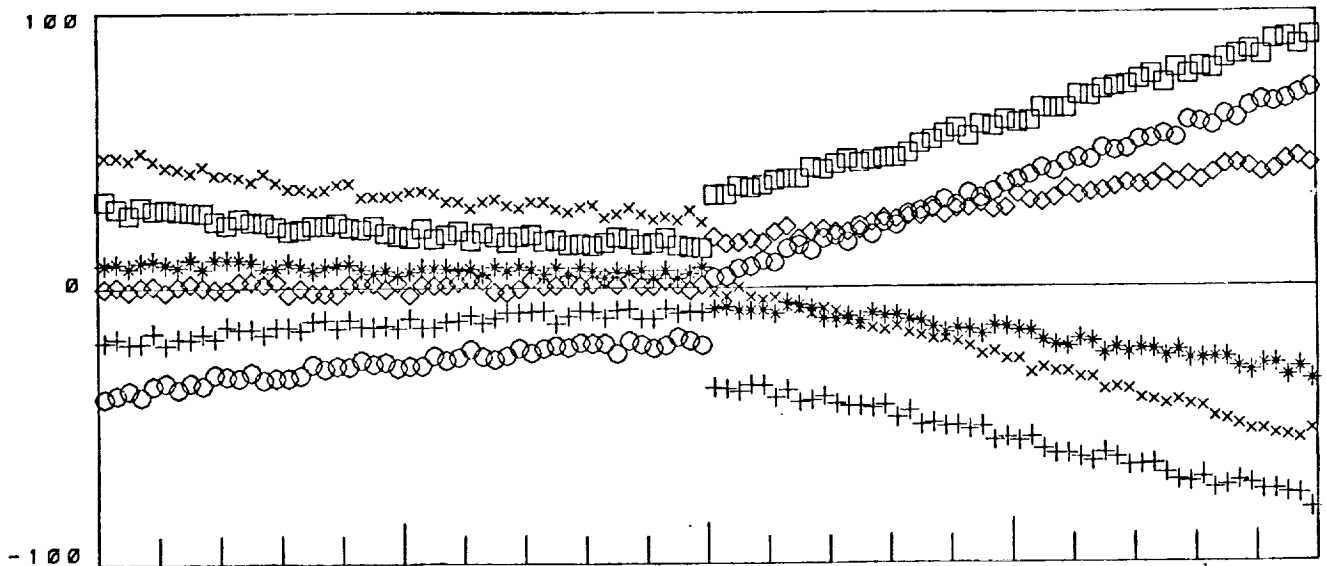
GAIN VECTOR: 0.0001   0.0001   0.0001   0.0001   0.0001   0.0001
PERCENT NOISE: CONTROL RELAX:
    5.0000   0.1000
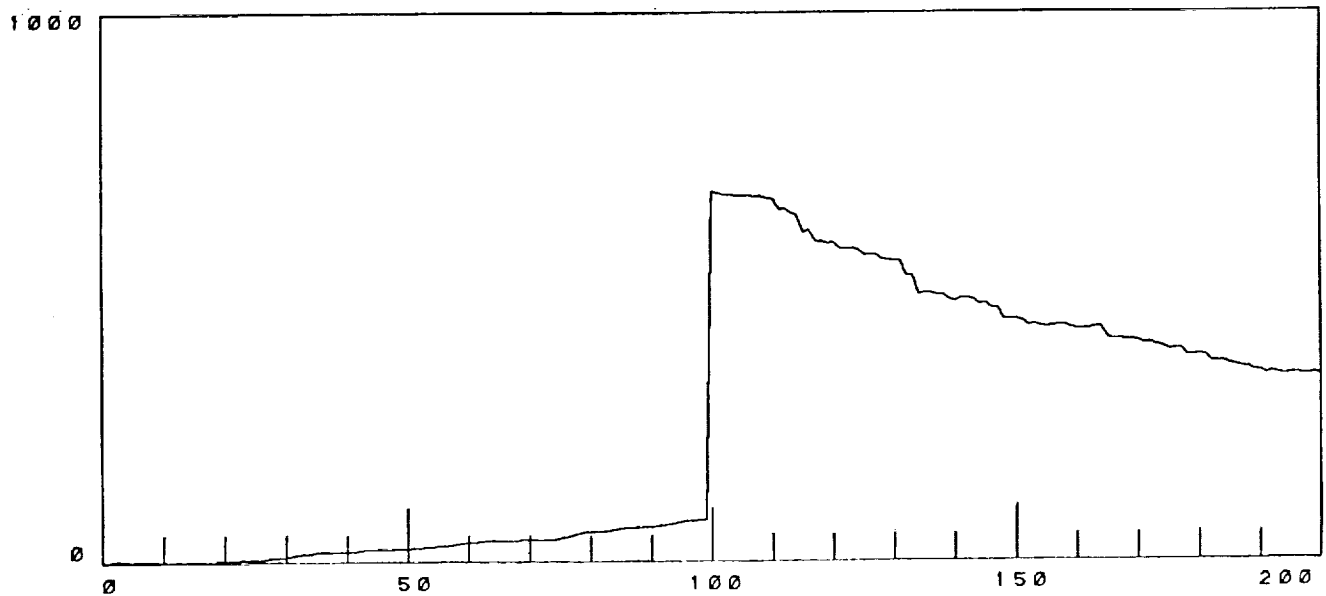
Figure 54A   LMS Adapative Inverse Control for Vibration Change at Step
              100, with Ks Diagonals = 0.0001, Control Relaxation of 0.10,
              and 5 Percent White Measurement Noise.

135

ITERATION	I.D. ERROR	VIBRATION
1	0.00000	0.00000
2	2.70784	149.91574
3	2.59698	128.22580
4	2.64891	115.54104
5	2.44081	101.01019
6	2.47238	102.48978
7	2.48193	91.37861
8	2.35151	77.14806
9	2.28532	65.54290
10	2.28890	64.40995
15	1.97084	37.56799
20	1.54230	15.48847
25	1.43040	10.37495
30	1.22658	14.63641
35	0.92553	8.32086
40	0.86039	8.65423
45	0.75268	7.86046
50	0.74101	9.94352
55	0.61290	8.81204
60	0.48714	9.62729
65	0.40817	9.51646
70	0.38369	9.14383
75	0.36201	7.53644
80	0.20626	7.52283
85	0.14886	7.37019
90	0.11373	9.29998
95	0.05785	6.60838
100	23.32772	122.44373
105	23.23248	95.42108
110	23.01586	73.50512
115	23.66547	60.39556
120	24.30606	47.06903
125	24.32661	41.76141
130	24.30917	28.40005
135	24.59439	27.22986
140	24.37214	24.59882
145	24.82065	15.94469
150	24.82135	10.12398
155	24.41597	14.00892
160	24.25171	9.65614
165	24.28445	13.57069
170	24.27261	5.69457
175	24.77578	9.32713
180	25.10926	4.04190
185	25.26221	8.84717
190	25.85704	6.40113
195	26.44195	7.77266
200	26.57766	7.72467

Figure 54B   Identification Error and Vibration Level for Vibration Change
at Step 100, with Ks Diagonals = 0.0001, Control
Relaxation of 0.10, and 5 Percent White Noise.

S E N S E D   V I B R A T I O N

I N V E R S E   I D E N T I F I C A T I O N   E R R O R S

GAIN VECTOR: 0.0010   0.0010   0.0010   0.0010   0.0010   0.0010
PERCENT NOISE: CONTROL RELAX:
    5.0000   0.0100

Figure 55   LMS Adapative Inverse Control for Vibration Change at Step
             100, with Ks Diagonals = 0.001, Control Relaxation of 0.01,
             and 5 Percent White Measurement Noise.

137

The noise problem was remedied by averaging the control and response signals over a small number of iterations. In this method, for example, the last ten vibration measurements and pitch control commands were stored in memory. When a new vibration measurement was taken, it was added to the previous nine vibration measurements. The average was then found and used as the current vibration measurement for use with the inverse control law. Similarly, the last ten cyclic pitch commands were averaged over ten cycles for use with the extended LMS estimator. Hence, for the case of ten averaging cycles,

$$\Delta \Theta(k) = \sum_{n=k-9}^{k} \Delta \Theta(n)$$

and,

$$\Delta Z(k) = \sum_{n=k-9}^{k} \Delta Z(n)$$

Figure 56 shows successful identification and control for K_s diagonal elements of 0.001 with control relaxation of 0.1, at the 5 percent, 10 percent, and 15 percent noise levels, using the averaging method. The vibration was reduced, and the identification error became smaller with increasing number of iterations. For 20 percent noise, the inverse identification was again unstable.
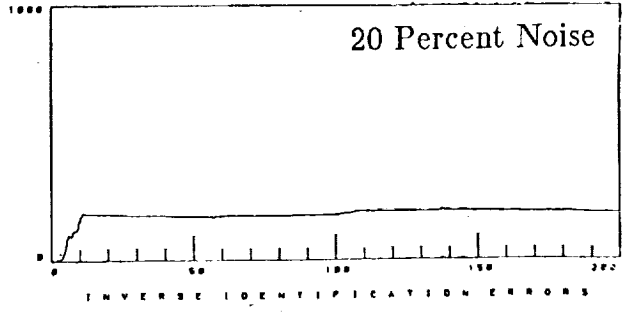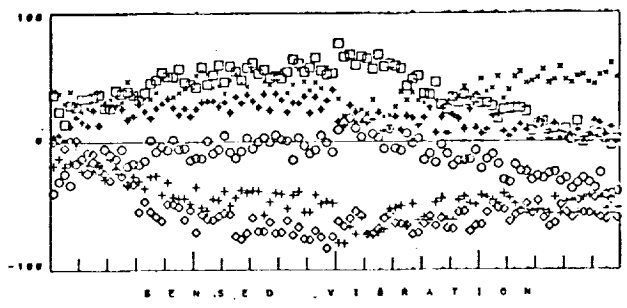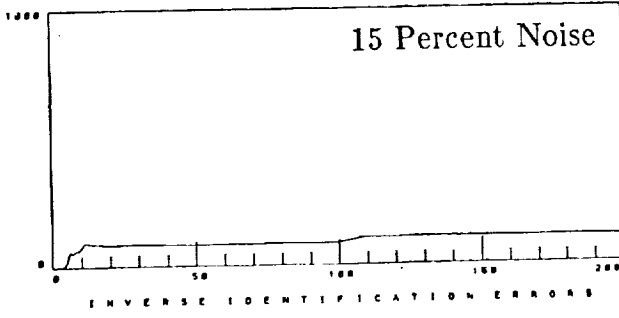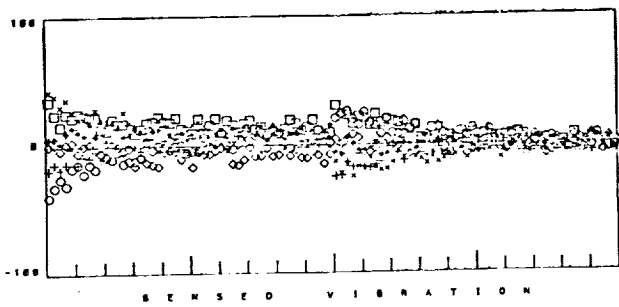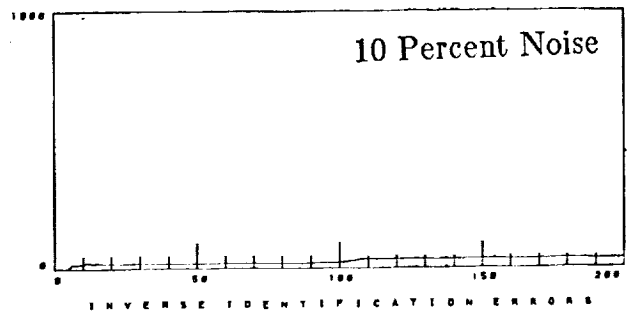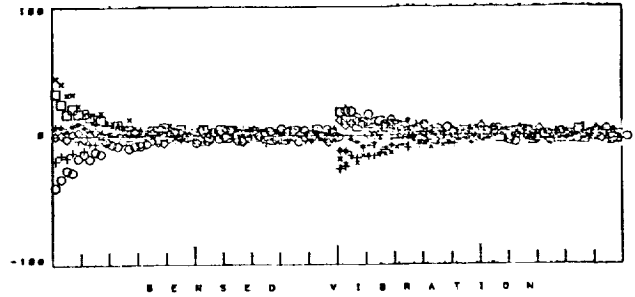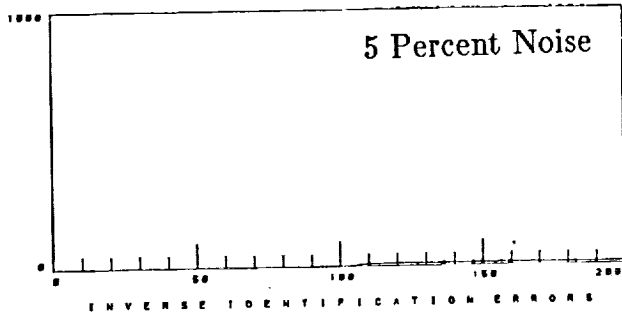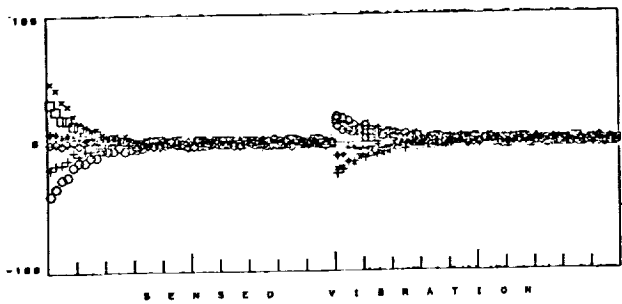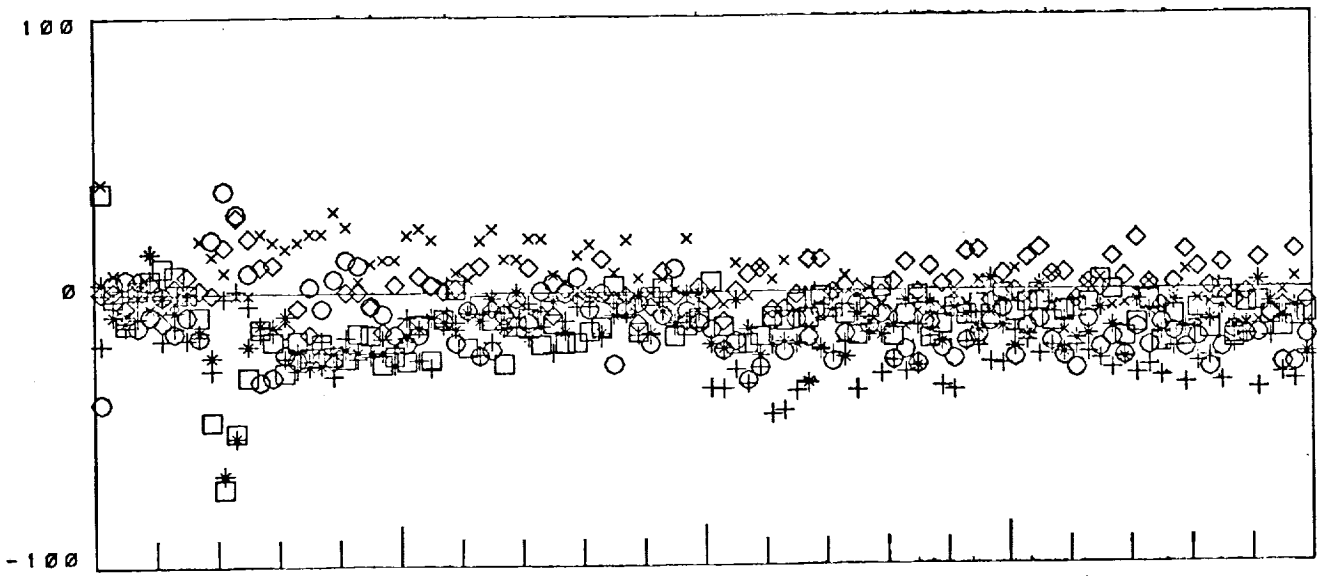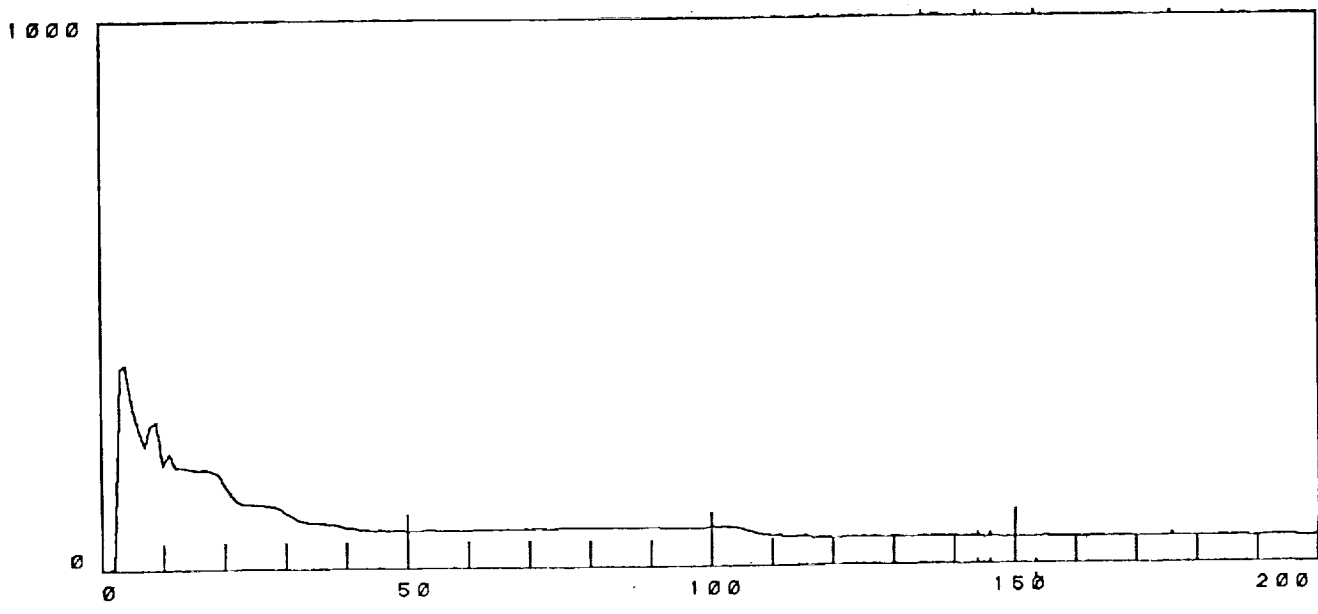
Figure 56   LMS Adaptive Inverse Control with Ks Diagonals = 0.001 and
0.10 Control Relaxation, with 5, 10, 15, and 20 Percent Noise
Using Averaging Method with 10 Cycles.

139

If the relaxation constant is increased from 0.1 to 0.8, the averaging method will allow accurate identification with 20 percent measurement noise (Figure 57). Figure 58 shows that thirty percent noise can also be handled if the control relaxation is set at .18. Furthermore, figure 59 illustrates that if the T matrix elements are changed by ten percent while executing the step change in vibration at iteration 100, the adaptive inverse control method using averaging will still be stable and responsive to changes in operating conditions.
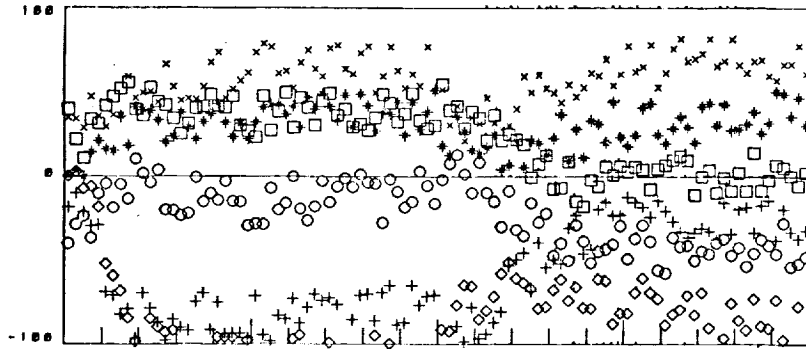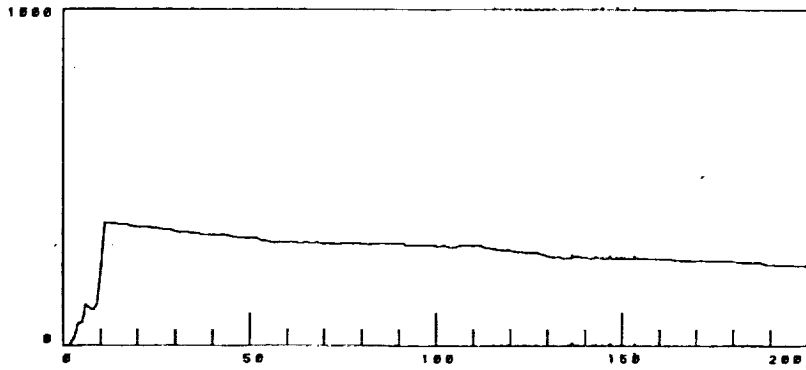
GAIN VECTOR: 0.0010   0.0010   0.0010   0.0010   0.0010   0.0010
PERCENT NOISE: CONTROL RELAX:
    20.0000   0.8000

Figure 57   LMS Adaptive Inverse Control with Ks Diagonals = 0.001 and
             0.80 Control Relaxation, with 20 Percent Noise and Change in
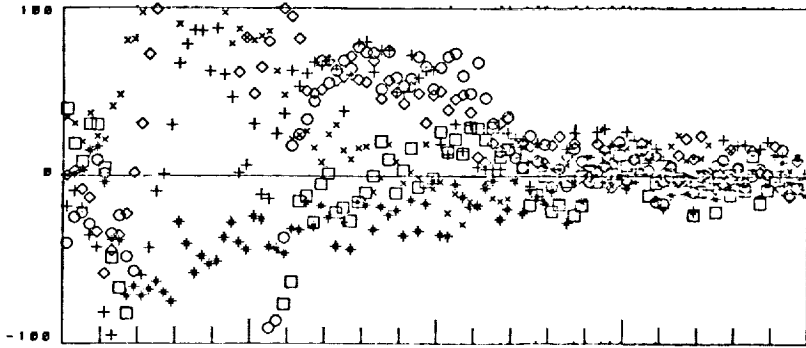   Vibration at 100 Using Averaging Method (10 Cycles.) .
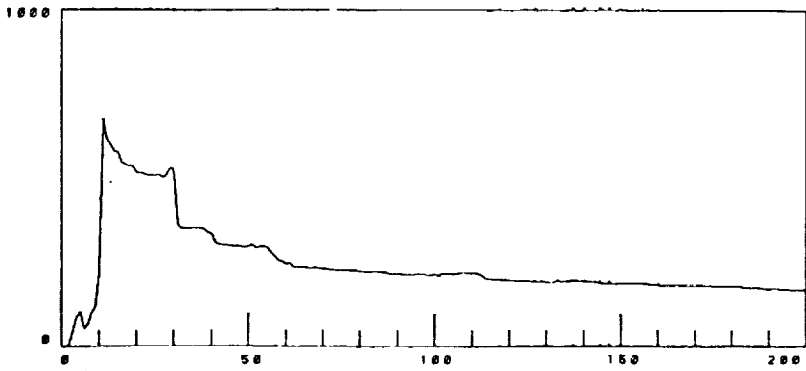
141

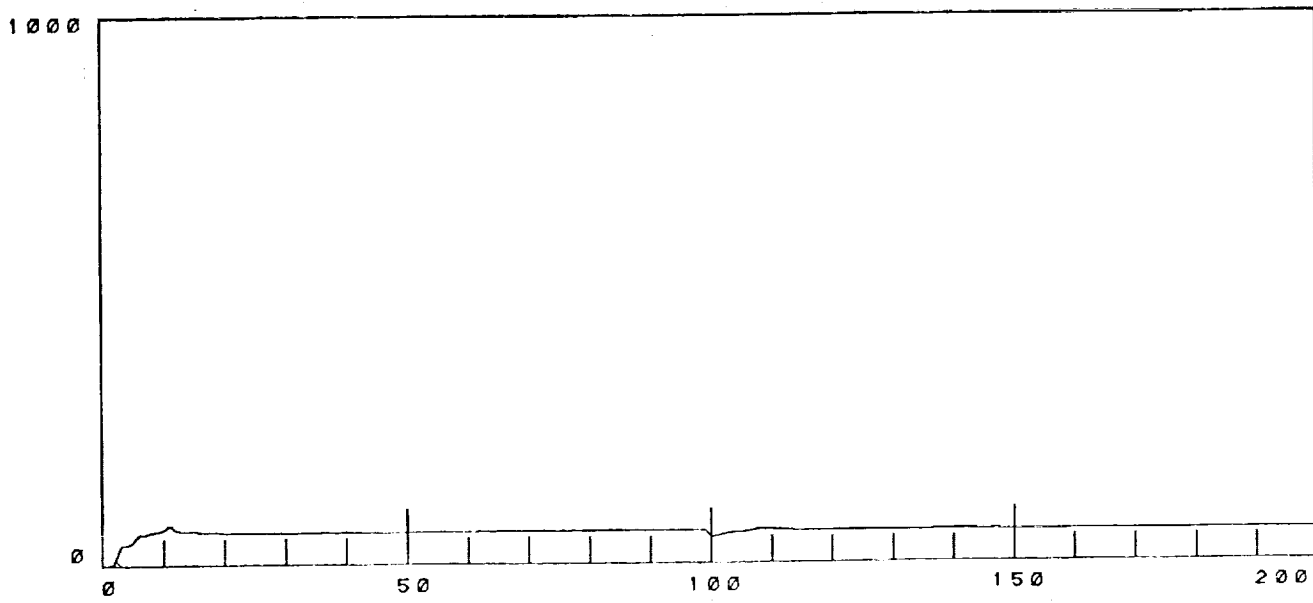30 Percent Noise

Control Relaxation
0.100

30 Percent Noise

Control Relaxation
0.180

Figure 58   LMS Adaptive Inverse Control with Ks Diagonals = 0.001,
30 Percent Measurement Noise, and Two Values of Control
Relaxation with 10 Cycle Averaging Method.   142
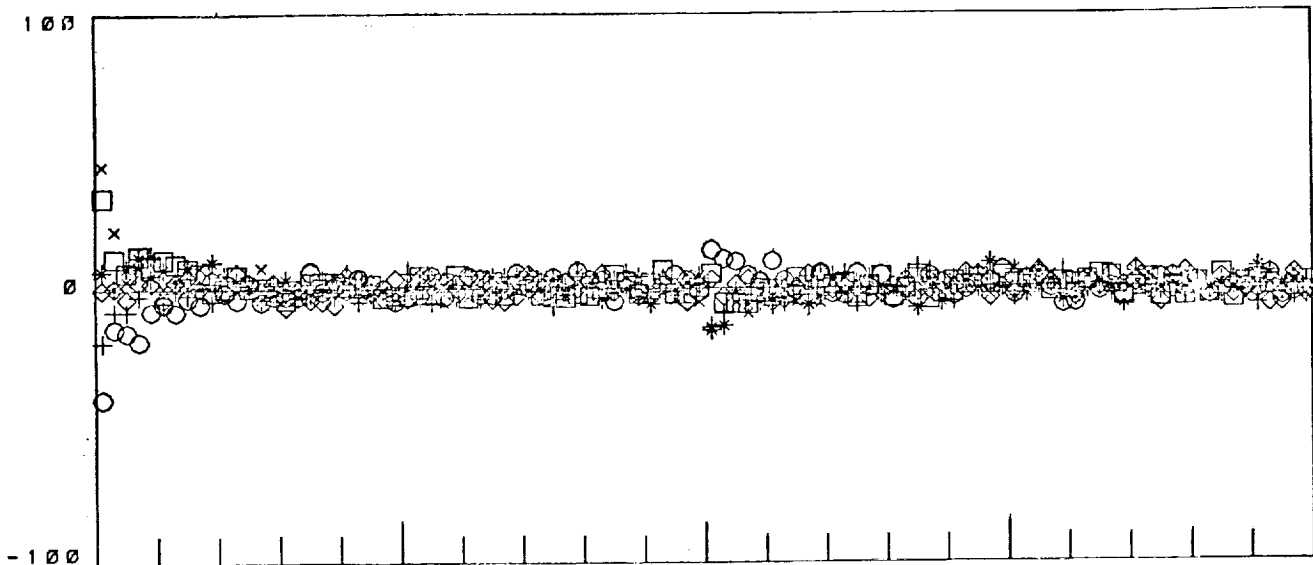
GAIN VECTOR: 0.0010   0.0010   0.0010   0.0010   0.0010   0.0010
PERCENT NOISE: CONTROL RELAX:
   10.0000   0.5000

Figure 59   LMS Adaptive Inverse Control with Ks Diagonals = 0.001 and
             0.50 Control Relaxation, with 10 Percent Noise and Step
             Change at 100 Using 10 Cycle Averaging.

143

The averaging method for reducing noise sensitivity appears to provide a simple, yet effective, means for improving the robustness of the adaptive inverse control method. If fact, if not done, the LMS adaptive inverse control method will not work at all. This does not invalidate the theory presented previously in the analysis section. This is because the extended LMS identification analysis (Section 5) only proved inverse identification convergence *in the limit* of many control and identification cycles. Nothing can really be said about any particular measurement. By averaging, the effect is to take out the measurement noise by building a memory into the extended LMS filter. The memory slows the adaptive response time somewhat, yet not to a significant degree, because for stable convergence, an amount of control relaxation is needed anyway. Hence, the loss in response time caused by averaging is more or less made up by the fact that less control relaxation is needed to stabilize the adaptive process when using the averaging method.

6.5

VIBRATION CONTROL USING THE AVERAGED
LMS ADAPTIVE INVERSE CONTROL METHOD

In the previous (6 x 6) simulations, the adaptive inverse transient identification behavior was simulated for only step changes in the uncontrolled vibration level. The reason for this was that there was much to be learned from that simple exercise. However, it is still desirable to know how well the

extended LMS algorithm can track rapid changes in operating conditions, such as those produced by wind gusts impending on the helicopter. For these simulations, the averaging method presented in the last section has been used.

The challenge presented by these simulation runs was to minimize a continuously changing uncontrolled vibration vector. The uncontrolled vibration vector elements were varied in a sinusoidal fashion. Furthermore, each element was varied at a different rate, to see when the LMS adaptive inverse process could no longer track the changes in operating conditions.

The case of uncontrolled vibration resulting from no adaptive inverse control is shown in Figure 60, along with the ideal inverse vibration control level possible, using an inverse with no error and a sensed vibration signal with no measurement noise. The latter forms the ideal baseline comparison case for the transient identification performance analysis to follow.
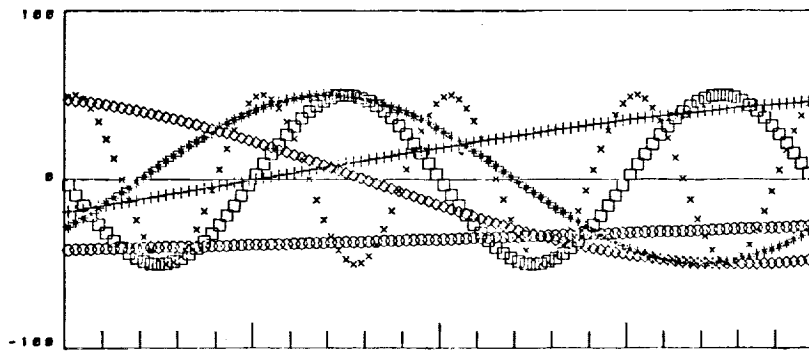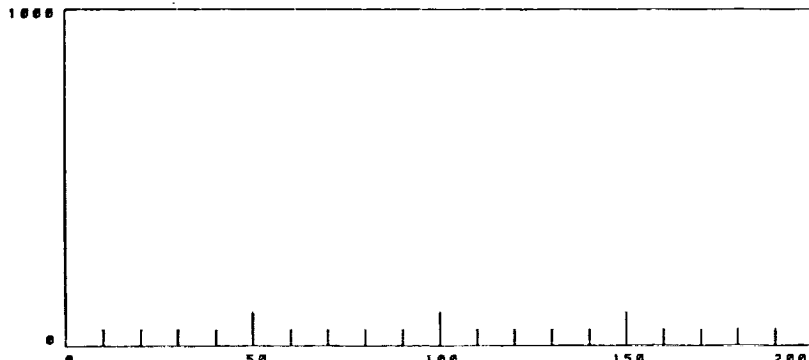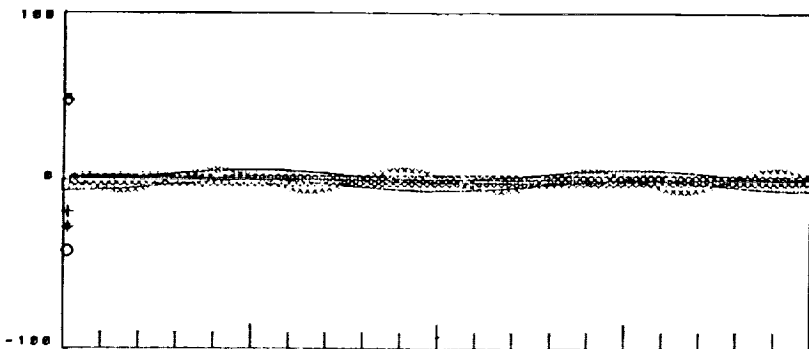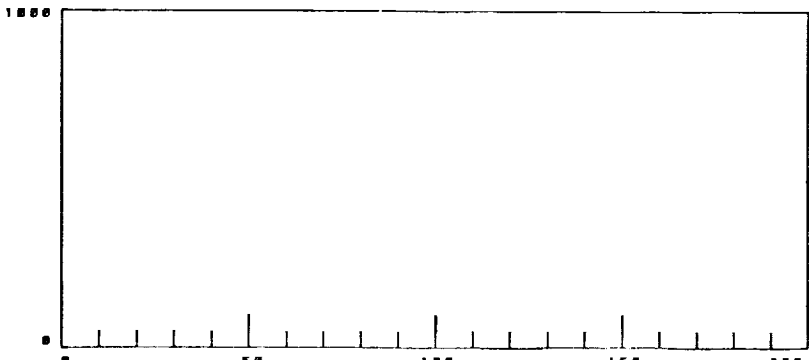
No Control of
Sinusoidally
Changing Vibration

Ideal Control of
Sinusoidally
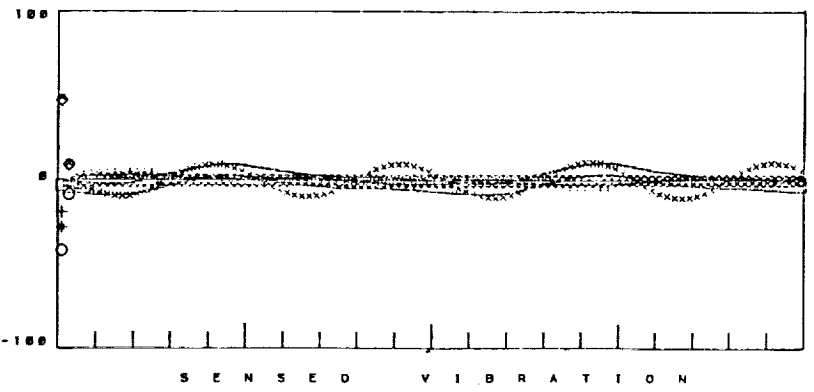Changing Vibration

(Perfect Inverse)
(No Noise)

Figure 60   Continuously Changing Uncontrolled Vibration for No Control
Control (Top), and Perfect Inverse Control (Bottom) with No Noise,
Using 10 Cycle Averaging

The case of no measurement noise is examined first. Figure 61 shows that for K_s diagonals of 0.001 and control relaxation of 0.4, the vibration of all but the fastest varying two channels has been controlled. By decreasing the control relaxation to 0.8, the vibration level for each channel has been controlled to an acceptable degree.

When measurement noise is added to the vibration measurement, the outcome is slightly different. Figure 62 repeats the case for the K_s diagonals of 0.001 with a control relaxation 0.8 . It it now seen that the fastest varying channel cannot really be controlled at all. The control for the other channels is acceptable. It is also seen that reducing the control relaxation to 0.5 does not change this outcome very much.
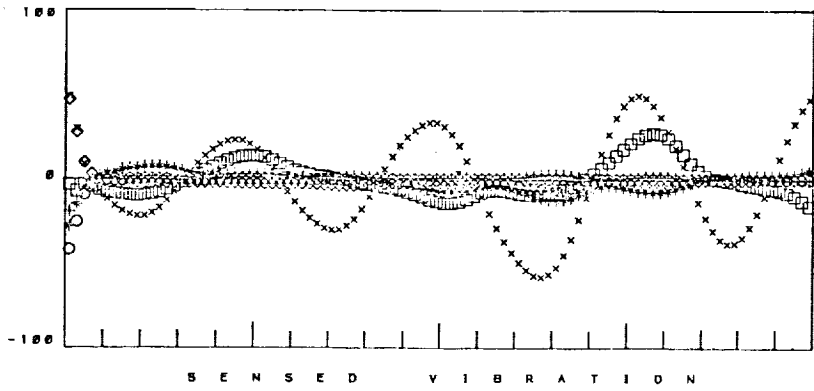
Control Relaxation
0.40

(No Noise)
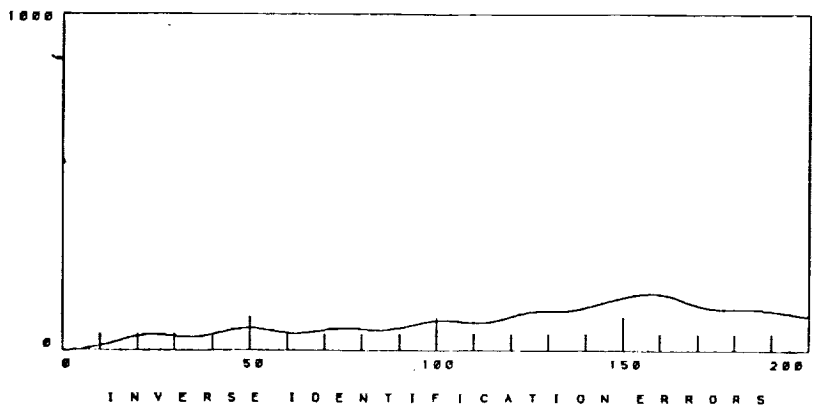
Control Relaxation
0.80

(No Noise)

Figure 61   LMS Adaptive Inverse Control of Continuously Changing
Vibration for Ks Diagonals = 0.001 and No Noise with 10
Cycle Averaging; Control Relax. 0.4 (top), 0.8 (Bottom).   148
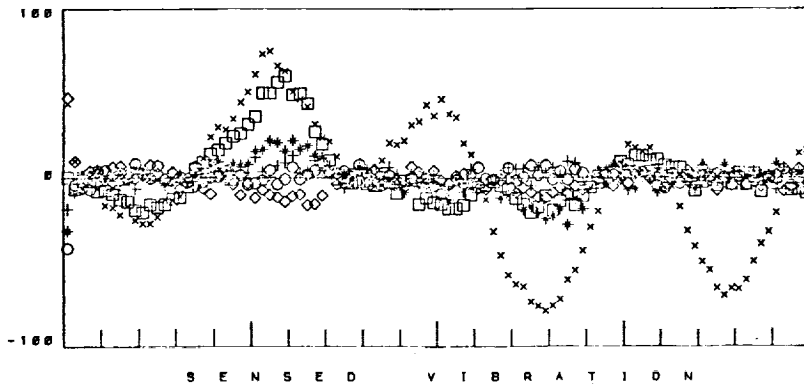
Control Relaxation
0.80

K_S Diagonals
0.001

10 Percent Noise

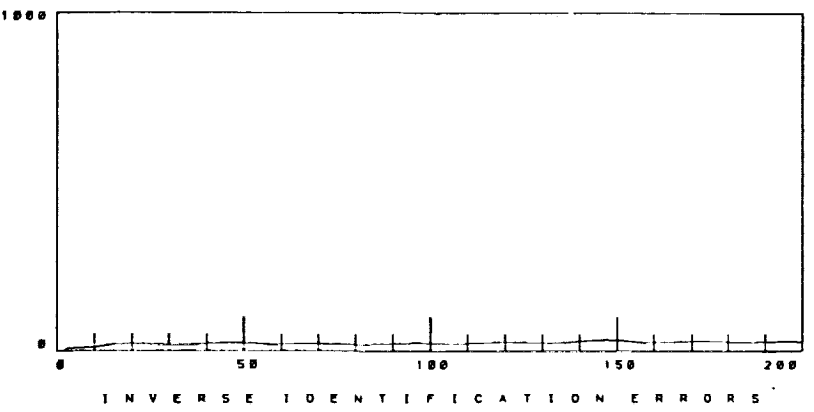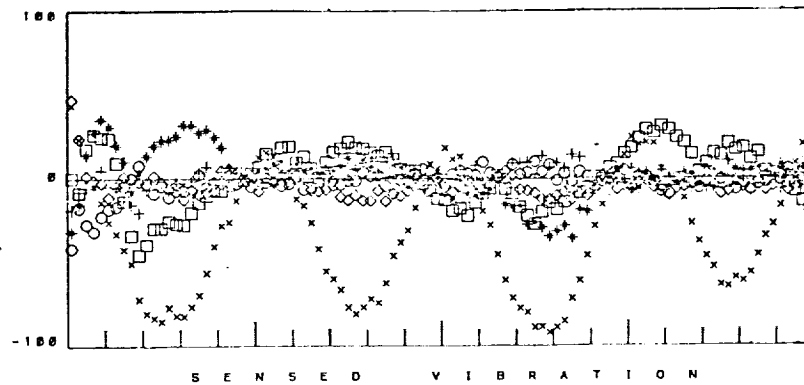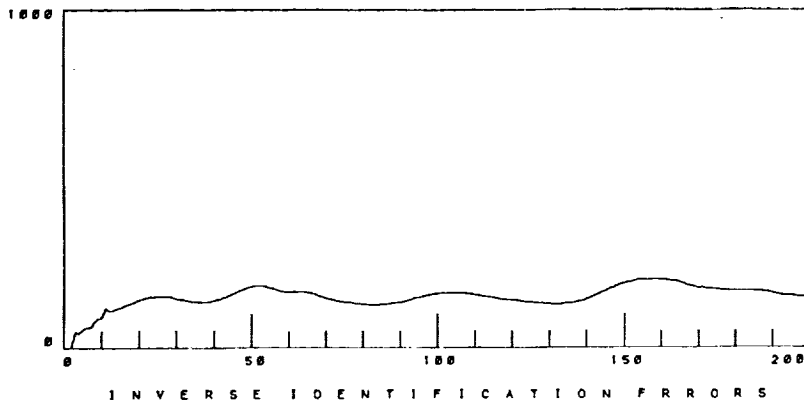Control Relaxation
0.50

K_S Diagonals
0.002

10 Percent Noise
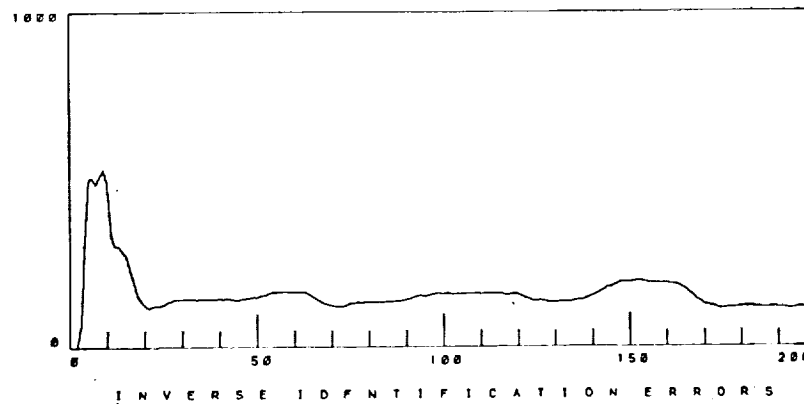
Figure 62   LMS Adaptive Inverse Control of Continuously Changing
Vibration for Ks 10 Percent Noise, with 10 Cycle Averaging,
and Similar Ks Diagonals and Control Relaxation.

149

Changing the amount of control relaxation did not enhance the tracking performance of the fastest varying channel. The most likely explanation is that the channel changed too fast relative to the time constant of the ten cycle averaging which took place on the measured vibration. Hence, the conclusion is that the averaged LMS adaptive inverse control technique can form a robust vibration control system, provided the changes in the vibration harmonics to be controlled do not change on the order of the averaging time constant of the identification process. Wind tunnel experimentation or actual flight testing is needed to determine the necessary degree to which the averaging technique is needed to make the LMS adaptive inverse control method work successfully.

VII. CONCLUSIONS

The extended LMS adaptive inverse control technique was shown to have good potential for reducing N/Rev helicopter fuselage vibration. The few number of operations required to implement the method makes it computationally attractive. Computer simulations using the (3 x 3) and (6 x 6) transfer matrix models were used to help validate and extend the results predicted by the theory. The overall conclusion is that the LMS adaptive inverse control method can form a robust vibration control system, but will require some tuning of the input sensor gains, the stability gain matrix, and the amount of control relaxation to be used.

The extended LMS algorithm can be used to adapt an initial estimate of the inverse prior to closed-loop control. For low rank order plants, such as the (3 x 3) simulation, the extended LMS algorithm can be started without any *a priori* knowledge of the inverse matrix. The learning phase of the method was shown to be capable of identifying the inverse, starting from an initial inverse estimate consisting of a matrix of zeros. The learning curve of the controller during the learning phase was then shown to be quantitatively close to that predicted by averaging the learning curves of the normal modes. The (6 x 6) simulation, however, indicated that for higher order transfer matrices, a rough estimate of the inverse is needed to start the algorithm efficiently. The more the starting estimate is in error, the more likely the identification process will become unstable.

For best performance, the stability gain matrix elements should be chosen small. Low control relaxation may then be chosen to quickly alleviate the

vibration. The eigenvalues of the signal information matrix predict the stability limits for the diagonal elements of the stability gain matrix only during the learning phase, when the control signals are known in advance. During the control phase, the signal information matrix is not known, and the selection of the stability gain matrix and the amount of control relaxation to be used must be found experimentally. The simulation results indicated that, in general, the product of the control relaxation and the magnitude of the stability gain matrix must be kept within limits. Low values of K_s make the controller less sensitive to control relaxation selection, and permits faster and more stable vibration reduction, than by choosing K_s large and the control relaxation coefficient small. Given a fixed amount of control relaxation, very low values of K_s make the inverse identification process smooth, but slow. The best selection of the stability gain matrix diagonal elements and the amount of control relaxation is basically a compromise between slow, stable convergence and fast, yet potentially unstable identification.

The LMS adaptive inverse control algorithm was shown to be capable of adapting the inverse (controller) matrix to track changes in the flight conditions. The algorithm converged quickly for moderate disturbances, while taking longer for larger disturbances. Perfect knowledge of the inverse matrix was not required for good control of the N/Rev vibration.

It was shown that measurement noise will prevent the LMS adaptive inverse control technique from controlling the vibration, unless the signal averaging method presented here is incorporated into the algorithm. This technique gives the LMS algorithm a memory, and greatly improves the robustness of the control system.

Wind tunnel or flight testing must now be done to tune the extended LMS adaptive inverse control technique for an actual application and validate the results found in simulation.

REFERENCES

Brown TJ and McCloud JL III: Multicyclic Control of a Helicopter Rotor Considering the Influence of Vibration, Loads, and Control Motion. Annual Forum of the American Helicopter Society, Washington, D.C., May 1980.

Bryson AE Jr. and Ho Y-C: Applied Optimal Control: Optimization, Estimation, and Control. Blaisdell Publishing Company, Waltham, Mass. 1969.

Chopra I and McCloud JL III: Considerations of Open-Loop, Closed-Loop, and Adaptive Multicyclic Control Systems. American Helicopter Society Northeast Region National Specialist's Meeting on Helicopter Vibration "Technology for the Jet Smooth Ride", Hartford, Conn., 1981.

Davis MW: Refinement and Evaluation of Helicopter Real-Time Self-Adaptive Active Vibration Controller Algorithms. NASA CR (No. pending), November 1983.

Gessow A and Meyers GC: Aerodynamics of the Helicopter. Frederick Ungar Publishing Company, New York, 1952.

Goodwin GC and Payne RL: Dynamic System Identification: Experiment Design and Data Analysis. Academic Press, New York, 1977.

Johnson W: Helicopter Theory. Princeton University Press, Princeton, New Jersey, 1980.

Johnson W: Self-Tuning Regulators for Multicyclic Control of Helicopter Vibration. NASA Technical Paper 1996, May 1982.

Kretz M, Aubrun J-N, and Larche M: Wind Tunnel Tests of the Dorand DH 2011 Jet-Flap Rotor. Volumes 1 and 2. NASA CR-114693, 1973.

McCloud, JL III: An Analytical Study of a Multicylic Controllable Twist Rotor. Paper No. 932, 31st Annual Forum of the American Helicopter Society, Washington, D.C., 1975.

154

McCloud JL III and Kretz M: Multicyclic Jet-Flap Control for Alleviation of Helicopter Blade Stresses and Fuselage Vibration. Rotorcraft Dynamics, NASA SP-352, 1974, pp. 233-238.

McCloud JL III and Weisbrich AL: Wind Tunnel Test Results of a Full-Scale Multicyclic Controllable Twist Rotor. Paper No. 78-60, Annual Forum of the American Helicopter Society, Washington, D.C., May 1978.

Molusis JA, Hammond CE, and Cline JH: A Unified Approach to the Optimal Design of Adaptive and Gain Scheduled Controllers to Achieve Minimum Helicopter Rotor Vibration. 37th Annual Forum of the American Helicopter Society, New Orleans, La., May 1981.

Powers RW: Application of Higher Harmonic Blade Feathering for Helicopter Vibration Reduction. NASA CR-158985, 1978.

Sage AP and Melsa JL: Estimation Theory with Applications to Communications and Control. McGraw Hill Book Company, New York, 1971.

Shaw J and Albion N: Active Control of the Helicopter Rotor for Vibration Reduction. Paper No. 80-68, 36th Annual Forum of the American Helicopter Society, Washington, D.C., 1980.

Sissingh GJ and Donham RE: Hingeless Rotor Theory and Experiment on Vibration Reduction by Periodic Variation of Conventional Control. Rotorcraft Dynamics, NASA SP-352, 1974, pp. 261-277.

Taylor RB, Farrar FA, and Miao W: An Active Control System for Helicopter Vibration Reduction by Higher Harmonic Pitch. Paper No. 80-71, 36th Annual Forum of the American Helicopter Society, Washington, D.C., 1980.

Widrow B: Adaptive Filters. Aspects of Network and System Theory, Holt, Rinehart, and Winston, Inc., New York, 1970

Widrow B: Adaptive Noise Cancelling: Principles and Applications. Proceedings IEEE, Volume 63, pp. 1692-1716, 1975.

Widrow B and Hoff ME Jr: Adaptive Switching Circuits. IRE WESCON Convention Record, pp 96-104, 1960.

Widrow B, Mantey P, Grifiths L, and Goode B: Adaptive Antenna Systems. Proceedings IEEE, Volume 55, No. 12, pp. 2143-2159, December

1967.

Widrow B, McCool JM, and Medoff BP: Adaptive Control by Inverse Modeling. Conference Record of 12th Asilomar Conference on Circuits, Systems, and Computers, pp. 90-94, November 1979.

1. Report No. TM-86829	2. Government Accession No.	3. Recipient's Catalog No.
4. Title and Subtitle Adaptive Inverse Control for Rotorcraft Vibration Reduction		5. Report Date October 1985
		6. Performing Organization Code
7. Author(s) Stephen A. Jacklin		8. Performing Organization Report No. 85396
		10. Work Unit No. (J.O. #) T7531
9. Performing Organization Name and Address Ames Research Center Moffett Field, CA 94035		11. Contract or Grant No.
		13. Type of Report and Period Covered Technical Memorandum
12. Sponsoring Agency Name and Address National Aeronautics and Space Admin. Washington, D.C. 20546		14. Sponsoring Agency Code (RTOP) 505-61-51

16. Abstract

This thesis extends the Least Mean Square (LMS) algorithm to solve the multiple-input, multiple-output problem of alleviating N/Rev helicopter fuselage vibration by means of adaptive inverse control. A frequency domain locally linear model is used to represent the transfer matrix relating the higher harmonic pitch control inputs to the harmonic vibration outputs to be controlled. By using the inverse matrix as the controller gain matrix, an adaptive inverse regulator is formed to alleviate the N/Rev vibration. The stability and rate of convergence properties of the extended LMS algorithm are discussed. It is shown that the stability ranges for the elements of the stability gain matrix are directly related to the eigenvalues of the vibration signal information matrix for the learning phase, but not for the control phase. The overall conclusion is that the LMS adaptive inverse control method can form a robust vibration control system, but will require some tuning of the input sensor gains, the stability gain matrix, and the amount of control relaxation to be used. The learning curve of the controller during the learning phase is shown to be quantitatively close to that predicted by averaging the learning curves of the normal modes. For higher order transfer matrices, a rough estimate of the inverse is needed to start the algorithm efficiently. The simulation results indicate that the factor which most influences LMS adaptive inverse control is the product of the control relaxation and the the stability gain matrix. A small stability gain matrix makes the controller less sensitive to relaxation selection, and permits faster and more stable vibration reduction, than by choosing the stability gain matrix large and the control relaxation term small. It is shown that the best selections of the stability gain matrix elements and the amount of control relaxation is basically a compromise between slow, stable convergence and fast convergence with increased possibility of unstable identification. In the simulation studies, the LMS adaptive inverse control algorithm is shown to be capable of adapting the inverse (controller) matrix to track changes in the flight conditions. The algorithm converges quickly for moderate disturbances, while taking longer for larger disturbances. Perfect knowledge of the inverse matrix is not required for good control of the N/Rev vibration. However it is shown that measurement noise will prevent the LMS adaptive inverse control technique from controlling the vibration, unless the signal averaging method presented is incorporated into the algorithm.

17. Key Words (Suggested by Author(s)) Active Control Rotorcraft Dynamics Higher Harmonic Control Multicyclic Control Adaptive Helicopter Vibration Control	18. Distribution Statement Unlimited Subject Category 63

19. Security Classif. (of this report) Unclassified	20. Security Classif. (of this page) Unclassified	21. No. of Pages 176	22. Price*